REPORT DOCUMENTATION PAGE

Form Approved
OMB No. 0704-0188

1. REPORT DATE *(DD-MM-YYYY)*	2. REPORT TYPE		3. DATES COVERED *(From - To)*
1/Oct/2001	THESIS		

4. TITLE AND SUBTITLE
VARIABILITY OF TROPICAL CYCOLNE WIND-PRESSURE RELATIONSHIPS

5a. CONTRACT NUMBER

5b. GRANT NUMBER

5c. PROGRAM ELEMENT NUMBER

6. AUTHOR(S)
CAPT VILPORS STEVEN E

5d. PROJECT NUMBER

5e. TASK NUMBER

5f. WORK UNIT NUMBER

7. PERFORMING ORGANIZATION NAME(S) AND ADDRESS(ES)
COLORADO STATE UNIVERSITY

8. PERFORMING ORGANIZATION REPORT NUMBER
CI01-259

9. SPONSORING/MONITORING AGENCY NAME(S) AND ADDRESS(ES)
THE DEPARTMENT OF THE AIR FORCE
AFIT/CIA, BLDG 125
2950 P STREET
WPAFB OH 45433

10. SPONSOR/MONITOR'S ACRONYM(S)

11. SPONSOR/MONITOR'S REPORT NUMBER(S)

12. DISTRIBUTION/AVAILABILITY STATEMENT
Unlimited distribution
In Accordance With AFI 35-205/AFIT Sup 1

13. SUPPLEMENTARY NOTES

14. ABSTRACT

20011016 182

15. SUBJECT TERMS

16. SECURITY CLASSIFICATION OF:			17. LIMITATION OF ABSTRACT	18. NUMBER OF PAGES	19a. NAME OF RESPONSIBLE PERSON
a. REPORT	b. ABSTRACT	c. THIS PAGE		110	19b. TELEPHONE NUMBER *(Include area code)*

Standard Form 298 (Rev. 8/98)
Prescribed by ANSI Std. Z39.18

THESIS

VARIABILITY OF TROPICAL CYCLONE WIND-PRESSURE RELATIONSHIPS

Submitted by

Steven E. Vilpors

Department of Atmospheric Science

In partial fulfillment of the requirements

for the degree of Master of Science

Colorado State University

Fort Collins, Colorado

Summer, 2001

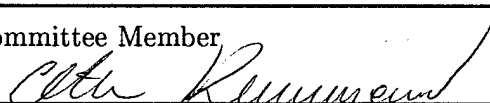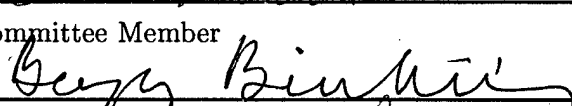COLORADO STATE UNIVERSITY

May 23, 2001

WE HEREBY RECOMMEND THAT THE THESIS PREPARED UNDER OUR
SUPERVISION BY STEVEN E. VILPORS ENTITLED VARIABILITY OF TROPICAL
CYCLONE WIND-PRESSURE RELATIONSHIPS BE ACCEPTED AS FULFILLING
IN PART REQUIREMENTS FOR THE DEGREE OF MASTER OF SCIENCE.
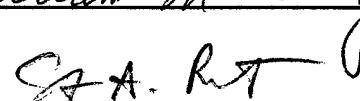
Committee on Graduate Work

Committee Member

Committee Member

Committee Member

William M. Gray

Adviser

Department Head

ABSTRACT OF THESIS

VARIABILITY OF TROPICAL CYCLONE WIND-PRESSURE RELATIONSHIPS

The variability of maximum sustained wind versus minimum sea level pressure (MSLP) in tropical cyclones is investigated using North Atlantic (1959–1999) and western North (NW) Pacific (1959–1999) best track data. A comparison is made of intensity estimates determined from aircraft reconnaissance, Dvorak (1975, 1984) satellite analysis, and Global Positioning System (GPS) dropwindsonde data. A review and comparison is made of past research on the variable relationship between maximum sustained wind versus MSLP in tropical cyclones (TCs). It is shown that the current analysis techniques are not reliable for assessing the large variability of maximum sustained wind versus MSLP for many cyclones of atypical structure.

The wind-pressure relationship for intensifying and filling stages of tropical cyclones is compared for 19 North Atlantic hurricanes from 1995-1999. The Kraft (1961) wind-pressure relationship for North Atlantic storms does not account for the temporal progression of the tropical cyclone wind structure. Winds tend to be overestimated for filling storms of a given pressure, especially at weaker intensities. A new relationship is established that better represents weakening storms.

The same storms are further divided into latitudinal categories and compared to wind-pressure relationships developed by Landsea et al. (2001). For a given pressure, filling storms north of 25° have lower winds than those south of 25°. Deepening storms do not show any latitudinal wind-pressure variations.

Data show greater variability of the maximum sustained wind versus MSLP relationships during the past 15 years in the Atlantic basin versus the NW Pacific where aircraft

penetrations into TCs are no longer conducted. Also, the NW Pacific best track intensities have smaller deviations from the Dvorak estimates, revealing the exclusive dependence of Joint Typhoon Warning Center (JTWC) on Dvorak's empirical intensity rules. We review, in this context, the prospect that the now universally used Dvorak technique can frequently have limitations which must be fully documented.

Steven E. Vilpors
Department of Atmospheric Science
Colorado State University
Fort Collins, Colorado 80523
Summer, 2001

ACKNOWLEDGEMENTS

TABLE OF CONTENTS

LIST OF FIGURES

LIST OF TABLES

LIST OF SYMBOLS AND ACRONYMS

AH: Atkinson and Holliday

AFGWC: Air Force Global Weather Center

AMSU: Advanced Microwave Sounding Unit

AOC: Aircraft Operations Center

AT: Atlantic

BT: Best Track

CI: Current Intensity

CIRA: Cooperative Institute for Research of the Atmosphere

f = Coriolis parameter ($2\Omega \sin \phi$)

GPS: Global Positioning System

HPD: Hurricane Prediction Center

HRD: Hurricane Research Division

INE: Inertial Navigation Equipment

JTWC: Joint Typhoon Warning Center

kts: Knots (nautical miles per hour)

KGWC: Identifier for AFGWC

km: Kilometers

mb: Millibars

MCP: Minimum Central Pressure

$MSLP_{am}$: Annual Average $MSLP_{mi}$

$MSLP_{mi}$: Minimum sea level pressure at time of max intensity

MSLP: Minimum Sea Level Pressure

MWS: Maximum sustained surface wind speed

NCAR: National Center for Atmospheric Research

NHC: National Hurricane Center

NHRP: National Hurricane Research Project

n mi: Nautical Mile

NOAA: National Oceanographic and Atmospheric Administration

NW: Northwestern

PAC: Pacific

P_c: Minimum sea level pressure

PGTW: Identifier for JTWC

r: Radius

RMSD: Root Mean Square Difference

RMW: Radius of Maximum tangential Wind

R_T = Radius of the trajectory

SAB: Satellite Analysis Branch

SLP: Sea Level Pressure

SSM/I: Special Sensor Microwave Imager

TAFB: Tropical Analysis Forecast Branch

TC: Tropical Cyclone

T number: Final T number

TPC: Tropical Prediction Center

TRMM: Tropical Rainfall Measurement Mission

V = Wind velocity

V_{am}: Annual Average V_{mi}

V_m: Maximum sustained surface wind speed

V_{mi}: Maximum wind speed at time of maximum intensity

WPAC: Western North Pacific Ocean

Chapter 1

INTRODUCTION

1.1 Introduction

Converting tropical cyclone maximum sustained surface winds to the minimum sea level pressure (MSLP), or vice versa, has been a useful tool for estimating tropical cyclone intensity when a limitted amount of data is available to forecasters and analysts. In tropical basins where aircraft reconnaissance data is not available, maximum surface winds are estimated using the Dvorak (1974, 1984) satellite intensity estimate technique, while MSLP measurements are determined through use of a wind-pressure relationship developed by Kraft (1961) in the Atlantic, or Atkinson and Holliday (1977) in the western North (NW) Pacific. While the Dvorak technique has proven to be an accurate tool to estimate storm intensity, the wind-pressure relationships used in his technique are not able to account for the range of maximum winds for a given MSLP, or vice versa, that can occur during a cyclone's life. A wind-pressure relationship that is able to account for wind-pressure changes due to life cycle or latitude changes can provide further insight into the tropical cyclone's wind structure to sufficiently improve the current relationships used by forecasting agencies around the world.

Since MSLP is the more accurate measurement, a meaningful relationship to obtain maximum surface wind estimates from MSLP is required. Kraft (1961) considered this requirement and worked to develop a more reliable wind-pressure relationship. Using data for 14 Atlantic hurricanes at peak intensity with land based wind observations, Kraft related MSLP in the eye to the maximum observed surface wind speed. From this he established the relationship between MSLP and maximum winds detailed in Table 1.1. Subsequently Atkinson and Holliday (1977) developed a similar wind-pressure relationship

using observations from NW Pacific tropical cyclones (Table 1.1). Note that for a given maximum wind speed, the MSLP values for Pacific TCs are lower than their Atlantic basin counterparts. This difference is shown in more detail in Fig. 1.1. Currently, the relationship developed by Kraft is widely used in the Atlantic while the Atkinson and Holliday (AH) relationship is used in the NW Pacific. Note that in other cyclone basins, the Atkinson and Holliday's relationship is typically used with small systematic adjustments. These wind-pressure relationships are relied upon to provide input to models, track cyclone intensity for the North Atlantic Hurricane Database, and are used in the Dvorak (1974, 1984) satellite intensity estimate techniques.

Table 1.1: Maximum surface winds (kts) and associated MSLP (mb) from Kraft 1961 (for Atlantic) and Atkinson-Holliday 1971 for (NW Pacific). Corresponding Dvorak Current Intensity (CI) Numbers are in the far left column.

CI Number	MWS (knots)	Kraft MSLP (Atlantic)	AH MSLP (NW Pacific)
1	25 K		
1.5	25 K		
2	30 K	1009 mb	1000 mb
2.5	35 K	1005 mb	997 mb
3	45 K	1000 mb	991 mb
3.5	55 K	994 mb	984 mb
4	65 K	987 mb	976 mb
4.5	77 K	979 mb	966 mb
5	90 K	970 mb	954 mb
5.5	102 K	960 mb	941 mb
6	115 K	948 mb	927 mb
6.5	127 K	935 mb	914 mb
7	140 K	921 mb	898 mb
7.5	155 K	906 mb	879 mb
8	170 K	890 mb	858 mb

Estimating the maximum wind speeds of tropical cyclones over the open ocean has always been a challenge for both analysts and forecasters. Atkinson and Holliday (1977) noted major problems in obtaining maximum wind observations for tropical cyclones (TCs), mainly sparseness of observations and inadequate wind equipment and exposure on ships and at existing stations wherein anemometers are often destroyed before record-
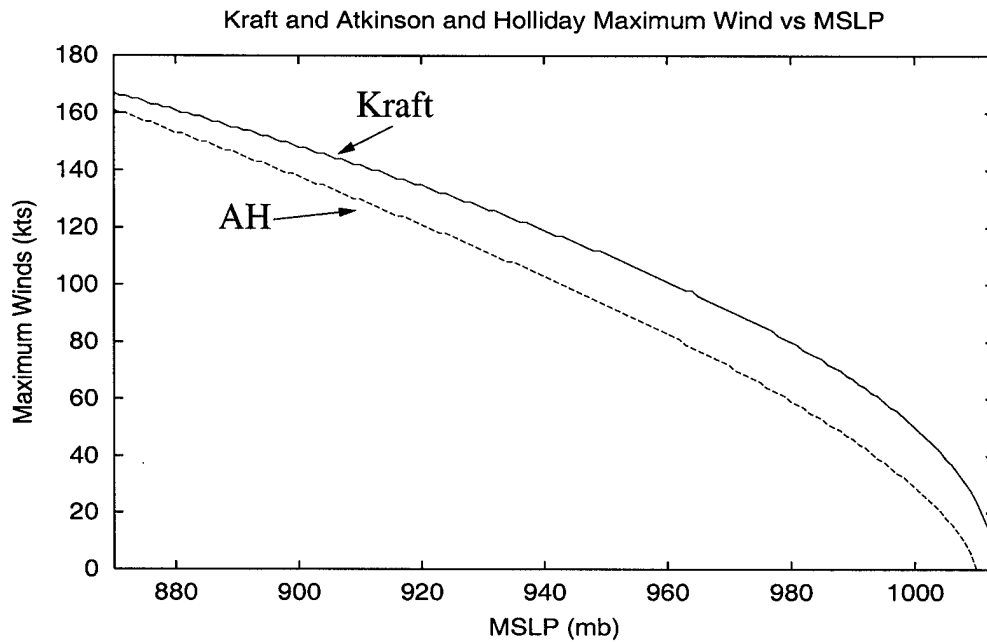
Figure 1.1: A comparison of Kraft versus AH wind-pressure relationships. Note that the AH curve gives 15-20 kts lower maximum wind speed for the same central pressure.

ing the peak winds. Other problems are the infrequency of ships/observations near the center of intense storms and the lack of wind measuring equipment on ships, the uncertainty of surface wind estimates from sea state observations during aircraft reconnaissance flights, and other difficulties. Moreover, even with recent technological advances such as the Global Positioning System (GPS) dropwindsondes, satellite imagery, satellite scatterometer data, and passive microwave imagery, truly accurate maximum surface wind measurements are very difficult or impossible to obtain.

Conversely, measurements of minimum sea level pressure (MSLP) in TCs tend to be more reliable and accurate, whether measured at flight level from aircraft or at the surface (Atkinson and Holliday 1977, Merrill 1982, Weatherford and Gray 1985). Weatherford and Gray produced a scatter plot of minimum 700 mb height versus the MSLP for aircraft reconnaissance of storms in the Northwest (NW) Pacific from 1979-1986 as shown in Fig. 1.2. Whereas the results in Fig. 1.2 convincingly show the accuracy of MSLP values

estimated from flight level data, there is little evidence for the accuracy of estimates of the maximum surface winds.
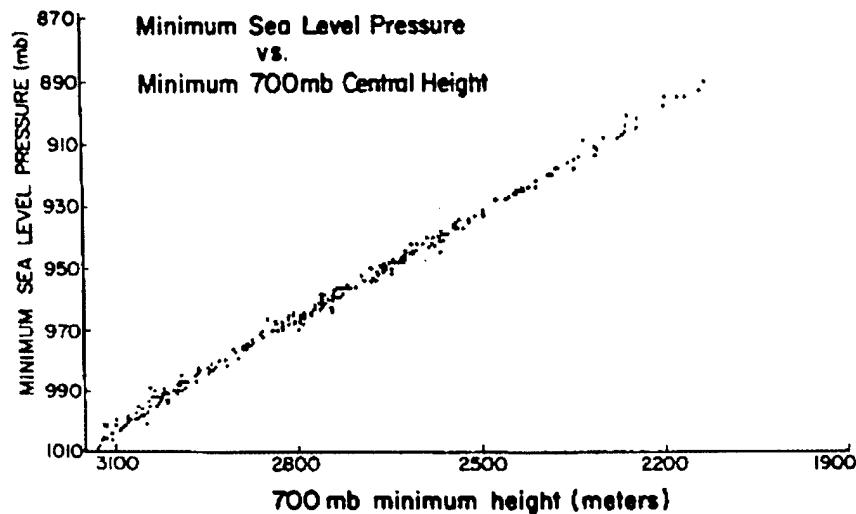
Figure 1.2: Scatter plot of central sea-level pressures versus 700 mb minimum height which correlates at .997 (Weatherford and Gray 1985).

The advent of satellite technology in the 1960's enabled scientists to observe the full cyclone life cycle over the open ocean. In the early 1970's, Vern Dvorak utilized these observations in developing a subjective technique for estimating tropical storm strength using visible satellite imagery (Dvorak 1974). This early technique used the extent of cloud banding features, eye size, central dense overcast, and other factors to determine the satellite inferred intensity. Dvorak later updated his scheme during the mid-1980s to include an infrared (satellite) imagery relationship (Dvorak 1984) that used equivalent black body brightness temperature of cloud tops and the eye (when present) to provide additional information. The current intensity number, or "CI", is computed after the analyst reviews the satellite images and applies Dvorak's rules. The CI number is correlated to a wind speed and then to a minimum sea level pressure, using Kraft's relation for the Atlantic, or Atkinson and Holliday's in the Pacific (See Table 1.1). The corresponding

pressure and wind is considered the intensity of the storm at the time of the satellite image.

Infrared satellite imagery enabled meteorologists to monitor tropical systems by both day and night. The Dvorak technique is still used by the Tropical Prediction Center (TPC) Miami, Florida, the Joint Typhoon Warning Center (JTWC) in Pearl Harbor, Hawaii, and by meteorological agencies and researchers in the other tropical cyclone basins where there are no routine aircraft reconnaissance. This is especially true at JTWC, currently in Pearl Harbor, Hawaii, where aerial reconnaissance flights from Guam were discontinued in 1986. The North Atlantic basin continues to be the only basin where aerial reconnaissance flights are routinely made. The Dvorak intensity technique must be relied upon when aircraft flights are not available.

The wind-pressure relationships summarized in Table 1.1 are too general to accommodate the range of peculiar wind-pressure qualities of individual cyclone variability. Consequently, the purpose of this study is to review prior TC research, try to document the various modes of individual TC maximum wind-pressure variability, and to develop quantitative parameters that describe this variability with the intent of better accommodating this improved information in operational analyses and forecasts. This study will also reveal the impact the exclusive use of satellite information without aerial reconnaissance on our determination of the tropical cyclone's maximum winds (V_m) to MSLP relationship.

1.2 Historical Background

1.2.1 Aerial Reconnaissance

Aerial reconnaissance (and hence, insitu observation(s)) is the most accurate way to measure hurricane maximum winds and minimum pressure. As shown in the timeline of Fig. 1.3 aircraft reconnaissance in the Atlantic Ocean began in 1943. Routine reconnaissance missions were initially flown after World War II and systematic research missions first began with the inception of the National Hurricane Research Project (NHRP) in 1956. Research flights are currently flown out of Tampa, FL by the National Oceanic and Atmospheric Administration(NOAA)/Hurricane Research Division and operational flights

by the 53rd Weather reconnaissance Squadron are flown out of Keesler Air Force Base, MS. Aircraft missions are typically made at least twice a day, with two center penetrations each flight, for cyclones located west of 55° west longitude.

Reconnaissance flights in the NW Pacific began at the end of World War II, and continued through the mid 1980's. With the inception of the Dvorak satellite intensity technique (Dvorak 1974, 1984) in the mid 70's, the need for the costly Guam based aircraft reconnaissance program was reduced and in early 1987, flights were discontinued. At that time, the Dvorak technique was thought to have been as accurate as aircraft intensity measurements, thus government agencies were convinced to halt tropical cyclone aircraft reconnaissance projects. Information on NW Pacific TCs since that time, has relied primarily on satellite observations.

Numerous studies have been conducted on the impact of the loss of aircraft investigation flights on forecasts in the NW Pacific. Shoemaker and Gray(1990) made statistical comparisons of the accuracy JTWC track forecasts from 1983-1986, separating similar forecast situations with and without aerial reconnaissance data available to the forecaster. They found that when synoptic aircraft reconnaissance missions were flown on the poleward side of the hurricanes, that average track forecast errors for 24 to 72 hour time periods were found to be approximately 10 to 20 percent smaller than when these aircraft data were not available. Their findings show that aircraft reconnaissance aided forecasts were consistently more accurate, thus making a case that improved long range forecasts in the NW Pacific won't occur without further advances in technology. This issue remains in question while the Joint Typhoon Warning Center, with greater satellite and computer model technology than ever before, has reported improving verification rates year after year. One can argue that these results are diluted since aircraft reconnaissance data is not available to provide accurate independent verifying information.

In the North Atlantic, the new NOAA synoptic Dropwindsonde Program (Burpee et al., 1996, Aberson and Franklin, 1999) has shown to add to the improvement of At-
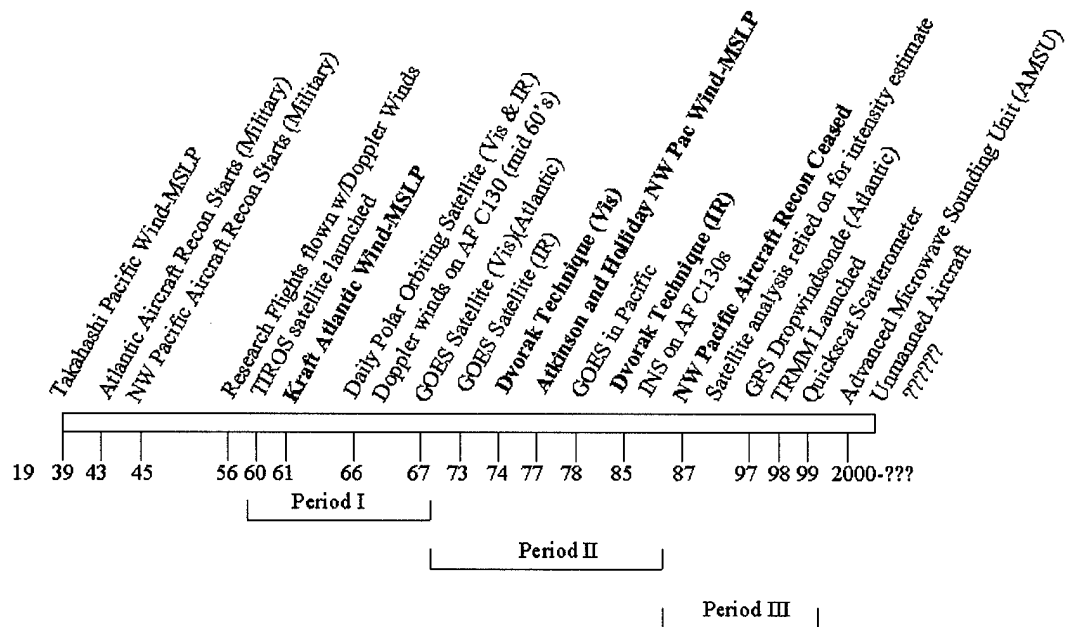
Figure 1.3: Wind-pressure relationship and satellite intensity estimate landmark events in the past 60 years. Period I, II, and III refer to the years that will be used for the time period comparison in Chapter 4.

lantic forecast tracks. This finding reveals that JTWC may find improved forecasts if dropwindsonde information were available.

In this study, information will be presented indicating a notable weakness in one of the Dvorak technique's applications for estimating the MSLP from satellite derived maximum surface wind estimates. We will investigate JTWC best track data with and without aircraft reconnaissance, and demonstrate the dependence of forecasters in the NW Pacific basin on the Dvorak technique and Atkinson and Holliday wind-pressure relationship. NW Pacific information with and without aircraft reconnaissance will be compared with Atlantic storm data that reveals a great range of winds for given pressures and vice-versa.

1.2.2 Dvorak Analysis

The development of earth satellites in the 1960's for delivering remote sensor images to meteorologists spawned a much more cost effective means of estimating tropical cyclone intensity and location assuming that the satellite would be placed in orbit regardless of its influence on tropical cyclone measurement. The feasibility of using satellite imagery to estimate tropical cyclone strength was early recognized by Fett (1961), Sadler (1964) and (Dvorak 1974) among others. Soon thereafter several methods were developed attempting to use the possible association between cloud features outer wind strength and inner-core intensity (Fett 1966, Fritz et al. 1966). But, the association that was developed did not prove fully adequate. During the next decade Vern Dvorak worked on further interpreting satellite imagery to determine intensity. Dvorak concentrated more on cloud-line banding features and the cyclone's central dense overcast rather than total cloud amount. This proved superior to the earlier techniques. The procedure developed by Dvorak (Dvorak, 1974) was adopted as the primary satellite intensity estimate technique in all TC basins and has, with a few modifications, withstood technological advances. Dvorak further updated his technique in 1984 to include cloud top temperatures derived from satellite infrared imagery, and when an eye is present, the temperature of the eye and the cloud top temperature of the ring of eye-wall clouds surrounding the eye. Combined infrared and visible relationships allow for an estimated Tropical number (or, "T" number) and maximum wind speed. The intensification and weakening trends of tropical cyclones are considered, and the intensity of the storm is deemed the "current intensity" number, or "CI". The CI value is the same as the T number as the storm deepens but may be 0.5 or 1.0 higher than the T number when the cyclone is in a weakening stage. This is based on the fact that as the storm weakens, the intensity typically remains higher than the weakening signals revealed by the changing cloud patterns. Using satellite imagery for both day and night storm intensity estimates was thought to prove reliable enough to allow the discontinuance of aerial reconnaissance in the Northwest Pacific basin.

Among the numerous analyses of operational Dvorak T-numbers, there are several benchmark studies which summarize its main findings. Shewchuk and Weir (1980) evaluated the Dvorak current intensity and 24-hour forecast intensities versus the JTWC best track data for the Northwest Pacific TCs. The best track data sets for Shewchuk and Weir's study (1980) benefited from aircraft reconnaissance data that have not been available to forecasters after 1987. Their study indicated an overall error bias errors of less than one CI number, and Dvorak and JTWC forecast errors were found to be approximately equal. Data tabulated in Table 1.1 provide corresponding wind speeds and MSLP for a given CI number. In addition, the Dvorak technique was found to be the most accurate of all objective aids available to forecasters at JTWC at that time (1987). The latter finding led to a much larger dependence on the Dvorak technique after aerial reconnaissance was discontinued. In addition, Shewchuk and Weir evaluated the performance of the Dvorak forecast data as a function of time throughout the tropical cyclone's life cycle. The latter tests showed that the Dvorak technique tends to over-forecast both intensifying and weakening trends. These biases are still believed to be present and no adjustment for these systematic differences has yet been provided and implemented.

Martin and Gray (1988) conducted studies to assess differences in Joint Typhoon Warning Center's Dvorak intensity estimates with and without aircraft investigation flight data. They also made a comparison of simultaneous satellite intensity estimates being made at several different analysis and forecast centers. Figure 1.4 shows the distribution of TC intensity differences as measured by the satellite versus aircraft at approximately the same time. Note that differences up to 20 mb (1 T number in the Dvorak intensity scheme) were common. Figure 1.5 shows intensity differences in millibars, irrespective of sign, for (independent) satellite observations made simultaneously at different analysis centers. The solid line at zero difference is a result of the concentration of many zero difference data points. Although large differences can occur between sites, the intensity estimates generally agreed, especially in comparison to differences with aircraft measurements. Martin and Gray speculate that the large differences present when aircraft were
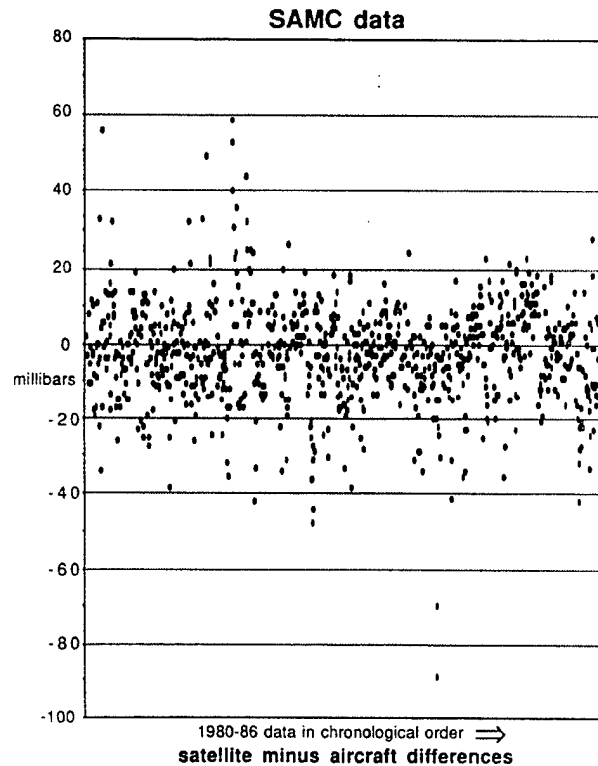
Figure 1.4: Distribution of differences (expressed in mb) of satellite estimated MSLP versus aircraft measured MSLP. Data from Satellite and Aircraft Measurement Comparison (SAMC) of Martin and Gray (1988).

flown within 12 hours of the estimate may be a result of the analysts' identifying similar cloud features not always related to intensity and their confusion when confronted with conflicting aircraft data and satellite estimates. When no aircraft data were available, the analysts followed the rules of the Dvorak technique and were less apt to have to deal with conflicting signals.

The Dvorak intensity estimates appear reliable and consistent, especially if no other conflicting data are available. However, as shown in Figs. 1.6–1.8, estimated intensity frequently shows a significant difference between aircraft and satellite determinations, especially during periods of rapid intensification, at the time of maximum intensity, and when the cyclone is weakening. Aircraft measurements clearly provide more accurate estimates during such periods. The results in Figs. 1.6–1.8 are examples of storms wherein the

SISO data

60 —

50 —

40 —

millibars

30 —

20 —

10 —

0 —

1979-86 data in chronological order $\Longrightarrow$
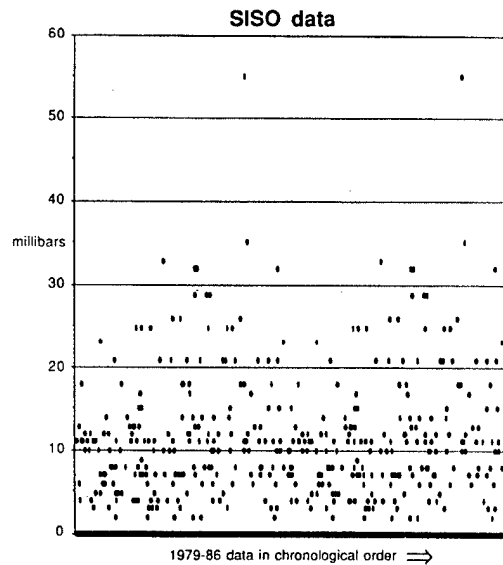
Figure 1.5: Distribution in time (1976–1986) of multiple simultaneous Independent Satellite Observations (SISO) of absolute TC Minimum Sea Level Pressure intensity differences. Data clustering at zero difference causes the thick black line at the base (from Martin and Gray 1988).

Dvorak intensity estimates were adjusted significantly due to the intensity measurements made by the aircraft investigation flights

Although the Dvorak technique has proven very valuable in all the global tropical cyclone basins and is by far the best technique for remote intensity estimation, it is not sufficiently accurate to depend upon exclusively in the western Atlantic where aircraft reconnaissance is still deployed. The West Atlantic reconnaissance flights continue to be made because of the known occasional inaccuracy of the Dvorak scheme and of the strong desire for a verifying redundancy in the measurements. This study will provide evidence of the often systematic lack of variability in Dvorak estimates of cyclone intensity as revealed by the maximum sustained surface wind-MSLP relationship recorded in the NW Pacific best track data set during and after aircraft reconnaissance.

1.2.3 Digital Dvorak Technique

Velden et al. (1997) created a digital Dvorak technique using computer algorithms, now being used experimentally at both the Tropical Prediction Center and the Joint Typhoon Warning Center. This algorithm is based on satellite derived temperatures of
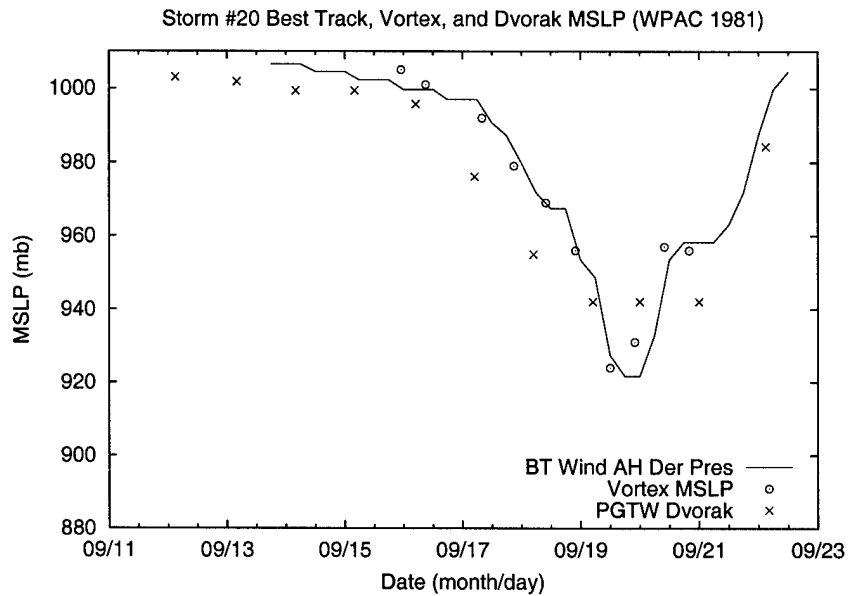
Figure 1.6: Time depiction of best track wind derived pressure using the Atkinson and Holliday relationship (solid line), aircraft measured minimum central pressure (o), and PGTW Dvorak intensity analysis estimates (x) for Typhoon Clara (1981) in the NW Pacific. The Dvorak estimates intensify the cyclones too quickly and often do not estimate maximum intensity accurately.
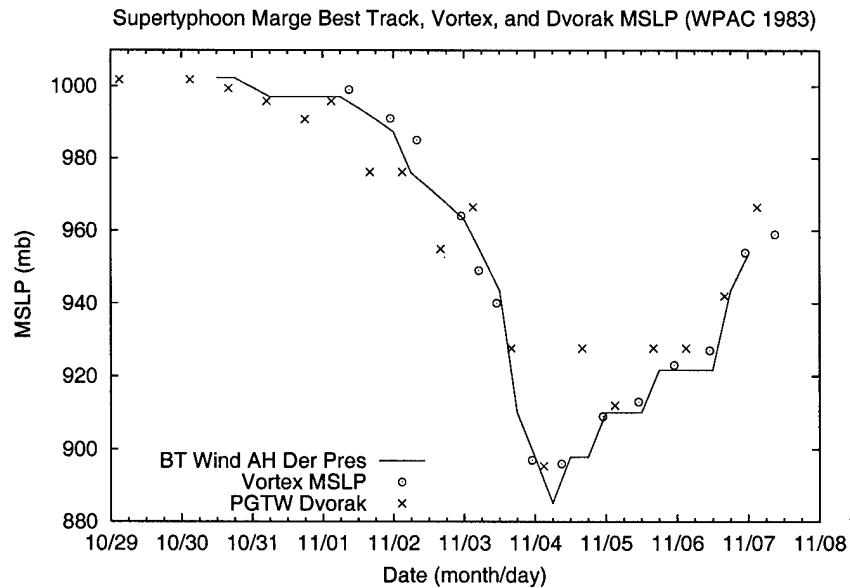
Figure 1.7: As in Fig. 1.6 but for Supertyphoon Marge 18 (1983) in the NW Pacific. The Dvorak estimates again intensify the storm too quickly, and do not well resolve the cyclone at maximum intensity, and fills the cyclone too quickly.
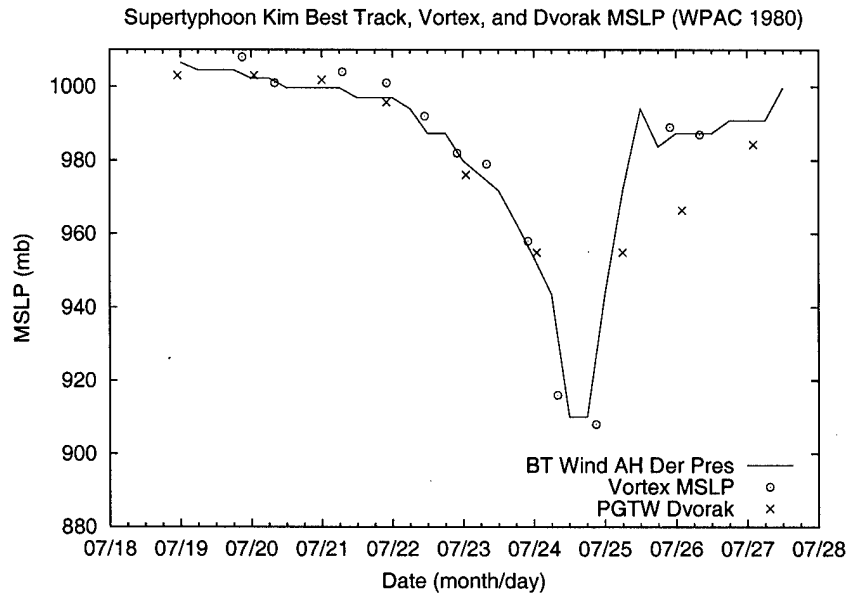
Figure 1.8: As in Figs. 1.6 and 1.7 but for Supertyphoon Kim 11 (1980) in the NW Pacific. The Dvorak estimates are inaccurate for maximum intensity accurately and tends to fill the storm too slowly.

the eye and cloud top temperatures of the surrounding cloud rings. Preliminary results using this technique are proving very valuable for the intense cyclones but there are some difficulties in accurately estimating the intensity of the weaker systems. This is due to inherent problems in measuring inner-core cloud top temperatures when no eye is present. Velden et al. (1997) technique, along with the more advanced high-resolution imagery that is coming in the near future is expected to provide a useful complement to the subjective Dvorak technique.

1.3 Research Objectives for This Study

Tropical cyclone forecasters and analysts all over the world depend on the Dvorak satellite intensity estimate to provide information on tropical cyclone intensity over the open ocean and, in some cases, the potential for wind damage once the storm makes landfall. Often the actual TC intensity is never known, or is not known until the system makes landfall or the system comes close enough to the coast that radar measurement can assist in the intensity determination. The accuracy of the Dvorak scheme is often exaggerated. This is because the intensity estimates made by forecasters in past-analysis

is used as a verification of the observations themselves. Clearly, this shortfall in tropical cyclone intensity determination will eventually lead to catastrophic mistakes when forecasters become too complacent in relying on satellite data only. This study will investigate the great variability of actual tropical cyclones versus various conventional relationships as presented by previous research. The results should enlighten tropical meteorologists as to the range of intensities that can exist for any given storm as observed either from aircraft or by satellite imagery.

In particular, though Kraft's original pressure-wind relationship has been in use by tropical meteorologists for nearly 40 years, it is also well understood in the tropical community that this relationship does not accommodate conditions in all cyclones, particularly in their weaker stages. To better understand the potential inaccuracy in the Dvorak scheme it is necessary to be familiar with the variations of tropical cyclones during their life cycles and the potential for occasional exceptions. The accurate determination of the maximum wind from the MSLP is crucial in better preparing the public for the actual strength of a storm as it approaches land. Future applications of this relationship include comparisons with the Advanced Microwave Sounding Unit (AMSU) intensity estimates, as input for initializing models, as well as other future applications that can accurately measure the MSLP but not the maximum surface winds.

The objective of this study is then to provide insight on the range of the winds for a given MSLP, or vice versa, from Atlantic best track and aircraft data of the period 1995–1999, and to compare this relationship with the Kraft (1961) curve. This study also analyzes the NW Pacific maximum wind-MSLP relationships from 1959-1999 using periods defined by aerial reconnaissance, and period defined only by satellite intensity data (1986 to present). This study will propose an adjustment to the Kraft maximum wind-MSLP relationship and for the Atkinson-Holliday relationship. An improved wind-MSLP relationship more suited to life cycle and latitudinal changes of a tropical cyclone is proposed. Finally, a $\frac{V_m}{MSLP}$ ratio is introduced that may provide forecasters and analysts

more insight in to the type of storm, and its potential damage solely by looking at the wind-MSLP relationship.

Chapter 2 contains a description of the data used in the study. Chapter 3 provides examples and discussion on the variability of the wind, pressure, and strength relationships for tropical systems and of the difficulties faced by current analysts and forecasters. Chapter 4 presents the results of the maximum wind-minimum sea level pressure study with a proposed adjustment to the current Kraft and Atkinson-Holliday relationships. Chapter 5 summarizes all findings and recommends a new technique for summarizing the V_m and MSLP relationship.

Chapter 2

DATA

2.1 Best Track

2.1.1 Atlantic Ocean

The primary data set used for this study is the Atlantic basin best track information from 1995-1999, prepared and maintained by the Tropical Prediction Center (TPC), formerly the National Hurricane Center. The Atlantic basin includes the North Atlantic Ocean, Caribbean Sea, and Gulf of Mexico. Data include the position, minimum sea level pressure (MSLP), and estimated maximum sustained one minute wind for six hour intervals. The data are in the form of a post-season analysis using synoptic station reports, aircraft reconnaissance data, ocean buoys, and all other available observations. These data are considered the most accurate information, or "best-track" because they are a composite of all available track and intensity data. The Atlantic years of 1995-1999 were used since this was a very active period from hurricanes and the data are considered to have been collected with the latest advanced observational techniques.

This study uses the maximum wind (V_m), MSLP, and latitude from the best track data set in order to investigate the V_m–MSLP relationship in the Atlantic basin. Additionally, the best track data set will be compared to Dvorak intensity estimates and aircraft data.

2.1.2 Northwest Pacific Ocean

The Joint Typhoon Warning Center in Pearl Harbor, Hawaii publishes a best track data set at the end of the calendar year, similar to the Atlantic TPC, but without the luxury of aircraft reconnaissance after 1987. Although data sets exist from 1945 to the

present, only the period of 1959 to present were used as both MSLP and maximum winds are available for those years. Whereas maximum winds are presented every six hours, similar to the Atlantic data set, MSLP is not. Due to the lack of reporting stations and ships in the NW Pacific Ocean, MSLP and maximum winds are simultaneously at maximum intensity in best track analyses. We make statistical comparisons of different time periods to show changing patterns of intensity estimates during the past two decades as well as a lack of the large maximum wind and pressure ranges observed in the Atlantic.

2.2 Global Positioning System Dropwindsonde Data

The National Center for Atmospheric Research (NCAR), in a joint effort with NOAA, has developed a dropwindsonde based on GPS satellite navigation (see Hock and Franklin 1999). Observations with this GPS dropwindsonde are providing important new insight into the structure and thermodynamics of tropical cyclones over data sparse oceanic areas. This technology represents a major advance in both accuracy and resolution of atmospheric measurements. It provides wind velocity accuracies of 0.5-2.0 m/s with vertical resolution of approximately 5 meters (Franklin and Black 1999). Franklin and Black also described the surprising and unexpected ability of the GPS dropwindsonde to measure wind speeds at or near 10 meters above ground level. Consequently, this growing GPS dropwindsonde data set provides wind measurements from flight level (generally below 5000m) to the surface at approximately five meter intervals down to 10 meters along the surface. To date GPS dropwindsondes have been used only in the North Atlantic and eastern North Pacific basins. Refer to LeeJoice (2000) for a more in depth description and history of the GPS dropwindsonde. These GPS measurements will be used in this study to demonstrate both the extreme wind measurements in storms and the great variability which occurs in tropical cyclone vertical wind profiles.

2.3 Aircraft Fix Data

2.3.1 Atlantic

Research aircraft in the Atlantic basin are flown into most storms west of 60 West longitude. Collected data on location and intensity are transmitted directly to the Tropical Prediction Center. The data are archived and maintained by the Hurricane Research Division (HRD) of NOAA. Flight patterns are determined prior to the mission and may deviate as appropriate if conditions warrant (Eastin 1999). The measurement of MSLP is considered the most accurate measurement. Data transmitted from the aircraft include the MSLP, maximum flight level winds, location relative to the center that the maximum flight level winds were measured, maximum surface winds, distance from the center of the maximum wind, the length of the long and short axis of elipitical (when present) eyes, and the location of the center of the storm.

For this study, the maximum flight level winds were reduced (extrapolated) to the surface using the relations devised by Black (2000). Specifically, if the flight level is 700 mb, winds are multiplied by 85 percent to estimate surface wind speed; if the flight level is 850mb, the flight level winds are multiplied by 90 percent. As the new GPS dropwindsondes show, these estimates of surface wind from flight level may not be as accurate as previously thought. Chapter 3 discusses the wide variability that can exist in the vertical wind profiles for several hurricanes. The length of the long axis of the eye will be used for a comparison of eye size. Aircraft fix data will provide additional data points.

2.3.2 Pacific

Aerial reconnaissance data from the Northwest Pacific basin will be studied for the 1979–1987 period. Since these flights were discontinued in 1987, only the Dvorak intensity estimates are available for best track representation. Doppler wind velocity estimates are only considered reliable since the early 1970's and thus limit the length of available record. Point values for maximum flight level winds (again extrapolated from flight level to estimate maximum surface winds) are used.

2.4 Dvorak Fix Data

2.4.1 Atlantic

Dvorak fix location and intensity estimates for the Atlantic basin are performed by analysts at three different sites including the Satellite Analysis Branch (SAB) of NCEP, Tropical Prediction Center (TAFB), and the Air Force Global Weather Central (KGWC) satellite group. Each of these centers has specific fix requirements. Typically storms are tracked by all three sites with many storms likely being analyzed simultaneously by all three sites at any given time. This redundancy provides this study with a large number of Dvorak intensity estimates for 1995–1999. The Dvorak T-number is converted to wind velocity by using the Kraft maximum wind-MSLP relationship (i.e., Table 1.1). Cases were presented in Chapter 1 wherein the Dvorak intensity estimates were improved for the best track data after aircraft reconnaissance data reviewed (also see Appendix A). An analysis of these cases show it is possible for the Dvorak technique in some cases to over or underestimate the intensity of the cyclone by a significant amount. Only the Dvorak CI estimates will be used for this portion of the study since these are the technique's best estimate for the intensity of the storm.

2.4.2 Northwest Pacific

Only CI estimates will be used for this study. Dvorak fix location and intensity estimates for the NW Pacific basin are performed at several locations including SAB, KGWC, Kadena Air Base (RODN), and by analysts at the Joint Typhoon Warning Center. Although many years of Dvorak data are available from the Joint Typhoon Warning Center, only a few cases were used for this study. Dvorak intensity numbers are converted to wind velocity by using the Aktinson and Holliday (1977) maximum wind-MSLP relationship (eg., Table 1.1). The Pacific best track data file will again be investigated and patterns of influence and reliance on the Dvorak intensity estimate by JTWC will be reconsidered (see Appendix A).

Chapter 3

TROPICAL CYCLONE VARIABILITY

3.1 Introduction

Tropical cyclones can best be characterized as coming in many different shapes and sizes. In particular, they take on different structural characteristics during their life cycle, have intraseasonal as well as interseasonal variations, and often appear to have complex vertical wind profiles as revealed by the GPS dropwindsonde. The advent of satellite imagery in the early 1960's has enabled scientists to better realize the great variability of tropical cyclones resulting in numerous studies on these differing characteristics. The following sections review and summarize basic conclusions drawn from previous studies and, where applicable, present additional results gathered during this study to illustrate the large variabilities of these tropical cyclones. This chapter provides background information reaffirming the fact that, although it's a very useful tool, the current Dvorak analysis technique is frequently insufficient to handle the multiple variabilities of tropical storms. We show again that the current wind-pressure relationships do not cover the wide variety of cyclone structure features which can be present.

3.2 Size Variability: Large and Small Cyclones

Cyclone size can vary enormously (Atkinson 1971, Merrill and Gray 1982). Several studies have considered large and small cyclones, one of which was conducted by Merrill and Gray (1982). In their study, they looked at the climatology of cyclone size, as indexed by the Radius of the Outer Closed Isobar (ROCI) in the Atlantic (1957-1977) and North-western Pacific (1961-1969) basins. Frequency distributions of TC size for both basins are shown in Figs. 3.1 and 3.2.

The climatology of cyclone sizes indicates that the Pacific storms are typically about twice as large in the area of cyclonic winds as Atlantic storms. Merrill and Gray concluded that the ROCI of the 'mean' Pacific cyclone is about 1.5 degrees larger than that of the Atlantic cyclone; this represents a 40 percent difference in the mean radius between the two basins.

The typical size of these cyclones also varies seasonally within each basin. Figures 3.3 and 3.4 (alas from Merrill and Gray 1982) suggest certain similarities between seasonal variation in the two basins wherein a relative size minimum occurs in mid-summer and a late season maximum in October. Merrill and Gray examined wind data and dispelled the theory that the size has much of a relationship to intensity. To do this they plotted a time series of the intensity variations for each basin and, by reviewing the trends, demonstrated that there is no direct correlation between size and intensity (ef., Figs. 3.3 and 3.4 versus Figs. 3.5 and 3.6). Note how Atlantic and Pacific September cyclones are at least as intense as October ones and how the size maximum in March leads the April intensity maximum in the Pacific basin. Whereas intensity may account for part of the seasonal trend in size, additional factors are involved.
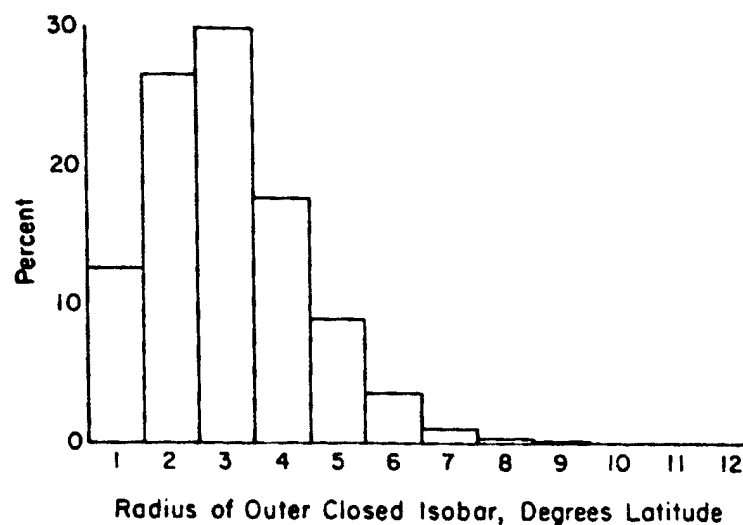
Figure 3.1: Percent frequency distribution of sizes of Atlantic tropical cyclones, 1957-1977, expressed in degree of latitude (from Merrill and Gray 1982).
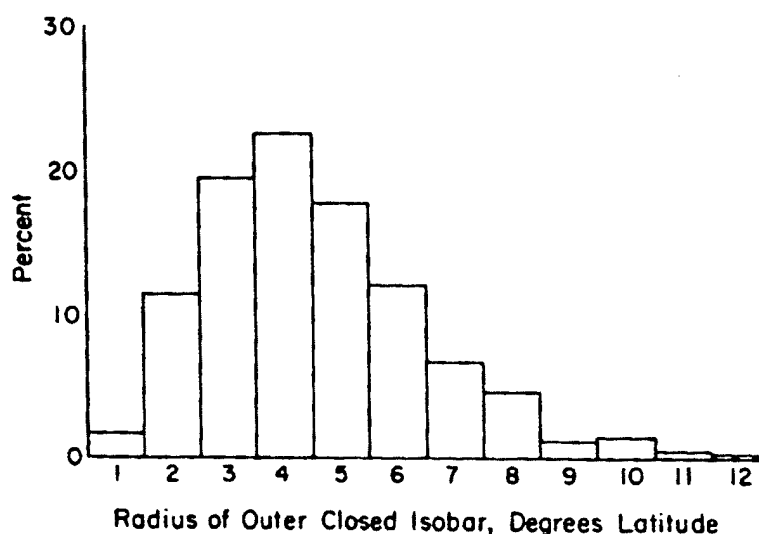
Figure 3.2: As in Fig. 3.1, but for the Pacific tropical cyclones, 1961-1969 (from Merrill and Gray (1982)

Merrill and Gray next considered maximum sustained winds versus ROCI for both basins. The least-squares regression line plotted in Figs. 3.7 and 3.8 reveals a clear relationship between size and intensity although the percentage variance explained by (less than 10 percent in both cases) is small.

Merrill and Gray's study further investigates the size and intensity of cyclones and came up with the following two additional conclusions.

1) Large cyclones occur more often in regions where low level environment vorticity is relatively large. Large TCs typically occur within the monsoon trough or between subtropical ridges.

2) Small cyclones occur more often in areas of minimum environmental vorticity. This consideration groups these small TCs in the trade winds in the margins of the subtropical ridge of the Gulf of Mexico and extreme NW Pacific Ocean, or within the westerly wind belt of very strong and high latitude monsoon troughs.
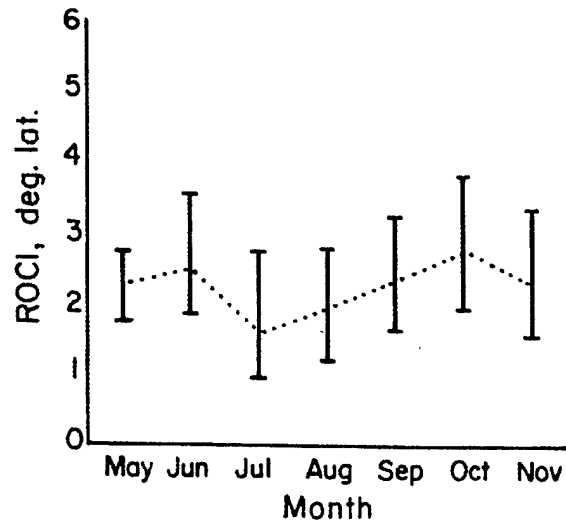
Figure 3.3: ROCI versus month for Atlantic (from Merrill and Gray 1982)
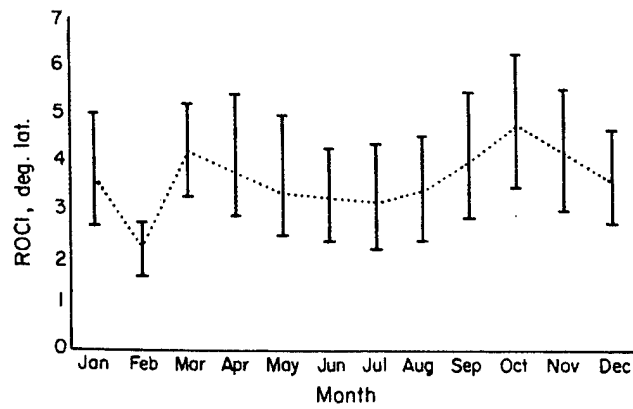
Figure 3.4: As in Fig. 3.3, but for the Pacific (from Merrill and Gray 1982)
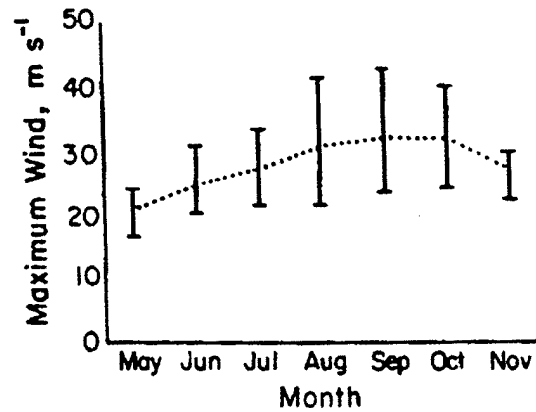
Figure 3.5: Monthly progression of median, 25th, and 75th percentile values of maximum sustained wind of Atlantic tropical cyclones, 1957-1977 (from Merrill and Gray 1982)
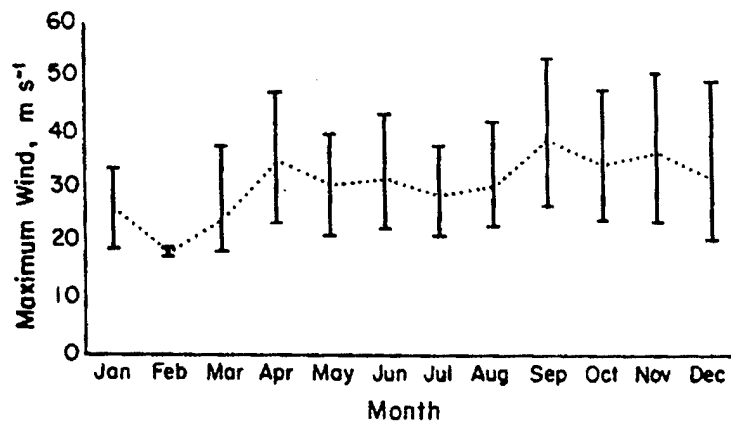
Figure 3.6: As in Fig. 3.5, but for the Pacific tropical cyclones, 1961-1969 (from Merrill and Gray 1982)
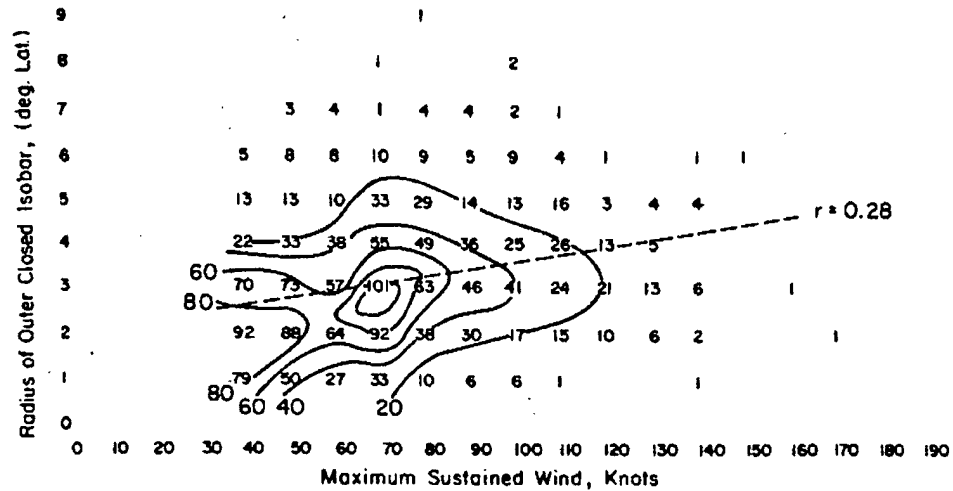
Figure 3.7: Distribution of tropical cyclone size as a function of maximum sustained wind for Atlantic tropical cyclones, 1957-1977. Observations were tabulated into classes of one degree latitude and 10 kts. The least square line is fitted to the raw data (from Merrill and Gray 1982)
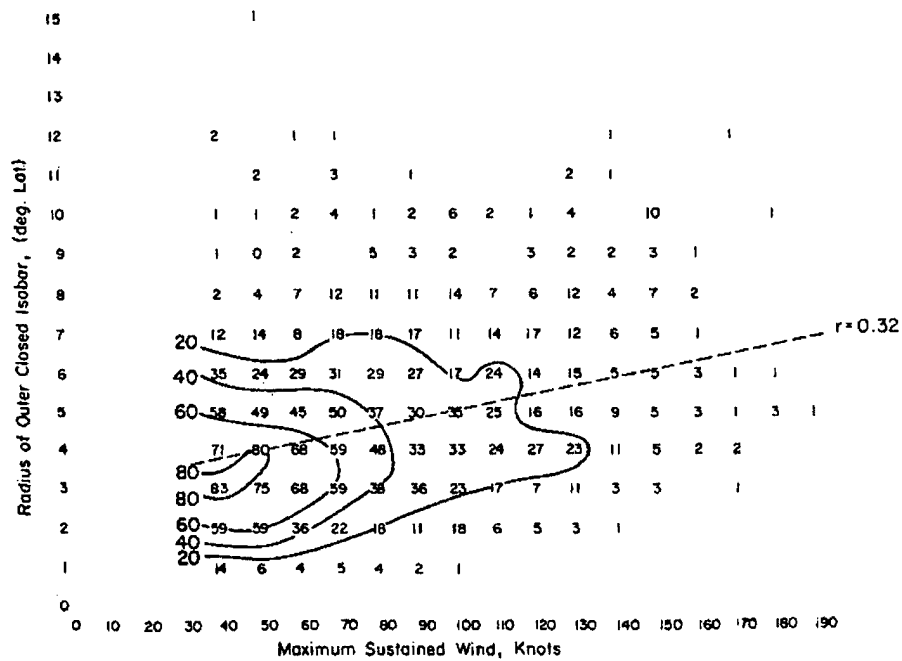
Figure 3.8: Same as previous figure, but for Pacific tropical cyclones (from Merrill and Gray 1982)

3.3 Very Small (Midget) Cyclones

Very small or midget cyclones have been observed in all TC basins. The 1996 JTWC Annual Tropical Cyclone Report describes midget cyclones as having a radius of the outermost closed isobar of less than 2 degrees latitude, or approximately 120 nautical miles. This radius is compared to that of an average typhoon of 3 to 6 degrees latitude, or approximately 180 to 360 nautical miles (Brand 1972, Merrill 1984). In 1952, Arakawa first mentioned these storms in his study of small intense tropical cyclones, naming them "mame taifu" which translates to English text as "midget typhoons". In 1967, Hawkins and Rubsam conducted a study on Hurricane Inez (21 September - 11 October, 1966) in the Caribbean and proposed that these small intense storms of hurricane intensity be named "micro-hurricanes". In 1972, Brand found that the midget typhoons of the NW Pacific tend to form in August and in the region south of the North Pacific High. Other areas of comparatively frequent formation are the Mozambique Channel and in the subtropical latitudes of both the Northwestern Pacific and the North Atlantic (Lander 2000). Midget typhoons typically maintain themselves for only 1-2 days.

Midget cyclones present a special challenge to forecasters since they often are undetected on synoptic charts and their early intensity is difficult to estimate using the Dvorak technique. Midget tropical cyclones' are often first observed as tropical storms; they intensity rapidly and are usually underforecast. Intensities vary greatly between overlapping advisory centers (Lander 2000). Lander describes several midget Pacific cyclones that caused great problems for forecasters. Specific characteristics of these storms were that they attained maximum intensity for only a few hours, forecast centers often have differing estimates of current intensities based on Dvorak analysis. Midgets developed and weakened very quickly (allowing warning centers very little time to make key decisions on forecasts). The real intensity of these storms is rarely known since they typically do not pass over any reporting stations and there have note been many aerial reconnaissance missions flown into these systems.

3.4 Variability of the Relationship Between Storm Intensity Versus Wind Strength

Weatherford and Gray (1985) investigated tropical cyclones which occurred from 1979-1986 in the Northwest Pacific in an attempt to relate the strength of the winds to the intensity, as measured by the minimum sea level pressure of the storm as shown in Fig. 3.9. Cyclone strength was determined as an area-weighted average tangential wind speed from 60 n mi (111 km) to 150 n mi (278 km) in a cyclone relative motion coordinate system. Figure 3.9 illustrates the large amount of variability that was observed. The least amount of scatter in this relationship was observed during the tropical storm stage but, once the storms develop to typhoon and/or formed an eye, virtually all the intensity-strength relationship is lost. For example, the most intense typhoon in Fig. 3.9 had a MSLP of 890 mb but with an average strength of only 35 knots. In contrast, several typhoons in Fig. 3.9 had a central pressures about 940 mb (50 mb higher) but with strength of 70 knots or twice as strong. Further evidence stems from the prospect that a typhoon with a sea level pressure of 960 mb may have strength as low as 20 knots and as high as 60 knots (i.e., a three-fold difference). Thus estimating variability of strength given only observations of minimum central pressure creates a major forecast challenge. Conversely, estimating the intensity of a cyclone from its outer core wind can be just as challenging.

Additional variability analyses were conducted concerning changing strength and intensity relationships as the storm goes through its life cycle. Weatherford and Gray concluded that cyclones may go through several different and illdefined patterns of changes. The example in Fig. 3.10 depicts how the two classes of rapid and slow deepening TCs may seem to have different outer core strength characteristics when compared to their intensities. Slow deepeners appear to have more outer core strength for a given pressure than do the rapid deepeners. This result illustrates how the outer core may act quite differently from the inner core of the tropical cyclone.
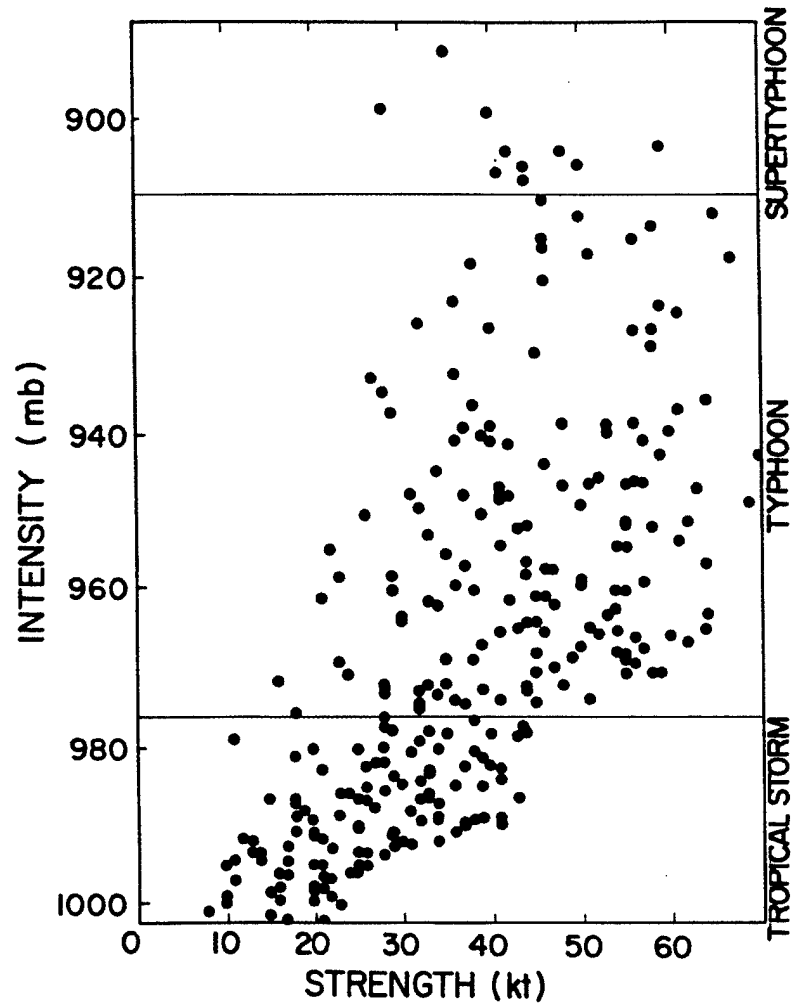
Figure 3.9: Wind strength (mean tangential wind between 1-2.5° radius) versus intensity (minimum sea-level pressure) for tropical cyclones. Note there is little correlation (from Weatherford and Gray 1985).
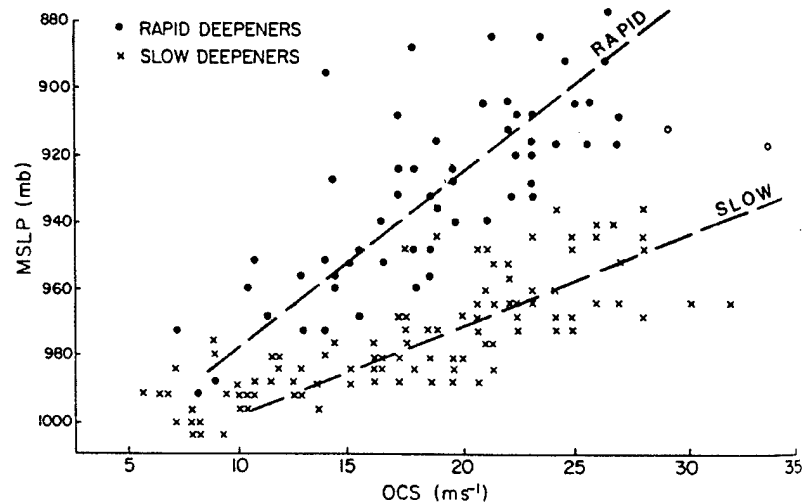
Figure 3.10: Wind strength (as OCS) versus minimum pressure for rapid and slow deepeners (from Weatherford and Gray 1989).

Croxford and Barnes (2000) also found that strength and intensity were poorly correlated with the intensity of 19 Atlantic tropical cyclones. Their analysis of aircraft reconnaissance data gathered by Hurricane Research Division within NOAA/AOML offered higher resolution (0.5 km) but the same conclusions. Hurricanes Frederic (79) and Diana (84) (shown in Fig. 3.11) had similar maximum tangential wind (V_T and yet their integrated total strength values are significantly different. Figure 3.12 shows Hurricane Diana's radial tangential wind for 9 August 1984, and then again three days. Diana's strength was relatively the same on both days, but the maximum tangential velocity on the 12th is nearly twice that than on the 9th. These are further examples where strength and intensity are uncorrelated.

3.5 Variability of the Eye and Its Characteristics

The eye is a basic characteristic of hurricanes-typhoons. The eye indicates that a cyclone has reached hurricane stagae. As observed from aircraft, satellite, and radar, the
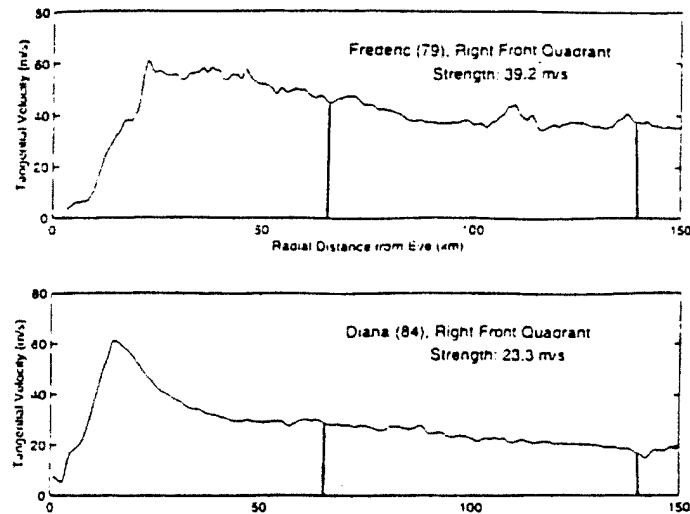
Figure 3.11: Radial profiles of storm-relative tangential velocity (m/s) in the right front quadrants of Hurricanes Diana (84) and Frederic (79) (from Coxford and Barnes 1998)

size and shape of the eye can vary through time as the storm matures and eventually weakens. Figure 3.15 gives typical eye classifications including circular, concentric, and elliptical eyes. The circular eye case has been dubbed as "annular hurricanes" by Knaff et al. (2001); concentric eyes are commonly referred to as double eyewall systems.

Measured as maximum sustained winds for Atlantic storm (based on best track data from 1995-1999) the eye forms when maximum winds are about 85 knots (Zehr, personal communication). Zehr based his eye versus non-eye criteria on infrared satellite imagery. Warm pixels signifying the presence of subsidence in the center. The following sections discuss the distinct ways in which the eye of a cyclone can vary.

3.5.1 Eye Diameter Variability

The satellite observed diameter of the eyes of a tropical cyclones is typically between 30 and 45 n mi (55-85 km) (Weatherford and Gray 1985) but can range from an aircraft-observed small value of 8 n mi (15 km) of Typhoon Tip (JTWC 1979), to as large as 200 n

EYEWALL SHAPES

CIRCULAR   CONCENTRIC   ELLIPTICAL
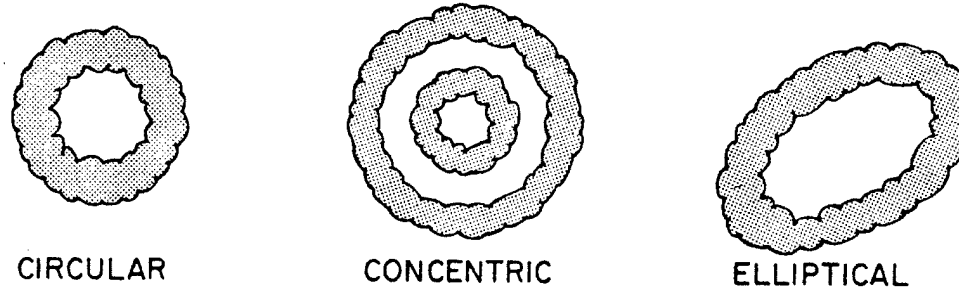
Figure 3.12: The different classifications of eye types (from Weatherford and Gray 1985).

mi (370 km) for the radar-observed eye diameter of Typhoon Carmen (1960) as it passed over Okinawa (Lander 1999). In this study, an eye is considered small for diameters less than 30 n mi (55 km) and large for diameters greater than that.

Lander (1999) conducted a case study on Supertyphoon Winnie (August 1997). Winnie passed over Okinawa with a complete ring of deep convection of nearly 200 n mi (370 km) diameter. The MSLP observed at Kadena AB, Okinawa was 964 hPa with gusts up to 82 kts as the center of the storm passed 80 n mi (150 km) south. The maximum winds and minimum sea level pressure for this storm are not known but, based on NEXRAD base velocity products, the maximum winds probably did not exceed 85 knots. This example is important since Winnie had concentric eyewalls and may have been going through an eyewall replacement cycle (Willoughby et al. 1982, 1990) at the time. The Dvorak technique has no rules for concentric eyes which can cause unrepresentative intensity estimates. Figure 3.17 is a Doppler radar picture concentric eyewalls for Hurricane Luis showing similar concentric eye features.

3.5.2 Eye Size and Intensity

Numerous studies have been conducted on the size of the eye in attempts to correlate eye size with intensity and/or as an aid in forecasting cyclone tendency. Weatherford and Gray (1985) used aircraft data collected from 1979-1986 from the Northwestern Pacific
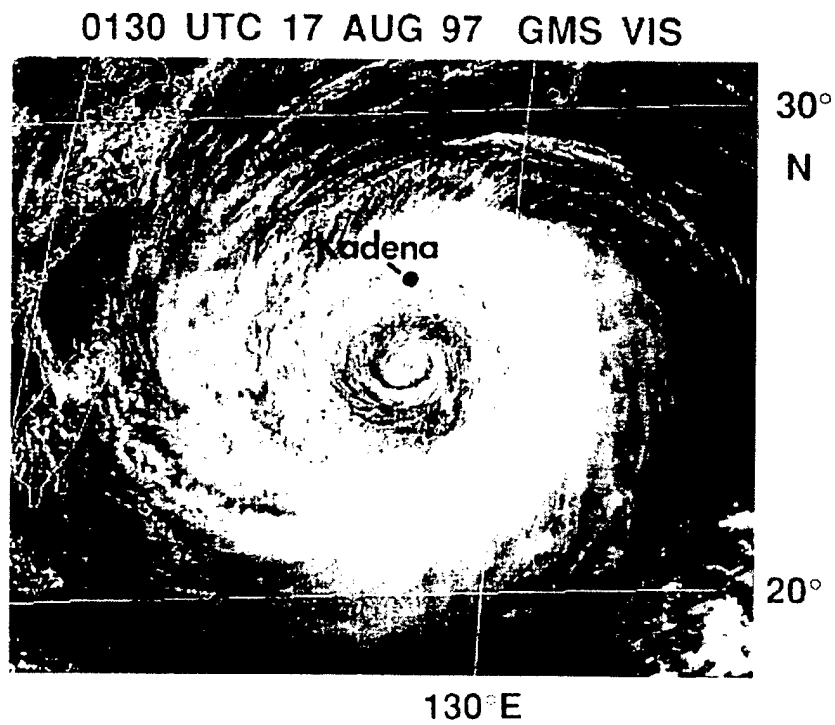
Figure 3.13: Satellite image of Typhoon Winnie (1997) as it passes south of Okinawa, Japan. Note the concentric eyewalls with a very large radius (from Lander 1999).
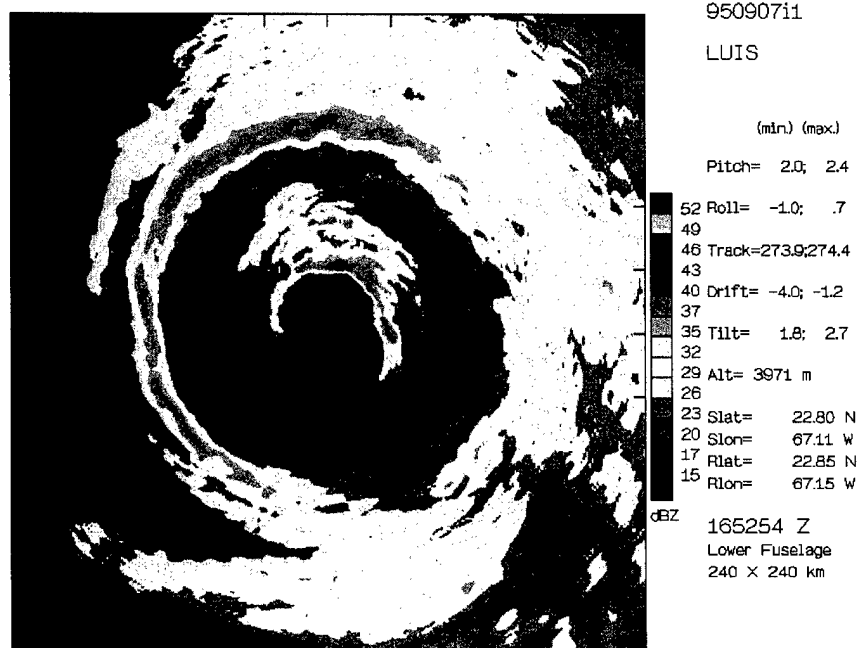
Figure 3.14: Doppler radar picture of Hurricane Luis' with concentric eyewalls in the Atlantic basin on 7 September 1995.

storms to compile a data set with eye size, intensity, and strength. Eye size was determined as the radius of the eye reported by aircraft, intensity was measured as minimum sea-level pressure and cyclone strength was determined from winds as described previously. Figure 3.18 summarizes the eye size distribution and corresponding eye classes used in their study.
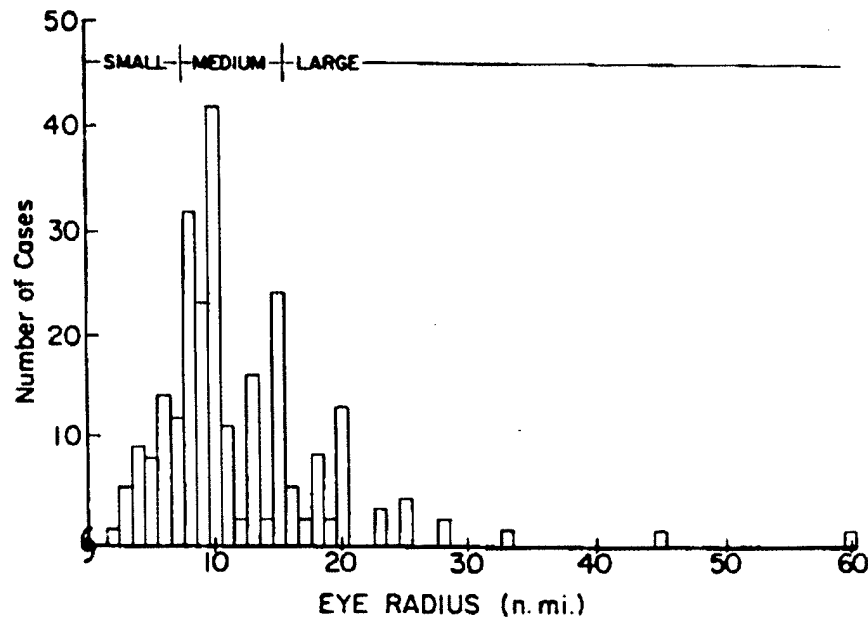
Figure 3.15: Eye size distribution and corresponding eye classes (from Weatherford and Gray 1985)

Figure 3.19 shows that there is little if any correlation between eye radius and intensity. There tends to be a large scatter of intensities for a given eye size, especially for smaller eyes and it would be difficult to use these data to estimate the intensity of a storm based solely on its eye size.

Although Weatherford and Gray found little correlation between eye size and intensity, they were able to show a relationship between the rate of intensity change and outer-core strength. They separated eye sizes into small (radius 2 to 7.5 n mi), medium (radius 8 to 15 n mi), and large (radius 15.5 to 60 n mi) to investigate relationships between eye size, intensity, and strength. Looking at the cases for small eye versus no eye in Figure 3.20, we infer that a storm with similar central pressure will have greater strength if no eye, or a larger eye exists. Also, cyclones with equal strength tend to be more intense
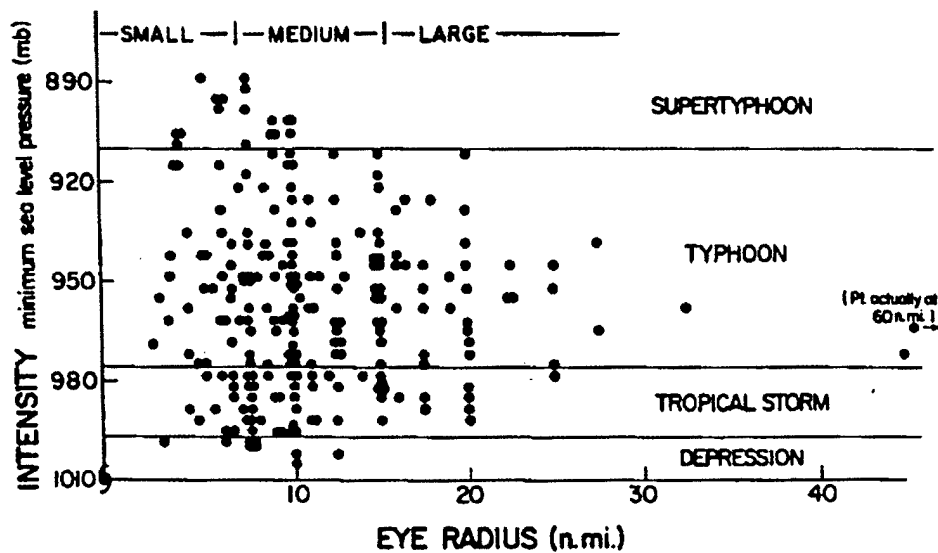
Figure 3.16: Eye size versus intensity (from Weatherford and Gray 1985).

with smaller eyes. This latter association is significant when attempting to forecast the outer winds of a storm that is over the open ocean when no data other than satellite are available.

3.5.3 Large Central Cold Cover

Lander (1999) showed an example of a typhoon with an extremely large Central Cold Cover (CCC). According to Dvorak (1984), the CCC pattern is defined when a more or less round, cold overcast mass of high could cirrus covers the TC center which obscures the expected signs of pattern evolution. The CCC spreads out from the inner core where there is an explosive growth of deep convection, and obscures the core and primary rain bands of the TC. The presence of a CCC signals an interruption in the development of the TC.

Lander's best example of this rare event was Typhoon Gloria, 1996 (Fig. 3.21). After showing few signs of significant development during the day of 23 July, an enormous CCC developed over Gloria's center close to local midnight. By that time the average diameter of the area within which the cloud-top temperature was at or below −70°C it was about 780
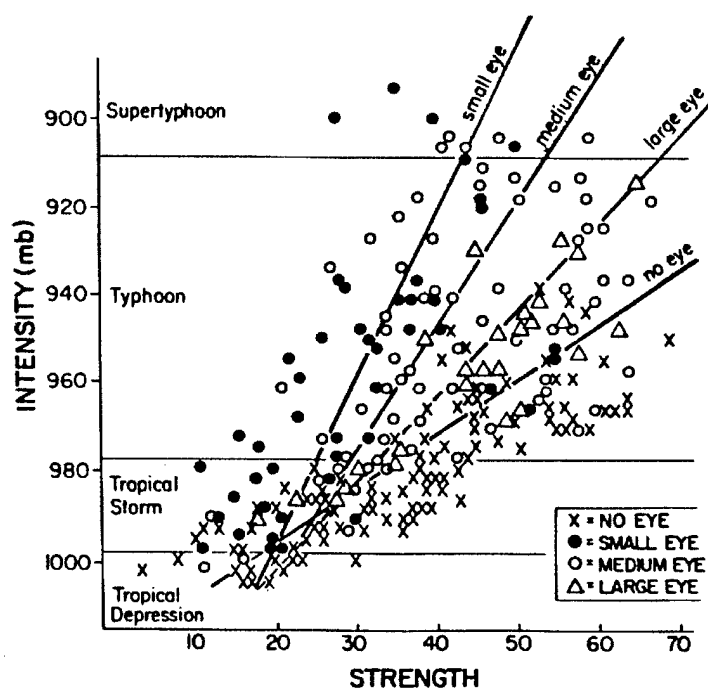
Figure 3.17: Intensity versus strength differs by eye class. Small eye: 0-7.5 n mi; Medium eye: 7.5-15 n mi; Large eye: 15-60 n mi (from Weatherford and Gray 1985
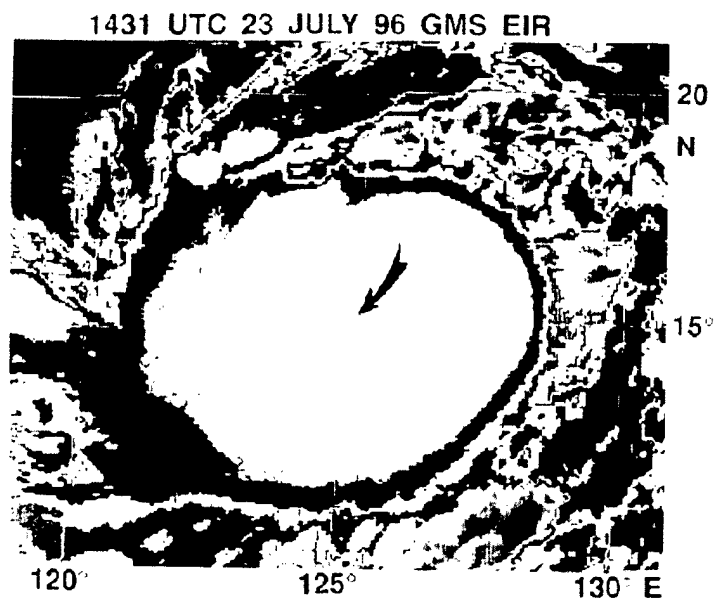
Figure 3.18: Infrared satellite image of Typhoon Gloria (1996) with "MB" curve enhancement. Arrow indicates the location of the coldest temperature of -100°C (from Lander 1999).
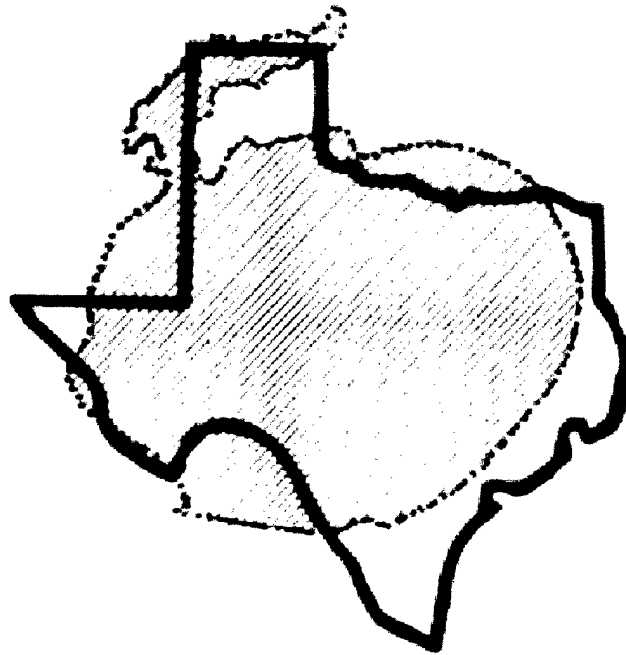
Figure 3.19: Gloria's Central Cold Cover (CCC) compared to the size of the state of Texas. The shaded region is the area at or below −70°C (from Lander 1999).

km in diameter, or almost the size of Texas (Fig. 3.22). Lander provides evidence that the storm intensified only slowly during this period. This is surprising since the cloud features underwent such an impressive change. Dvorak's belief that a CCC, no matter how large it may be, is not a sign of explosive intensification, but rather an arrestment in development is still accepted.

3.5.4 "Annular" Hurricane

Knaff et al. (2001) examined a select set of storms observed in the Atlantic and Pacific basins with large symmetric cloud shields and eyes (see Fig. 3.23). He refers to these storms as "Annular Hurricane".

These storms are unique not only because of their annular appearance but because they generally possess no banding features, sustain their intensity for only a few days, and usually exist in waters below 28.5°C. Though there are only a few cases of these storms during the past five years, they pose a forecast challenge due to the fact that they appear after peak intensity, and seem to go through a weakening period before intensifying and
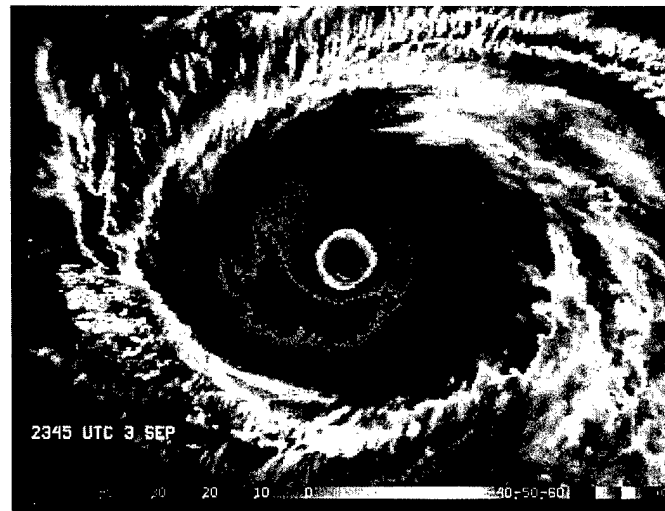
Figure 3.20: Satellite picture of annular hurricane Luis (from Knaff 2001).

forming a large eye and thereby going against current forecast logic. Figure 3.24 is a composite time series of tangential wind, relative to the time of the maximum intensity of the average hurricane that did not encounter cold water or make landfall reported by Emanuel (2000) and the average annular hurricane from Knaff (2001). Tangential wind is normalized by mean maximum intensity. Notice how the annular hurricane maintains a strong intensity after the maximum intensity has been reached.

3.6 Life Cycle Variability

Tropical cyclones that only develop into comparatively weak hurricanes or typhoons usually go through a deepening period, then weaken and fill. The variability of the storms behavior during these two periods is not so well understood. Kubat and Gray (KG) (1995) and Weatherford and Gray (1985) investigated different aspects of tropical cyclone behavior during this portion of the typical life cycle and came up with distinct differences in wind field and characteristics.

Weatherford and Gray (1985 1989) describe the typical events of a tropical cyclone as it deepens, reaches a maximum intensity, and then weakens, or fills (see Fig. 3.25). They investigated inner and outer core wind strength (OCS) during different stages of the storms' life cycle, concluding that the storms' structure changes as it goes through its
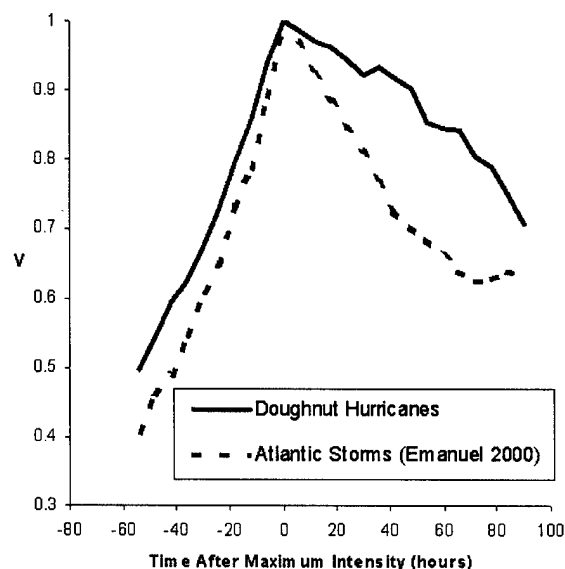
Figure 3.21: Composite time series relative to the time of maximum intensity, of the intensity associated with average Atlantic hurricanes that did not encounter cold water or make landfall (56 cases) as reported by Emanuel (2000) and annular hurricanes, normalized by mean maximum intensity (from Knaff 2001).

life cycle. They divide life cyclones into three phases (Figs. 3.25 and 3.26). Phase one is described as an intensification period where both the inner and outer core intensify. Phase two follows with the inner core weakening while the outer core continues to strengthen. Phase three concludes all intensification with weakening of both the inner core and outer core areas.

Figure 3.27 offers a depiction of the tangential wind field of a typical storm during intensifying versus filling periods. Note that the intensifying storms have higher maximum winds and lower outer core strength while the filling storms' outer core strength is greater but with a lower maximum wind. This condition will be discussed further in the next chapter where an adjustment to the wind-pressure relationship will be recommended for the Atlantic basin.

The magnitude of the differences between deepening and filling storms is more apparent in comparisons of radial kinetic energy difference between filling and deepening storms (Fig. 3.28). An increase of kinetic energy up to 60 percent in the outer radii occurs with

THE LIFE CYCLE OF THE TYPHOON

Figure 3.22: Con WIND cyclone. From W SPEED ... typical tropical
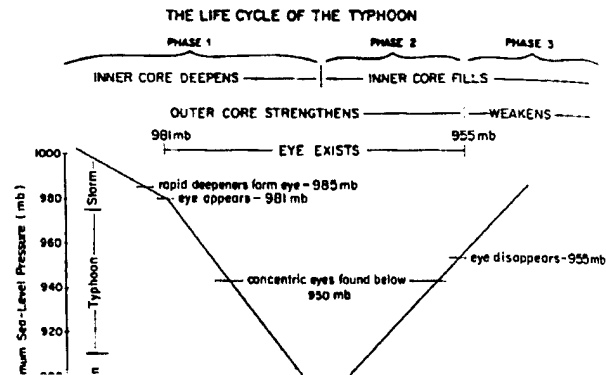
PHASE 1
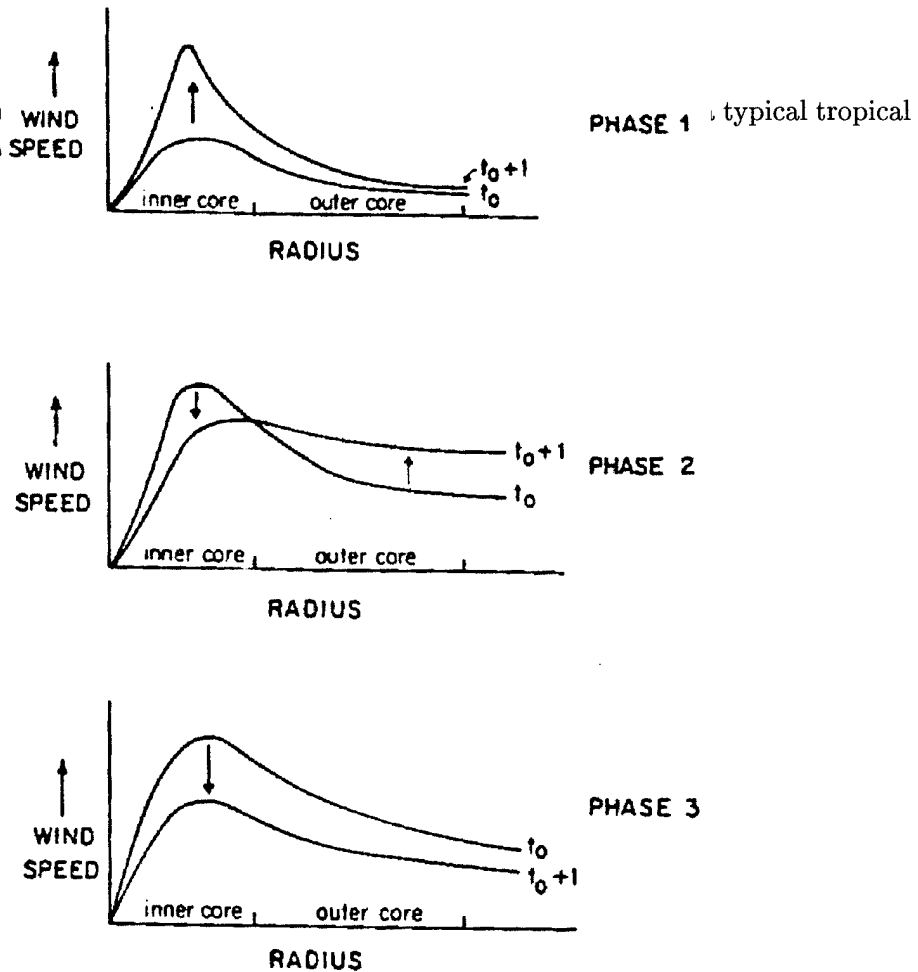
PHASE 2

PHASE 3

Figure 3.23: Schematic of the three phase life cycle of cyclone wind profiles: In phase 1 the inner core intensifies as the outer core strengthens; phase 2, inner core fills as the outer core strengthens; phase 3, the inner core fills as the outer core weakens. From Weatherford and Gray (1989)
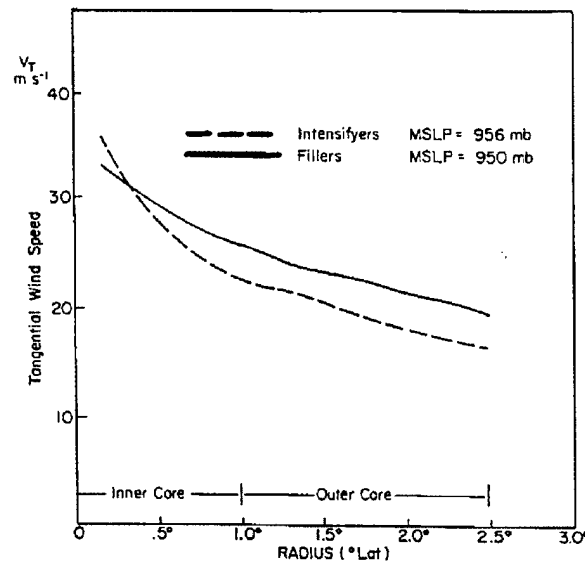
Figure 3.24: Radial profiles of azimuthally-averaged tangential winds for intensifying (dashed) and filling (solid) cyclones of the same MSLP. Note the max winds are greater for an intensifying storm (from Weatherford and Gray 1989).

the typical filling cyclone, revealing an increase in outer core strength at the expense of the inner core.

It is important to know about these typical structure changes during the cyclone's life cycle.

3.7 Variabilities Revealed by GPS Dropwindsondes

The role of aircraft reconnaissance entered a new era with the development of the National Center for Atmospheric Research (NCAR) GPS dropwindsonde program. The GPS dropwindsonde, as described in Chapter 2, has revealed structure and variability of surface wind speeds in tropical cyclones that were not measured accurately by previous dropwindsonde systems. The accuracy of wind estimates are 0.5 to 2.0 m/s (Hock and Franklin, 1998) with vertical resolution as small as 5 m.

Black and Franklin (1999) first noted the great variability in GPS dropwindsonde measurements at the 10m height above the ocean. Results shown in Figs. 3.29 and 3.30
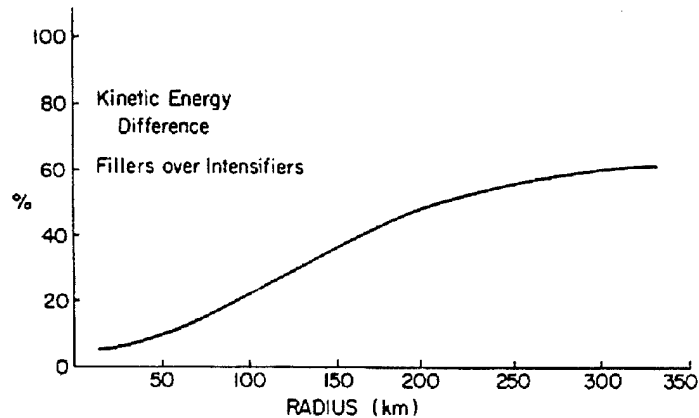
Figure 3.25: Kinetic energy differences between fillers and intensifiers (from Weatherford and Gray 1989).

reveal the difficulties with estimating the surface winds based on the 700 mb and 850 mb winds above, the technique currently used operationally in the Atlantic basin. The two examples, from Hurricanes Erika (1997) and Linda (1997), in Fig. 3.29 shows three vertical wind profiles measured at roughly simultaneously three different areas of the eyewall. Whereas winds are similar at 1500m the surface winds vary considerably. On the other hand, Fig. 3.30 shows two vertical wind profiles which have similar surface winds but very different winds aloft. The two examples in Figs. 3.29 and 3.30 reveal some of the uncertainty in making accurate surface wind estimates from typical reconnaissance flight level winds.

3.8 Summary

The examples of studies and data from this chapter exemplify the need for a wind-pressure relationship that can account for all the changes a storm goes through during its life cycle. The wind-pressure tables used by the Dvorak technique, and depended
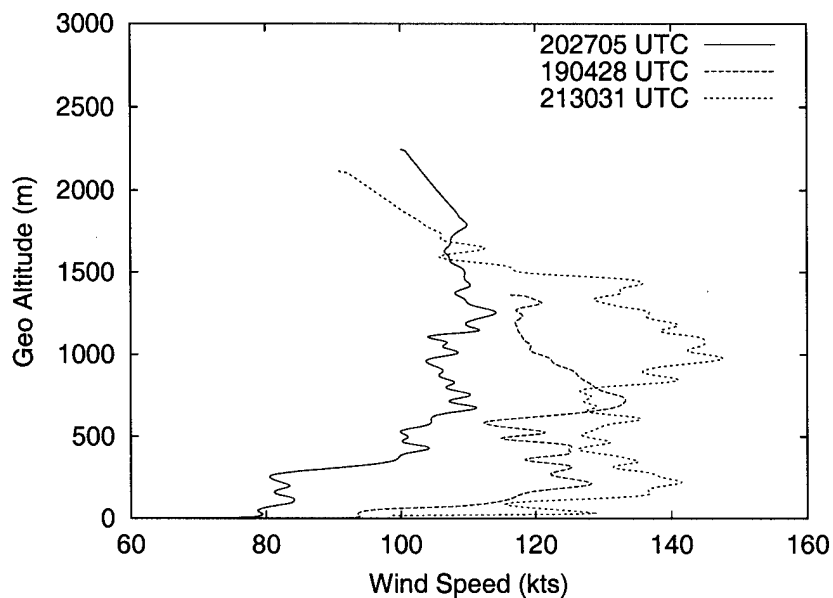
Figure 3.26: Wind speed profiles from the eyewall of Hurricane Erika, from 1904-2130 UTC 8 September 1997. From Franklin et al., 1999
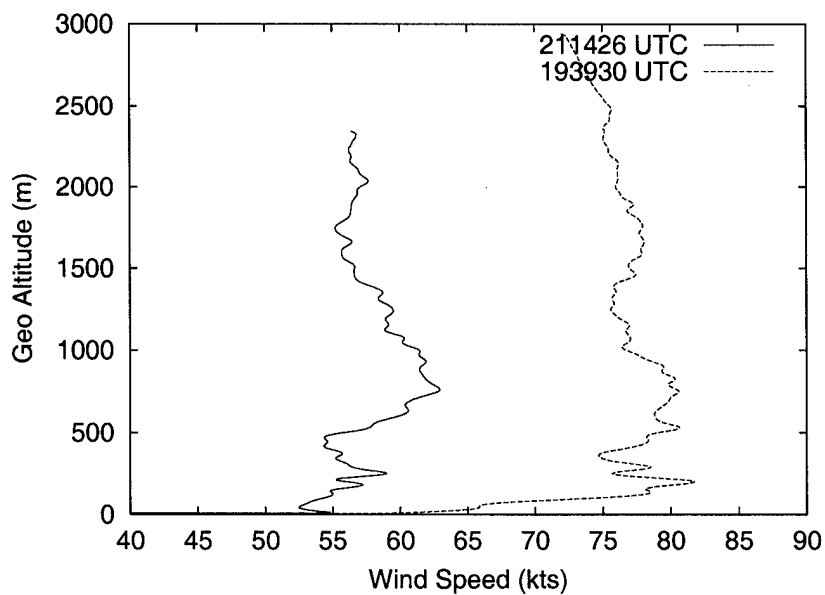
Figure 3.27: Wind speed profiles from the eyewall of Eastern Pacific Hurricane Linda on 14 September 1997. From Franklin et al., 1999.

on by tropical forecasting agencies all over the world, do not account for any range of possible values of wind or pressure that a tropical cyclone can have. The recent GPS dropsonde data has revealed the difficulty in estimating maximum surface winds from aircraft measured maximum flight level winds. MSLP can be measured accurately by aircraft, while maximum surface winds continue to be difficult. The wind-pressure tables need to be updated in order to improve the conversion of winds to pressure, or vice versa.

Chapter 4

PREVIOUS RESEARCH AND RESULTS

4.1 Introduction

The most important and sought after characteristic of tropical cyclones excepting location is intensity. Diagnosing the intensity of tropical cyclones over the open ocean is extremely difficult. Much of this difficulty lies in the large variability of the maximum surface wind relationship with Minimum Sea Level Pressure (MSLP), storm size, inner-core wind strength, outer winds, eye characteristics, etc. Concerning maximum sustained surface wind (V_m) and MSLP of tropical cyclones in the North Atlantic and NW Pacific it will be shown that a single "universal" V_m versus MSLP relationship cannot be assumed. A set of relationships which account for life cycle and latitude among other variables needs also to be consulted. Relationships between these two variables will demonstrate how the lack of aerial reconnaissance impedes analysts' ability to fully accommodate diverse individual storm V_m versus MSLP. Information from both ocean basins include best track (BT) data, aircraft vortex messages, and Dvorak intensity estimates.

4.2 Previous Research on MSLP Versus Wind Structure Relationships

4.2.1 The Atlantic Basin

Previous studies on the relationship between maximum wind and MSLP in Atlantic tropical cyclones include Takahashi (1939), Kraft (1961), Wang (1978), Holland (1980), Vickery et al. (2000), Landsea et al. (2000), among others. Kraft, whose relationship is operationally employed by the Miami Tropical Prediction Center (NHC), developed his association from 14 1950s tropical storms and hurricanes that passed over or near observation stations on the coastal United States. Kraft analysis improved on Takahashi's

earlier study wherein Kraft used V_m and MSLP recorded in the eye and eye-wall cloud of 14 cyclones. He obtained the following relationship:

$$V_m = 14(1013 - P_c)^{0.5} \tag{4.1}$$

or,

$$P_c = -((V_m/14)^2) + 1013 \tag{4.2}$$

where V_m is the maximum surface wind in knots and P_c is the minimum sea level pressure in millibars. His study did not take into account either the life cycle or location of the storm, but consisted entirely of data points for each storm's maximum intensity. The relationship developed by Kraft is still used today in the North Atlantic as the primary tool for converting minimum sea level pressure to maximum winds when reliable wind and pressure measurements near the center are unavailable.

Holland (1980) proposed a new analytic model of the radial profile of the relationship between pressure and tangential winds. Holland's model was superior to the prior relationships but required data that often can only be measured by aircraft reconnaissance. His model was able to account for differing radial pressure profiles and thus different radial wind profiles. He found that when the model was applied to pressure profiles, it could not resolve very strong pressure gradients over small distances and supergradient winds could not be accommodated. The model's inability to resolve the eyewall or radius of maximum winds resulted in underestimates of maximum winds. It is difficult to apply Holland's model when accurate environmental pressure and reconnaissance data are not available, and hence is difficult to apply operationally.

Landsea et al. (2001) have been engaged in a cyclone re-analysis project for the North Atlantic hurricane database. They are tracing cyclone tracks and intensity observations back into the 19th Century. They find that Kraft's wind-pressure relationship does not accurately depict all storms in all locations and have chosen to separate the Atlantic basin into different latitudinal areas and to include a special relationship for the Gulf of Mexico. Their maximum wind and MSLP data came from the Atlantic hurricane database, 1970-

1997. The latter were separated into data bases for four areas. This leads to the following set of best-fit equations for the areas as indicated:

Gulf of Mexico, sample size 664:

$$V_m = 10.63(1013 - P_c)^{0.56} \tag{4.3}$$

, or

$$P_c = -((V_m/10.63))^{1.77} + 1013 \tag{4.4}$$

South of 25N, sample size 1033:

$$V_m = 12.02(1013 - P_c)^{0.53} \tag{4.5}$$

, or

$$P_c = -((V_m/12.02))^{1.89} + 1013 \tag{4.6}$$

25 - 35N, sample size 922:

$$V_m = 14.17(1013 - P_c)^{0.48} \tag{4.7}$$

, or

$$P_c = -((V_m/14.13))^{2.08} + 1013 \tag{4.8}$$

35 - 45N, sample size 492:

$$V_m = 16.09(1013 - P_c)^{0.43} \tag{4.9}$$

, or

$$P_c = -((V_m/14.13))^{2.33} + 1013 \tag{4.10}$$

These four curves and the Kraft curve (i.e., from Fig. 1) are shown in Fig. 4.1. The Kraft relationship best matched Landsea et al.'s mid-latitude representation for TCs of below hurricane intensity and for TCs at southerly latitudes for hurricane winds. They found that the Kraft formula over-estimates wind speeds for mid- and high latitude hurricanes. Kraft's curve would assign a 960 mb hurricane 102 kt sustained surface winds, which is quite close to the 100 kt estimated by Landsea's Gulf of Mexico and low latitude relationships. On the other hand, Landsea's mid-latitude and high latitude equations suggest 94 and 90 kts, respectively, concluding that wind speeds for a given central pressure
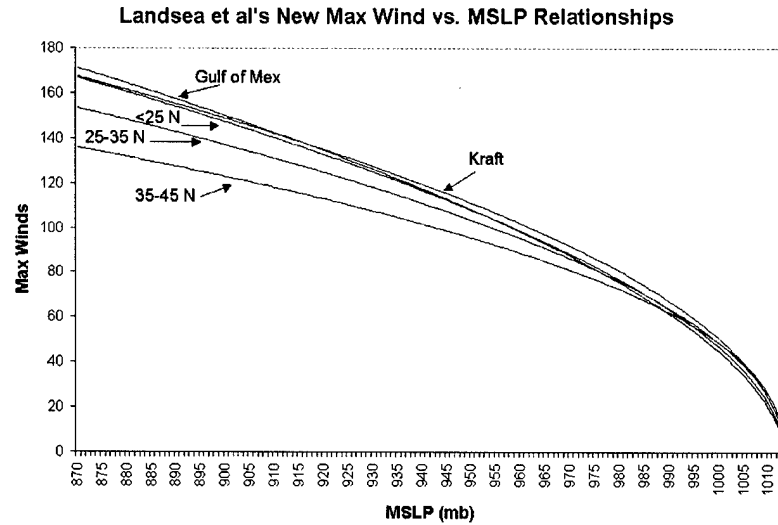
Figure 4.1: Landsea et al.'s adjusted curves of V_m versus MSLP for different latitudes. The Kraft curve is overlayed.

decrease for increasing latitudes (except for the Gulf of Mexico). This topic is treated later in this chapter.

4.2.2 Northwest Pacific

Takahashi's (1939) wind-pressure relationship was the first developed for typhoons in the NW Pacific basin using wind data from ships and island stations near or in Japan. He often had to interpolate and/or use a simple model to estimate central pressure. Although an improvement for its time, Takahashi's relationship can be improved upon using more recent data. In studies at the Joint Typhoon Warning Center (JTWC), Guam, particularly by Atkinson and Holliday (1977). Takahashi's original equation was modified several times during the next 35 years to include latitudinal variations and aircraft reconnaissance data. Atkinson and Holliday (AH) eventually developed an equation using more extensive and accurate NW Pacific wind measurements from aircraft, observation stations, buoys, and ships. In these studies AH did rigorous adjustments for anemometer heights and gust

measurements to standardize all the data. The resulting equation obtained for the NW Pacific basin is given by Eqs. 4.11 and 4.12.

$$V_m = 6.7(1010 - P_c)^{0.644} \qquad (4.11)$$

or,

$$P_c = (-V_m/6.7)^{1.553}) + 1010 \qquad (4.12)$$

The value of 1010 mb appears to be representative of the environmental pressure in the western NW Pacific area. Somewhat different standard pressure values are appropriate in other basins. The appropriate Atlantic mean environmental pressure, for example, is known to be 3 to 5 mb higher than this (1010 mb) value. This relationship in Eqs. 4.11 and 4.12 is currently used by Joint Typhoon Warning Center (JTWC), and by other international meteorological agencies in the Eastern Hemisphere. Since aircraft reconnaissance no longer occurs in any of the Eastern Hemisphere, the AH curve is greatly relied upon for analyzing and verifying maximum surface winds and minimum sea level pressure values.

Lubeck and Shewchuck (1980) conducted a study to test and verify the Atkinson and Holliday database by analyzing 13 new storm cases not in the original data set. They also attempted to correct the curve by adjusting the 10-minute averaged maximum winds assumed by Atkinson and Holliday to 1-minute averaged winds used by the NPC in the Atlantic and by including variable environmental pressure and latitude parameters. The additional data made little difference in the original curve and they concluded that the Atkinson and Holliday curve was indeed representative of conditions in the NW Pacific basin.

4.3   New Results for the Atlantic Basin

Observations for nineteen hurricanes from Atlantic best track and aircraft fix (1995–1999) data sets were used in this study to examin variability in the relationship between maximum surface wind V_m and MSLP for different portions of a life cycle and for different latitudes. Aircraft fix data were also used to make similar comparisons V_m to MSLP with

varying eye sizes. Table 4.1 lists the number of cases used from the Atlantic best track and aircraft fix data.

Table 4.1: Number of cases from the Atlantic 1995-1999 best track data set and aircraft vortex message archives (Large Eye and Small Eye) used for the sustained surface maximum wind versus minimum sea level pressure study.

	Number of Samples
All	2358
Deepening	468
Filling	381
Large Eye	93
Small Eye	177

4.3.1 Life Cycle

Concepts relating to variability of a storm's maximum sustained surface wind (V_m) during its intensifying and filling stages were introduced in the previous chapter. Weatherford and Gray (1985) and Kubat (1995) noted that V_m tends to be greater for a given minimum sea level pressure (MSLP) as a cyclone intensifies versus when it weakens. Figure 4.2 is a depiction of maximum sustained surface wind versus MSLP for all best track data points from 1995-1999 irrespective of intensity. The Kraft relationship for the Atlantic Ocean is also shown. Tables 4.2 and 4.3 display the large range of MSLPs for a given V_m (up to 60 mb in extreme cases), as well as ranges of V_m for a given MSLP (up to 65 kts). Note that the more extreme ranges occur at lower intensities while at higher intensities, the relationship is less variable.

Table 4.2: Range of MSLP for given V_m for 90% and 50% of the cases for all Atlantic storms, 1995–1999.

V_m (kts)	MSLP 90% (mb)	Range (mb)	MSLP 50% (mb)	Range (mb)
60	960-1000	40	975-990	15
80	955-995	40	965-980	15
100	935-965	30	945-960	15
120	925-955	30	930-940	10
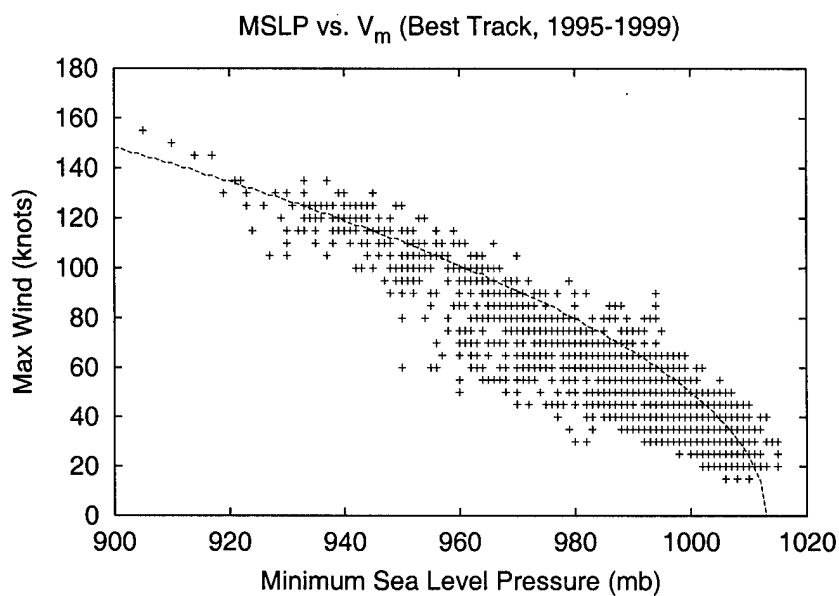
Figure 4.2: Atlantic best track MSLP for 1995-1999 in mb versus maximum sustained surface winds (V_m) in knots for all cases. Dashed line is the Kraft (1961) curve.

Table 4.3: Range of V_m for given MSLP for 90% and 50% of the cases for all Atlantic storms 1995–1999.

MSLP (mb)	V_m 90% (kts)	Range (kts)	V_m 50% (kts)	Range (kts)
1000	25-60	35	35-55	20
980	40-85	45	50-70	20
960	60-120	60	75-100	25
940	95-135	40	105-120	15
920	120-150	30	125-140	15

Figure 4.2 suggests that one single relationship may not account for the variability of maximum wind versus MSLP for all storms. In order to investigate this further, the cyclones were broken into intensifying and filling categories. Cyclones that did not have definite intensifying and filling periods, or that did not intensify into hurricanes, were not included. All landfall points were also excluded so as to emphasize representative points over the open ocean. Figure 4.3 shows the maximum surface wind versus MSLP for intensifying storms while Fig. 4.4 shows the same data but for weakening storms. Note how the filling storms have a wider range of values than intensifying storms for given MSLP and V_m (see Tables 4.4–4.7). The range of MSLP for intensifying storms and a given V_m varies from 15–30 mb for 90 % of the cases, while the range for filling storms was from 35–40 mb. By eliminating 50 % of the cases, these ranges decrease significantly although there are still significant differences for each. In filling storms the Kraft curve overestimates wind speeds for a given MSLP while intensifying storms lie closer to the Kraft curve. This result verifies Kubat and Gray (1995) who also found that maximum wind (V_m) for a given MSLP tend to be lower for weakening than for intensifying storms. The average wind deviation for a given pressure from the Kraft curve for deepening storms was 6.5 knots while the deviation for filling storms was 12.8 kts.

Figure 4.5 shows a plot of the maximum winds versus MSLP when the same storms were at their maximum intensity. Note how the points fit the curve very well and there is less spread in the data points. These points have the same criteria that Kraft used when he initially set up the curve using storm data at their maximum intensity.

Table 4.4: Range of MSLP for given V_m for 90% and 50% of the cases for Atlantic data (1995–1999).

V_m (kts)	MSLP 90% (mb)	Range (mb)	MSLP 50% (mb)	Range (mb)
60	980-1000	20	985-995	10
80	965-980	15	965-975	10
100	945-965	20	950-960	10
120	920-950	30	935-945	10
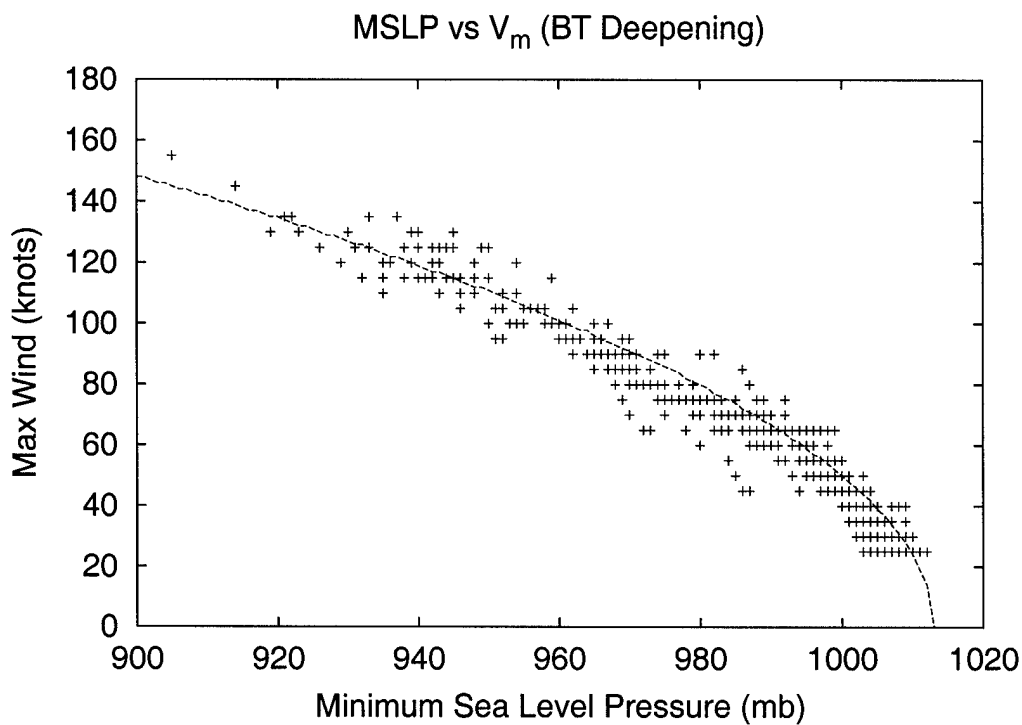
Figure 4.3: Atlantic best track MSLP for 1995-1999 in mb versus V_m in knots for intensifying storms. Kraft's relationship (1961) is shown by the dashed line.
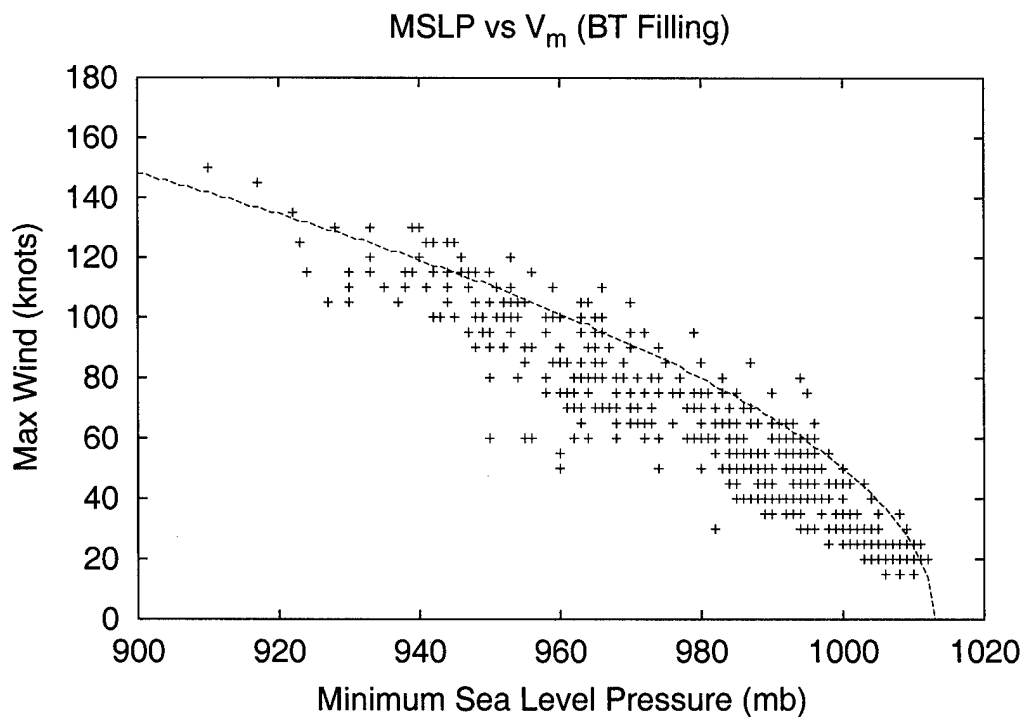
Figure 4.4: Atlantic best track MSLP for 1995-1999 in mb versus V_m in knots for weakening storms. Kraft's relationship (1961) is shown by the dashed line.
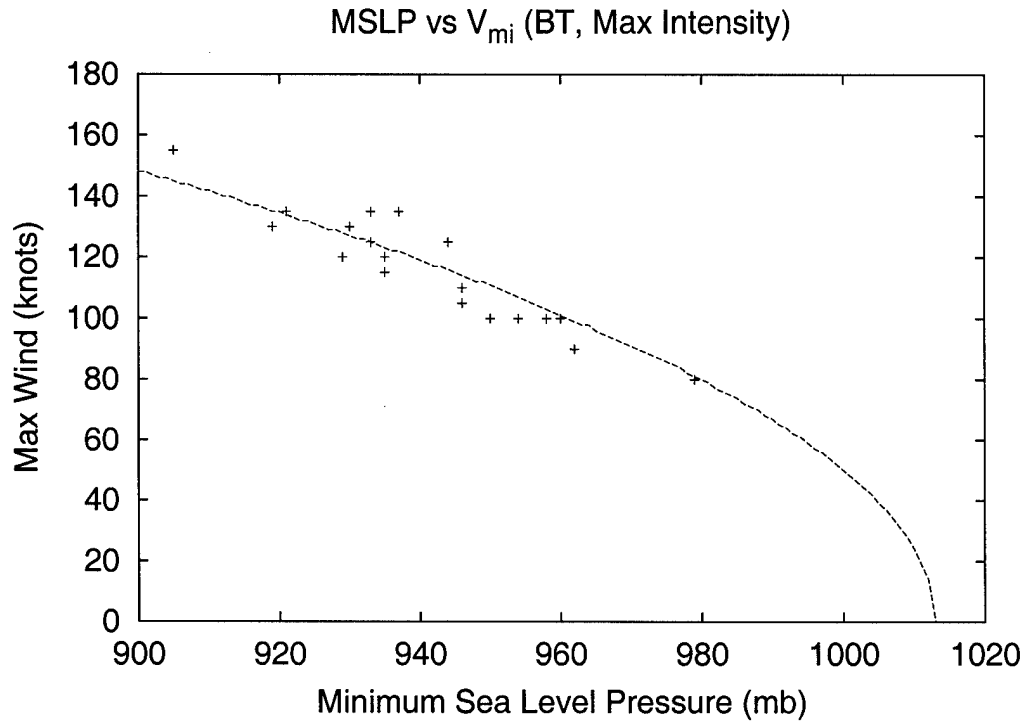
Figure 4.5: Atlantic best track MSLP for 1995-1999 in mb versus V_m at max intensity (V_{mi}) in knots. Kraft's relationship (1961) is shown by the dashed line.

Table 4.5: Range of V_m for given MSLP for 90% and 50% of the cases of deepening Atlantic storms for 1995–1999.

MSLP (mb)	V_m 90% (kts)	Range (kts)	V_m 50% (kts)	Range (kts)
1000	35-60	25	40-50	10
980	60-85	25	65-75	10
960	90-115	25	95-105	10
940	105-130	25	115-125	10
920	120-150	30	130-140	10

Table 4.6: Range of MSLP for given V_m for 90% and 50% of the cases of filling Atlantic storms for 1995–1999.

V_m (kts)	MSLP 90% (mb)	Range (mb)	MSLP 50% (mb)	Range (mb)
60	965-1000	35	975-990	15
80	950-990	40	955-970	15
100	930-970	40	940-955	15
120	920-955	35	930-940	10

Table 4.7: Range of V_m for given MSLP for 90% and 50% of the cases of filling Atlantic storms for 1995–1999.

MSLP (mb)	V_m 90% (kts)	Range (kts)	V_m 50% (kts)	Range (kts)
1000	25-50	25	30-40	10
980	45-80	35	60-70	10
960	65-105	40	80-95	15
940	100-130	30	105-120	15
920	115-145	30	125-135	10

Figure 4.6 depicts a composite graph centered on the time of maximum intensity for the 19 storms used in the life cycle comparison. The two curves in Fig. 4.6 include the best track minimum sea level pressure (solid line) and the maximum sustained surface winds converted to pressure values using Kraft's relationship (dashed line). If the Kraft relationship were used exclusively to convert MSLP to V_m, or vice versa, the two lines would overlap. Note the average difference between the Kraft pressure and best track MSLP for intensifying storms is 3.8 mb whereas the difference for filling storms is 9.5 mb. This net difference between the intensifying versus filling storms is almost one half of a Dvorak T number.

4.4 Adjustments to the Kraft Relationship

The results just presented show clearly that deepening versus filling storms have significant differences in their minimum pressure-maximum wind relationships and the relationships for both cases differ from the Kraft curve. For the Atlantic 1995–1999 best track data, the absolute average difference from the Kraft curve for intensifying storms was 6.5 knots while the average difference for the filling storms was 12.8 knots. Forecasters and analysts must be aware of and effectively account for these differences when preparing products for their area of responsibility.

One obvious solution is to restructure the Kraft curve for each of these modes of variability using subsets of the data. Figure 4.7 shows how a cyclone "filling" relationship better fit the data points, but still does not account for the wide spread of values. The
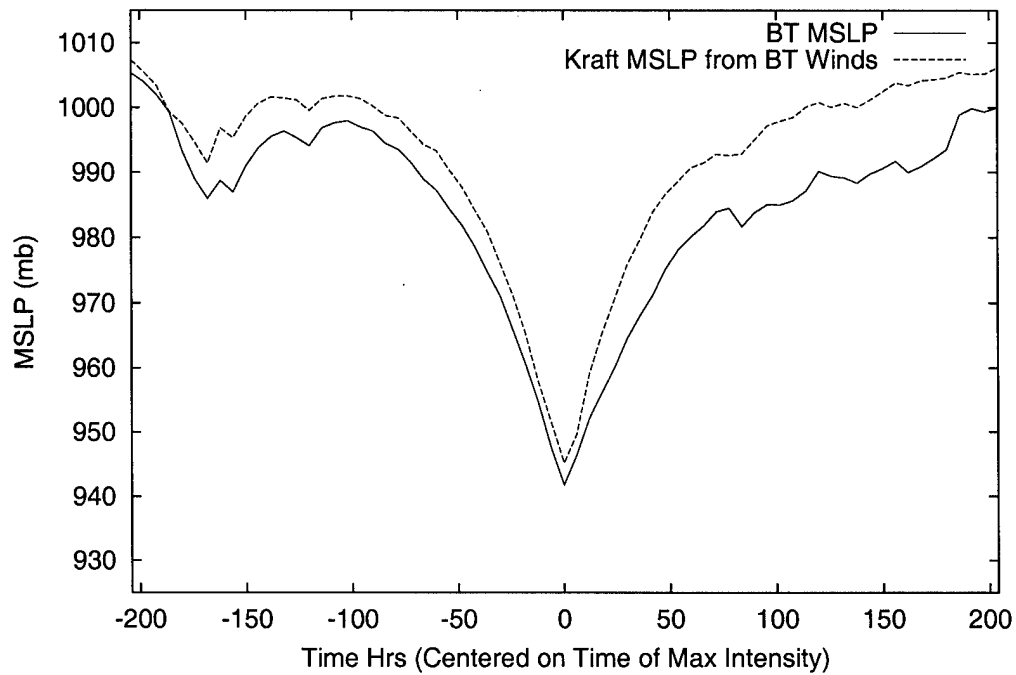
Figure 4.6: Composite (time-centered on maximum intensity) of 1995-1999 Atlantic best track minimum central pressure (solid line) and minimum central pressure from best track winds derived using Kraft relationship (dashed line). Note that on average at a given pressure weaker winds occur for filling storms versus intensifying storms.

similar regression curves for the deepening storms followed closely Kraft's curve although slight differences occur for the more intense stages (see Table 4.8 and Figure 4.8).

The new best fit equations, in the same form as derived by Kraft, are as follows:

Deepening Equations:

$$V_m = 10.62(1013 - P_c)^{0.56} \tag{4.13}$$

$$P_c = (-V_m/10.62)^{1.78} + 1013 \tag{4.14}$$

Filling Equation:

$$V_m = 7.28(1013 - P_c)^{0.629} \tag{4.15}$$

$$P_c = (-V_m/7.28)^{1.59} + 1013 \tag{4.16}$$

The improvement of these new relationships over the Kraft curve, especially for the filling storms is summarized in Tables 4.9 and 4.10. The average absolute difference for

Table 4.8: Maximum sustained surface winds (kts) and corresponding MSLP (mb) for Kraft, deepening, and filling relationships for the Atlantic basin. Corresponding Dvorak current intensity numbers are in the far left column.

CI Number	MWS (knots)	MSLP (Kraft)	MSLP (Deepening)	MSLP (Filling)
1	25 K			
1.5	25 K			
2	30 K	1009 mb	1007 mb	1005 mb
2.5	35 K	1005 mb	1005 mb	1002 mb
3	45 K	1000 mb	1000 mb	996 mb
3.5	55 K	994 mb	994 mb	990 mb
4	65 K	987 mb	988 mb	982 mb
4.5	77 K	979 mb	979 mb	972 mb
5	90 K	970 mb	968 mb	960 mb
5.5	102 K	960 mb	957 mb	948 mb
6	115 K	948 mb	944 mb	933 mb
6.5	127 K	935 mb	930 mb	918 mb
7	140 K	921 mb	915 mb	902 mb
7.5	155 K	906 mb	895 mb	881 mb
8	170 K	890 mb	874 mb	859 mb
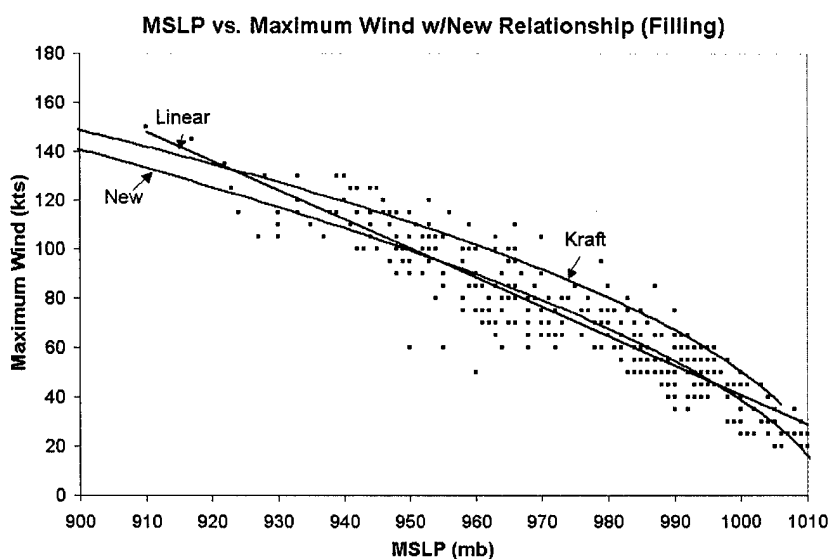
Figure 4.7: Atlantic best track MSLP (mb) for 1995-1999 versus maximum sustained surface winds (kts) for filling storms. The Kraft, best fit linear regression, and new non-linear regression curves are overlayed.

filling storms was reduced from 12.8 to 8.3 knots while the average absolute difference

for deepening storms was reduced slightly from 6.5 to 5.1 knots. Figure 4.8 presents a

comparison of the curves for the new relationships versus Kraft. The new filling curve

shows the lower wind speeds expected for a filling versus an intensifying storms for the

same pressure. These results will discussed further in section 4.4.3.

Table 4.9: **Deepening Storms**: The average absolute difference for the maximum sustained surface winds and minimum sea level pressures from the Kraft and new best-fit curves for the Atlantic 1995-1999.

	Kraft	New Deepening Equation
Avg Diff (kts)	6.5	5.1
Avg Diff (mb)	4.4	3.6

Table 4.10: **Filling Storms**: The average absolute difference for the maximum sustained winds and MSLP from the Kraft and new best-fit curves for the Atlantic 1995–1999.

	Kraft	New Equation
Avg Diff (kts)	12.8	8.3
Avg Diff (mb)	9.6	7.0

4.4.1 Latitudinal Variations

Results showing the tendency for filling storms in the Atlantic basin to occur at

higher latitudes than do intensifying storms are summarized in Figs. 4.9 and 4.10. The

average latitude of the 1995–1999 best track deepening storm data points was 18° North

while the average latitude for filling storm data points was 33° North. The deepening

storms generally intensify over open water in the southern latitude belts where the water

is warmer, there is less vertical wind shear, and conditions are generally more favorable

for development. Conversely, filling storms are typically recurving and moving northward

towards cooler water when where there is greater vertical shear and hence, much less

favorable conditions for maintenance of high wind speeds near the center. Latitudinal

variations are discussed in the next section.
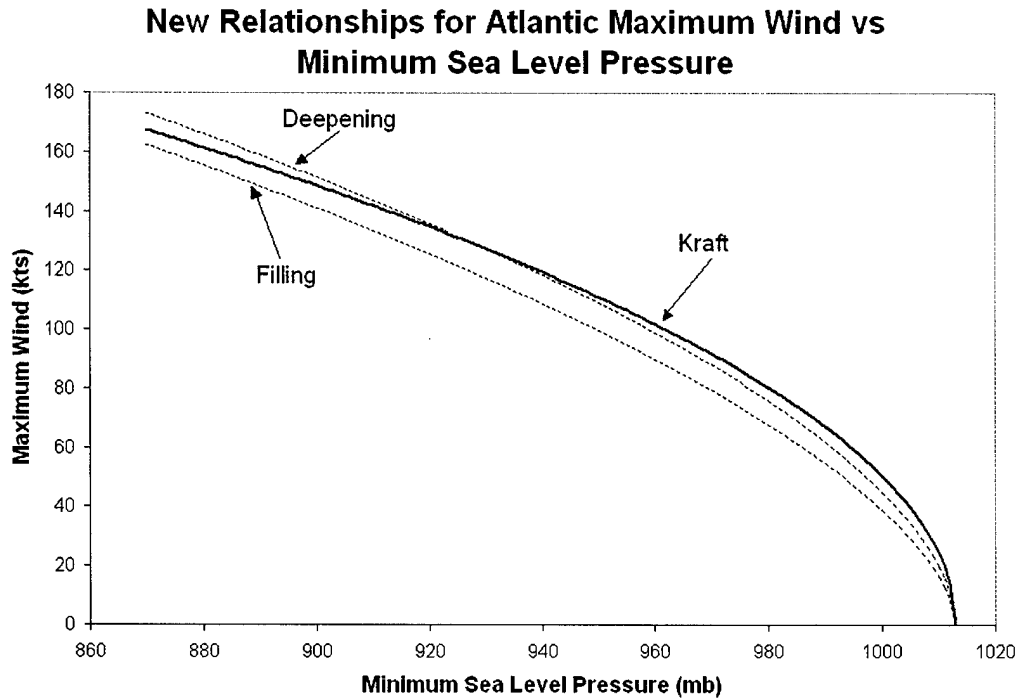
Figure 4.8: Comparative plots of the new non-linear regression curves for deepening and filling storms with Kraft curve overlayed. Note the drop in maximum winds at a given pressure for the filling relationship.
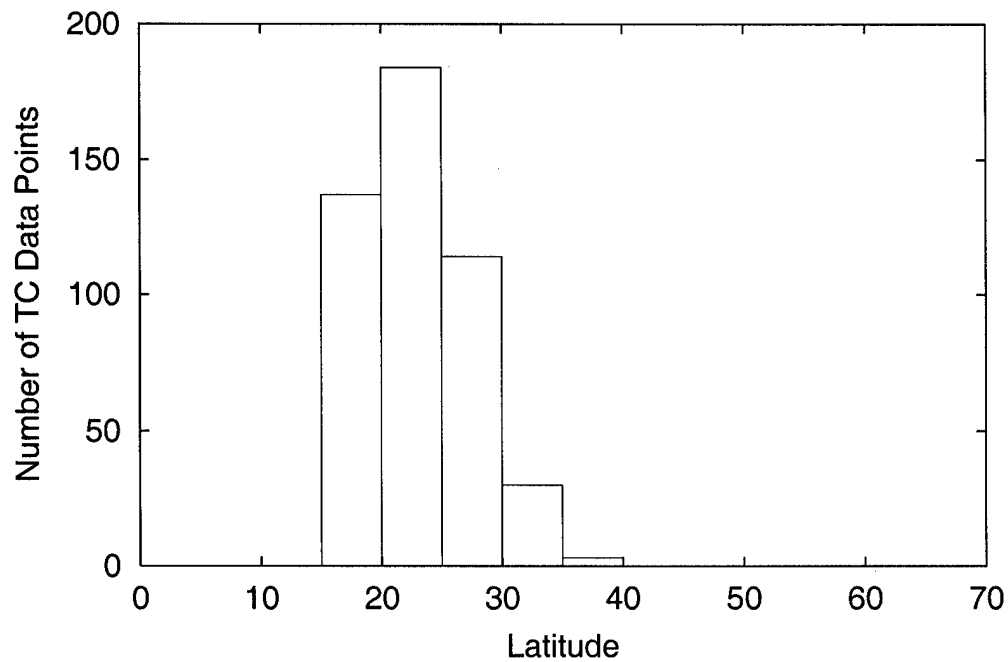
Figure 4.9: Number of Atlantic deepening data points per 5 degree latitude belt in 1995–1999 best track data.
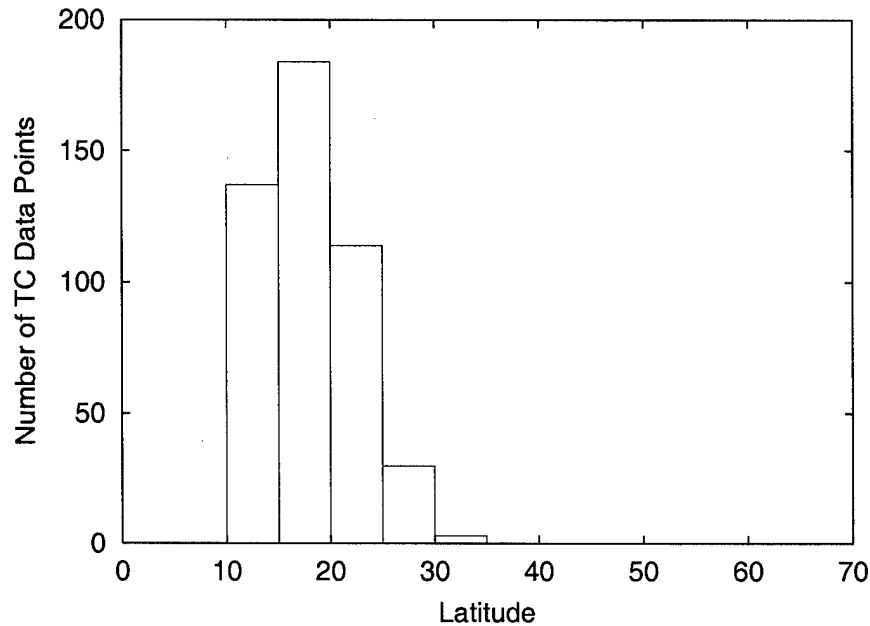
Figure 4.10: Number of Atlantic filling data points per 5 degree latitude belt in 1995–1999 best track.

4.4.2 Comparison With New Work By Landsea et al.

Landsea et al. separated Atlantic tropical storms into groups by latitude and Gulf of Mexico. For the present study, filling, intensifying, and "all other" classes of storms (eg., steady-state) were grouped into the same latitude areas prescribed by Landsea et al. Gulf of Mexico storms were not considered separately in this study. We next stratify our data to see if Landsea et al. latitudinal maximum wind (V_m) versus minimum sea level pressure (MSLP) relationships can be further adjusted when the cyclone's life cycle is also accounted for.

Figure 4.11 depicts the V_m versus MSLP for deepening storms separated according to Landsea et al's latitudinal criteria. All 19 storms were observed to deepen south of 25° latitude while only 7 continued to deepen as they moved North from 25 to 35° latitude. There were no deepening storms north of 35°. All the curves fit the data points well for all cases. The only substantial discrepancy between the relationship curves is for storms located 25-35° wherein Landsea et al's curve shows a weaker wind for a given pressure at the higher intensities. For storms less than 25°, all three deepening storm curves
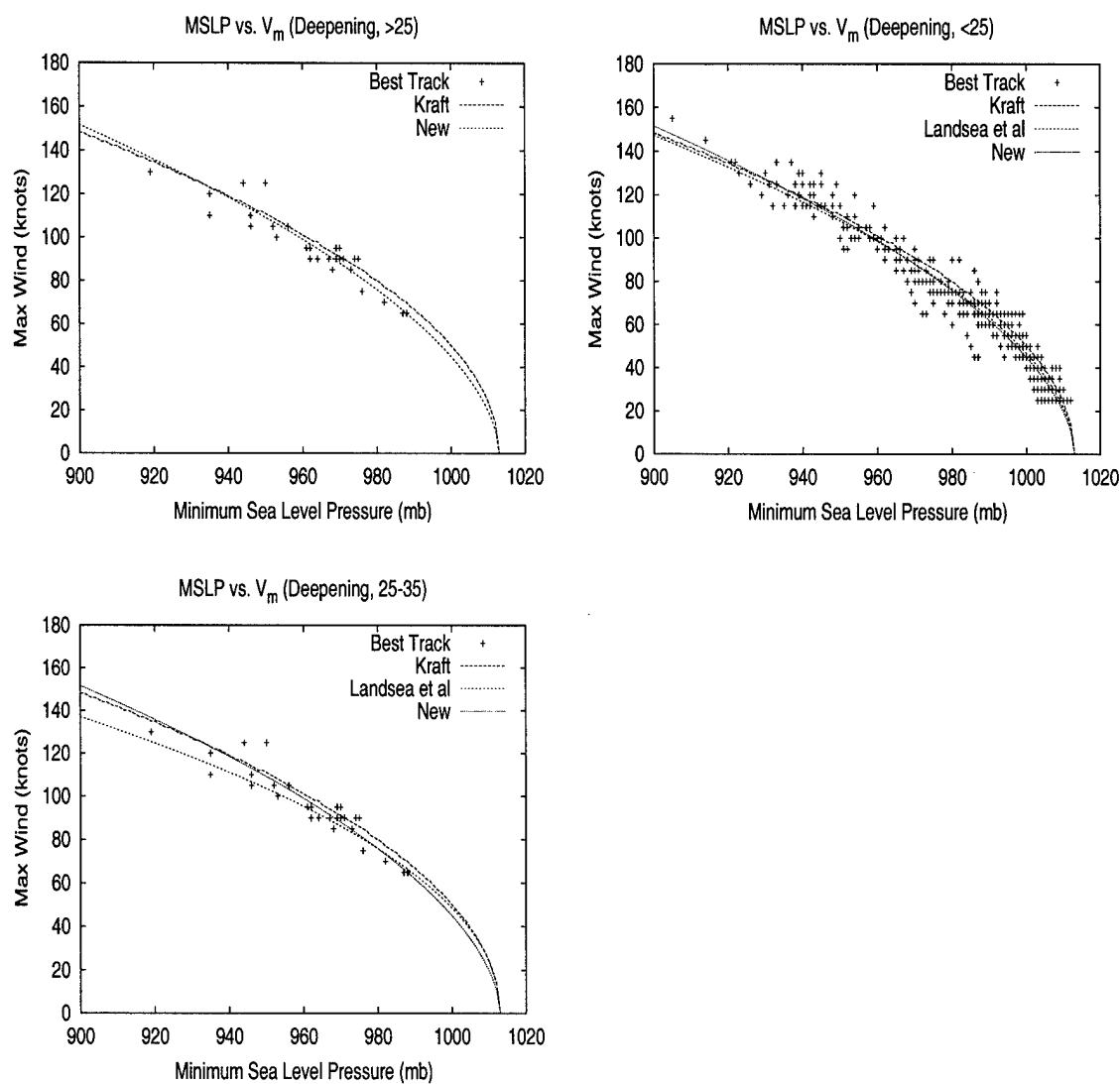
Figure 4.11: North Atlantic best track (1995-1999) MSLP versus. V_m for deepening storms located >25° (top left), < 25° (top right), and between 25 and 35° (lower left). Kraft (1961), Landsea et al. (2001), and this study's new deepening relationships are overlayed.

appear representative. Additional years of data need to be added to the analysis before conclusions are made for that latitudinal belt, but the following best-fit equation has been made using this data set for deepening storms located 25-35°:

Deepening Equations (25–35 °):

$$V_m = 12.999(1013 - P_c)^{0.510} \tag{4.17}$$

$$P_c = (-V_m/12.999)^1.96 + 1013 \tag{4.18}$$

Figure 4.12 shows V_m versus MSLP for filling storms, separated according to Landsea et al's criteria. Only 9 storms were observed south of 25°, whereas 17 between 25 and 35°, and 15 were located between 35 and 45°. Looking at the upper left panel in Fig. 4.12 for storms north of 25° the filling relationship developed for this study fits those points quite well. On the other hand, the upper right panel for storms south of 25° shows that the filling equation derived here underestimates (V_m) for a given MSLP while both Landsea et al's and Kraft's curves fit the winds somewhat better, except at weaker intensities. The life cycle linked relationships fit the data points better at higher latitudes as shown in the lower two panels. The latter is a consequence of filling storms at lower latitudes maintaining slightly higher V_m for given MSLP than do filling storms at higher latitudes. Landsea et al's curve for filling storms north of 25° would overestimate winds, thus the following filling relationships derived here is more representative:

Filling Equations (25–35°):

$$V_m = 7.294(1013 - P_c)^{0.627} \tag{4.19}$$

$$P_c = (-V_m/7.294)^1.60 + 1013 \tag{4.20}$$

Filling Equations (35–45°):

$$V_m = 9.223(1013 - P_c)^{0.544} \tag{4.21}$$

$$P_c = (-V_m/9.223)^1.84 + 1013 \tag{4.22}$$
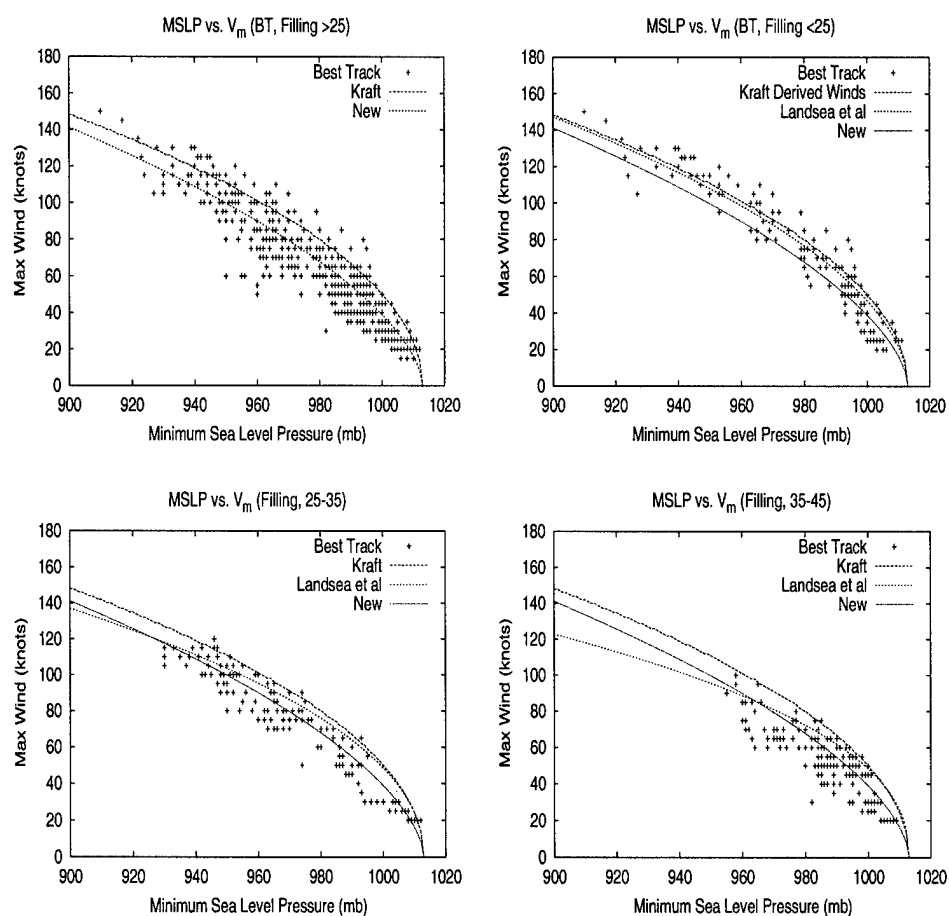
Figure 4.12: As in Fig. 4.11 and 4.12 but for North Atlantic best track (1995-1999) MSLP versus V_m for filling storms located $>25°$ (top left), $<25°$ (top right), between 25 and 35° (lower left), and between 35 and 45° (lower right). Kraft (1961), Landsea et al. (2001), and the new filling relationships from this study are overlayed.

4.4.3 Interpretation and Discussion

In general we observe that filling storms with the same minimum sea level pressure as deepening storms will have lower maximum winds. To explain this observation, it becomes necessary to explore the average characteristics of filling versus deepening storms. In general, filling storms have greater outer wind strength (Weatherford and Gray 1985), are further north or moving towards more northerly latitudes, have encountered cooler waters and/or westerly shear and have decreasing winds and pressure gradients.

The gradient wind equation can explain the latitudinal variation of the pressure-wind relationship in terms of the opposing effects of the Coriolis parameter and changing pressure gradient following Kubat and Gray (1995). The gradient wind equation which balances the pressure gradient term, Coriolis parameter, and centrifugal forces is given by Eq. 4.17:

$$\nabla P = \frac{V^2}{R_r} + fV \tag{4.23}$$

where:

$\nabla P = \frac{-1}{\rho} \frac{\partial P}{\partial R}$

V = Wind velocity

R_T = Radius of the trajectory

f = Coriolis parameter ($2\Omega \sin \phi$)

For simplicity, the first term on the right side of the equation can be neglected. With the Coriolis effect held constant, weakening the pressure gradient term (i.e., by filling the eye or by having the TC expand) decreases the wind velocity. Likewise, holding the pressure gradient term constant while f increases as a storm moves poleward also results in slightly weaker wind velocity. As a TC moves north during phase 2 (see Fig. 3.26), and maintains constant MSLP, the wind velocity must decrease to maintain gradient wind balance.

4.4.4 Eye Size (Atlantic)
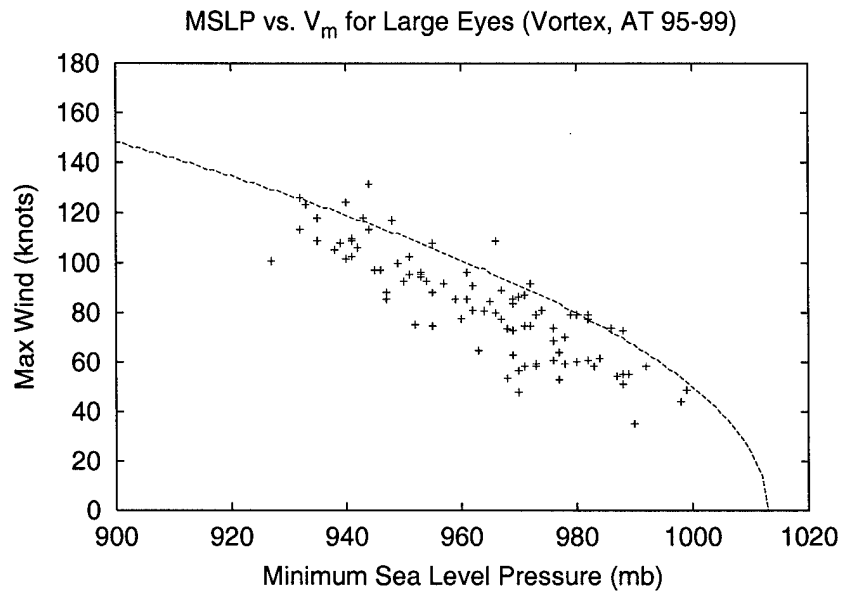
Figure 4.13: Atlantic vortex message MSLP (mb) for 1995-1999 versus maximum surface winds (kts) reduced from flight level for large eyes (radius greater than 27.5 km) at all time periods irrespective of intensity. Dashed line is the Kraft curve.

Figure 4.14: Atlantic vortex message MSLP (mb) for 1995-1999 versus maximum surface winds (kts) reduced from flight level for Small Eyes (radius less than 27.5 km) at all time periods irrespective of intensity. Dashed line is the Kraft curve.

We investigated the prospect that the V_m versus MSLP relationship might be refined by incorporating knowledge of the size of the eye. The eye radius for this study was determined from the long axis measurement made from aircraft reconnaissance. Following Lander (1999) an eye radius greater than 27.5 km was considered large and a radius less than 27.5 km was small. The minimum sea level pressure is as reported by aircraft reconnaissance and the maximum winds were extrapolated from flight level winds using the reduction factors recommended by Franklin et al. (2000). As can be seen in Figs. 4.14 and 4.15 and contrary to our expectations, variable eye size had very little impact on the overall relationship of minimum pressure and maximum winds of the storms. This non result also agrees with the findings of Weatherford and Gray (1985) wherein eye size was unrelated to intensity of the storm. Perhaps the only observation of note was that there was relatively more scatter for the small eye cases (see Tables 4.11–4.14). For example, for V_m equal to 100 kts, the corresponding MSLP's for large eyes ranged 35 mb, from 930 to 965 mb, while for small eyes the MSLP's ranged 45 mb, from 925 to 970 mb. Also, note that MSLPs lower than 930 mb were common only to small eyes.

Table 4.11: Summary of V$_m$ versus MSLP for Atlantic storms with large eyes reported by aircraft, 1995-1999. Range of MSLP for given V_m for 90% and 50% of the cases.

V_m (kts)	MSLP 90% (mb)	Range (mb)	MSLP 50% (mb)	Range (mb)
60	965-995	30	975-985	10
80	945-975	30	955-965	10
100	930-965	35	940-950	10
120	915-945	30	930-935	5

Table 4.12: Atlantic Storms with Large Eyes reported by aircraft, 1995-1999. Range of V_m for given MSLP for 90% and 50% of the cases.

MSLP (mb)	V_m 90% (kts)	Range (kts)	V_m 50% (kts)	Range (kts)
980	50-80	30	60-65	5
960	65-105	40	80-90	10
940	95-125	30	100-115	15
920	N/A	N/A	N/A	N/A

Table 4.13: Atlantic Storms with Small Eyes reported by aircraft, 1995-1999. Range of MSLP for given V_m for 90% and 50% of the cases.

V_m (kts)	MSLP 90% (mb)	Range (mb)	MSLP 50% (mb)	Range (mb)
60	955-990	35	970-985	15
80	940-975	35	950-965	15
100	925-970	45	930-950	20
120	915-950	35	920-930	10

Table 4.14: Atlantic Storms with Small Eyes reported by aircraft, 1995-1999. Range of V_m for given MSLP for 90% and 50% of the cases.

MSLP (mb)	V_m 90 (kts)	Range (kts)	V_m 50% (kts)	Range (kts)
980	40-80	20	50-60	10
960	60-100	40	70-90	20
940	80-125	45	90-110	20
920	110-140	30	120-130	10

4.4.5 Eye Size (Western North Pacific)

The findings for eye size as a factor in the wind-pressure relationship for the western North (NW) Pacific tropical basin were similar to those found for the North Atlantic. As shown in the Figs. 4.16 and 4.17 there is little difference in the wind-pressure relationship based on eye size alone. However, similar to the North Atlantic, the range of MSLP for a given V_m is greater for small eye versus large eye systems (see Tables 4.15-4.18). Also, the ranges are significantly greater for the Pacific than the Atlantic storms. Given a V_m, the NW Pacific MSLPs may range 45 to 70 mb, while in the Atlantic the MSLPs range was 35-45 mb under the same circumstances. Note also that large eye storms in the Pacific have far fewer occurrences of V_m greater than 120 kts and MSLP less than 920 mb compared to small eye storms.

4.5 Time Period Comparison: 1959-1999

Time period comparisons between the North Atlantic and NW Pacific basins were conducted to compare the intensity analysis trends during and after aircraft reconnaissance data were available in the western North (NW) Pacific tropical basin. The number of data

MSLP vs. V$_m$ for Large Eyes (Vortex, NW Pac 79-86)
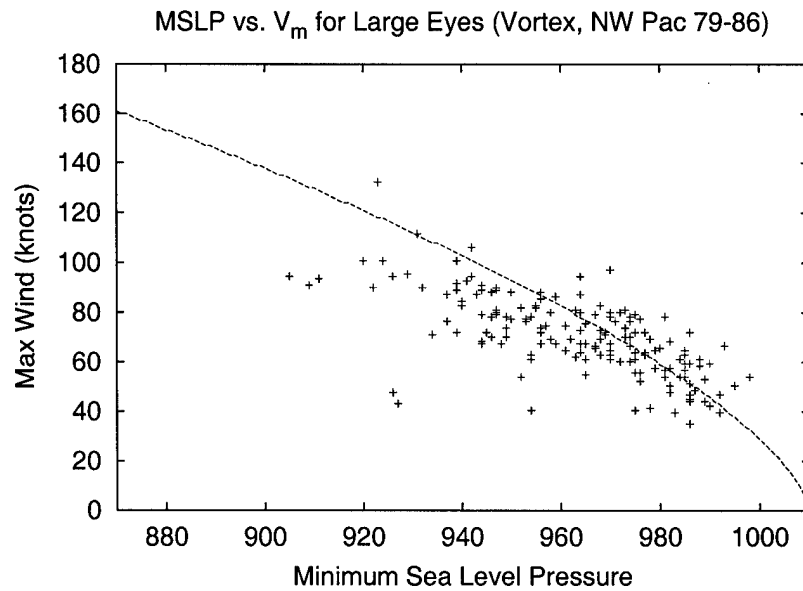
Figure 4.15: 1979-1986 Pacific vortex message MSLP (mb) versus V_m (kts) reduced from flight level for Large Eyes (radius greater than 27.5 km) at all time periods irrespective of intensity. The dashed line is the Atkinson and Holliday curve.
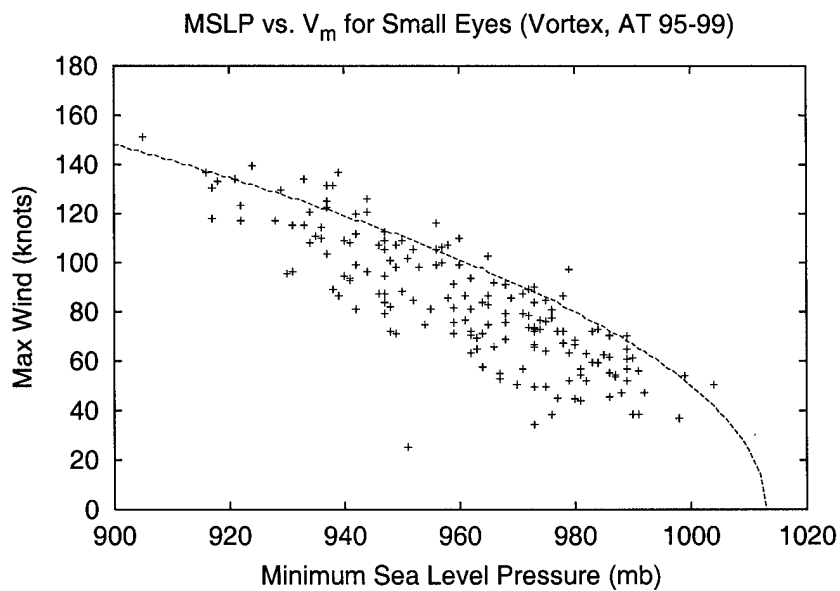
MSLP vs. V$_m$ for Small Eyes (Vortex, NW Pac 79-86)
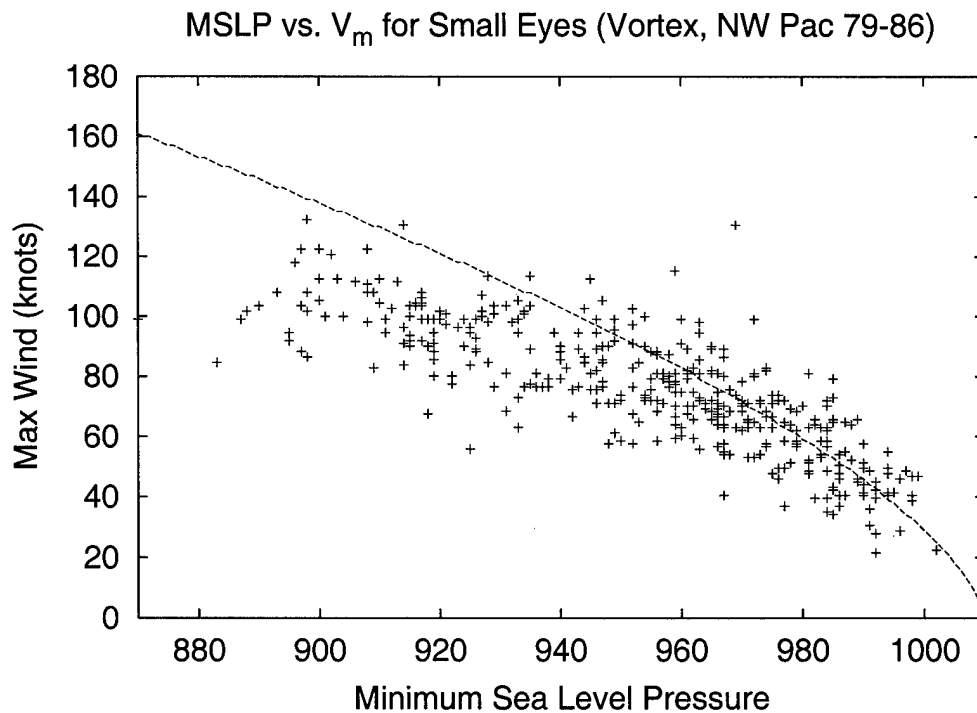
Figure 4.16: 1979-1986 Pacific vortex message MSLP (mb) versus V_m (kts) reduced from flight level for Small Eyes (radius less than 27.5 km) at all time periods irrespective of intensity. The dashed line is the Atkinson and Holliday curve.

Table 4.15: Pacific storms with large eyes as reported by aircraft, 1979-1986. Range of MSLP for given V_m for 90% and 50% of the cases.

V_m (kts)	MSLP 90% (mb)	Range (mb)	MSLP 50% (mb)	Range (mb)
60	950-990	40	965-980	15
80	920-975	55	940-955	15
100	900-940	40	920-935	15
120	N/A	N/A	N/A	N/A

Table 4.16: Pacific storms with small eyes as reported by aircraft, 1979-1986. Range of V_m for given MSLP for 90% and 50% of the cases.

MSLP (mb)	V_m 90% (kts)	Range (kts)	V_m 50% (kts)	Range (kts)
980	40-75	35	55-65	10
960	50-95	45	65-80	15
940	70-105	35	80-90	10
920	80-125	45	100-115	15

Table 4.17: Pacific storms with small eyes as reported by aircraft, 1979-1986. Range of MSLP for given V_m for 90% and 50% of the cases.

V_m (kts)	MSLP 90% (mb)	Range (mb)	MSLP 50% (mb)	Range (mb)
60	950-995	45	970-985	15
80	910-975	65	930-935	5
100	885-955	70	900-920	20
120	860-920	60	870-895	25

Table 4.18: Pacific Storms with large eyes as reported by aircraft, 1979-1986. Range of $V_{(m)}$ for given MSLP for 90% and 50% of the cases.

MSLP (mb)	V_m 90% (kts)	Range (kts)	V_m 50% (kts)	Range (kts)
980	40-80	40	50-65	15
960	60-100	40	65-80	15
940	70-105	35	80-95	15
920	80-125	45	90-105	15
900	85-140	55	100-115	15

points available for each basin, as summarized in Table 4.19 show that the NW Pacific has many more data points since it averages 18 typhoons a year while the North Atlantic averages only 6 hurricanes a season. Three study periods were designated as follows:

Period I: From 1959 to 1969 and hence, prior to the Atkinson and Holliday (AH) wind-pressure relationship being established, before use of accurate doppler or inertial navigation wind measuring devices, and when maximum winds were generally over-estimated in comparison with the comparatively accurate aircraft measured minimum sea level pressures (Figs. 4.18, 4.21 and 4.22).

Period II: From 1970 to 1986 when both Doppler determined winds and MSLP were simultaneously available. It was during these years that the AH relationship was established (Figs. 4.19, 4.23, 4.24).

Period III: Observation system again changed after 1986, so from 1987 to 1999, aircraft reconnaissance was no longer available and intensity estimates depended exclusively on satellite imagery which employed the Dvorak wind estimates and the AH relationship (Figs. 4.20, 4.25, 4.26).

The best track data set, which is compiled and maintained by The Joint Typhoon Warning Center (JTWC), consists of maximum sustained surface winds every 6 hours and MSLP for the time of maximum intensity. The JTWC maintains the MSLP only at maximum intensity in their best track owing to a lack of MSLP measurements in the data sparse area of responsibility. For this reason a life cycle based analysis for the Pacific data, similar to that done for the Atlantic in Section 4.3 was not possible. In view of the limitation of MSLP data in the NW Pacific to the time of maximum intensity only, a study of the variability of the relationship between maximum wind and MSLP at maximum intensity was done. For this the following definitions of terms is required:

V_m = Maximum Sustained Surface Wind Speed

V_{mi} = V_m at time of Max Intensity

$MSLP_{mi}$ = Minimum Sea Level Pressure (MSLP) at time of Max Intensity

V_{am} = Annual Average V_{mi}

$MSLP_{am}$ = Annual Average $MSLP_{mi}$

For the NW Pacific, the V_{mi} and $MSLP_{mi}$ were averaged for all storms occurring in each year, yielding a set of average annual maximum wind and minimum sea level pressure at maximum intensity (V_{am} and $MSLP_{am}$) for each year. As indicated in Table 4.19, these annual average data would not yield conclusive results for the Atlantic as there are so comparatively few hurricanes per year. Inspection of Figs. 4.18, 4.19, and 4.20, and Tables 4.20 and 4.21, indicates appreciable discrepancy in annual averages for the three periods designated previously. Notably, Period III closely matches the AH curve with an absolute average difference of only 1.7 knots from the curve. During Period II, when accurate wind measurements from aircraft were comparatively abundant, the annual averages show an appreciable range of variability, yet not so great as 1959-1969 owing to the constraints of the AH curve. It is interesting to note that each time period had a distinct range of intensities for average values.

Table 4.19: Number of samples for North Atlantic and NW Pacific V_{mi} and $MSLP_{(mi)}$ time period comparison.

Period	Atlantic	NW Pacific
I	56	213
II	64	266
III	80	237

Table 4.20: The average absolute difference of V_{am} and $MSLP_{am}$ from the Atkinson and Holliday curve per time period for the NW Pacific (typhoons only).

Period	Avg Diff Wind (kts)	Avg Diff Pressure (mb)
1959-1999	10.1	6.7
I	16.6	17.3
II	3.3	3.5
III	1.7	1.8

We also investigated the V_{mi} versus $MSLP_{mi}$ relationship for the North Atlantic in comparison with the NW Pacific for periods I, II, and III wherein the average absolute differences from each respective wind-pressure relationship were compared. While the

Table 4.21: The average absolute difference of V_{am} and $MSLP_{am}$ from the best-fit linear curve per time period for the NW Pacific (typhoons only).

Period	Avg Diff Wind (kts)	Avg Diff Pressure (mb)
1959-1999	5.5	14.0
I	6.9	26.1
II	3.2	9.2
III	0.4	0.5

Figure 4.17: $MSLP_{am}$ (mb) versus V_{am} for typhoons for Period I, 1959-1969, with best-fit linear regression and Atkinson and Holliday curves.

Figure 4.18: $MSLP_{am}$ (mb) versus V_{am} (kts) for typhoons for Period II, 1970-1986, with best-fit linear regression and Atkinson and Holliday curves.

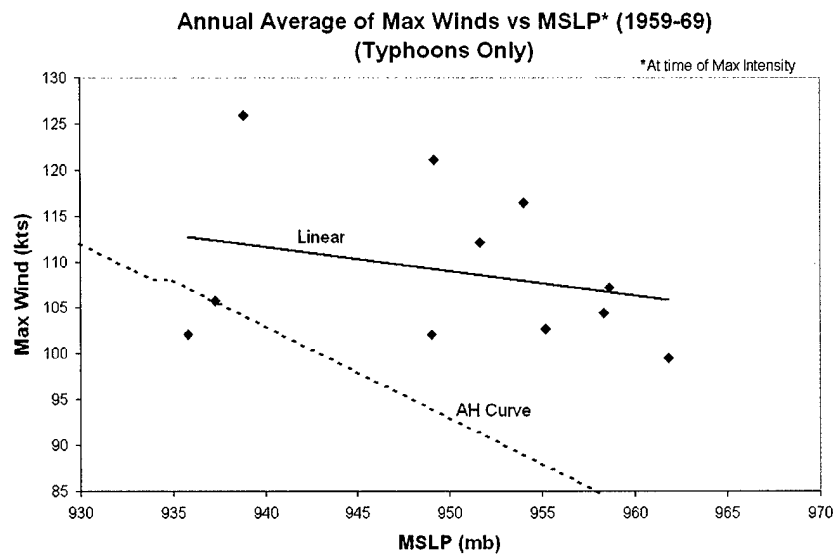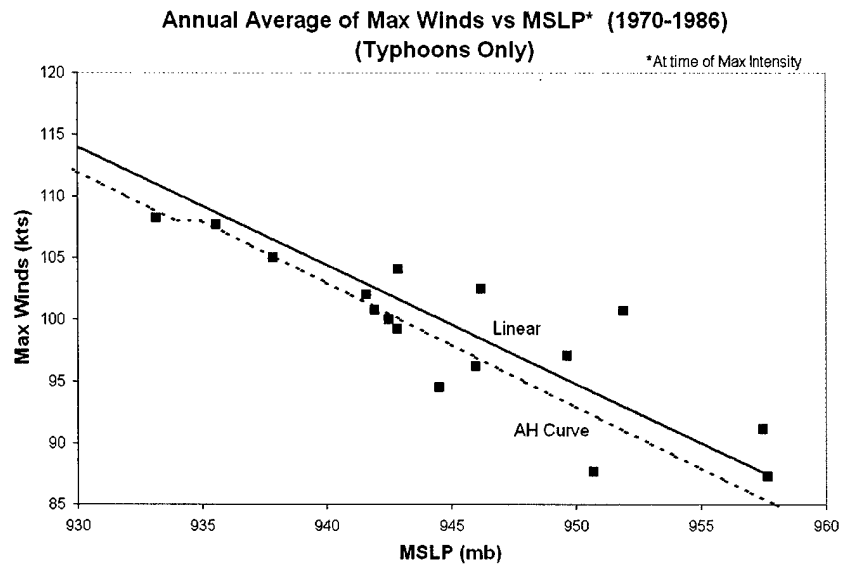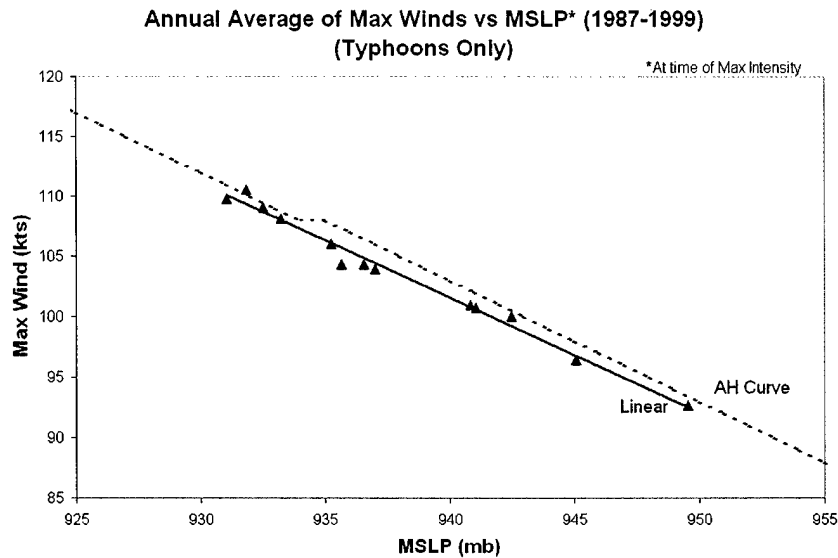Figure 4.19: $MSLP_{am}$ (mb) versus V_{am} (kts) for typhoons for Period III, 1987-1999, with best-fit linear regression and Atkinson and Holliday curves.

North Atlantic data yielded absolute average maximum wind speed deviations of 9.6 kts, 7.1 kts, and 6.6 kts from the Kraft curve for periods I, II, and III (Table 4.22 and Figures 4.22, 4.24, and 4.26) respectively, the NW Pacific had average absolute differences of 20.9 kts, 6.3 kts, and .79 kts respectively from the AH curve (see Table 4.23 and Figs. 4.21, 4.23 and 4.25). The same patterns of deviations are found for the average absolute deviations from the best-fit linear curves (see Tables 4.24 and 4.25). During Period II, the average absolute difference of the Atlantic data from the Kraft curve was 7.1 kts versus the Pacific difference (from AH) of 6.3 kts. These differences occurred during a time when both basins had aircraft reconnaissance into the center of these storms. In the NW Pacific, the observed variability does not occur during Period III owing to the loss of in situ measurements. Rather, for the last 15 years, JTWC analysts have relied on the AH curve to convert maximum winds to MSLP, therefore eliminating any variability in the wind-pressure relationship that may have been present.

Table 4.22: The average absolute difference of all V_{mi} and $MSLP_{mi}$ from the Kraft curve per time period for the Atlantic (hurricanes only).

Period	Avg Diff Wind (kts)	Avg Diff Pressure (mb)
1959-1999	7.5	7.2
I	9.6	9.8
II	7.1	6.5
III	6.6	6.2

Table 4.23: The average absolute difference of V_{mi} and $MSLP_{mi}$ from the Atkinson and Holliday curve per time period for the NW Pacific (typhoons only).

Period	Avg Diff Wind (kts)	Avg Diff Pressure (mb)
1959-1999	8.8	9.1
I	20.9	21.6
II	6.3	6.4
III	.79	.79

Table 4.24: The average absolute difference of all V_{mi} and $MSLP_{mi}$ from the best-fit linear curve per time period for the Atlantic (hurricanes only).

Years Period	Avg Diff Wind (kts)	Avg Diff Pressure (mb)
1959-1999	6.9	7.5
I	8.6	7.8
II	6.0	6.0
III	5.8	5.8

Table 4.25: The average absolute difference of V_{mi} and $MSLP_{mi}$ from the best-fit linear curve per time period for the NW Pacific (typhoons only).

Period	Avg Diff Wind (kts)	Avg Diff Pressure (mb)
1959-1999	9.2	10.5
I	12.9	13.7
II	6.0	6.6
III	1.8	2.0

Figure 4.20: V_{mi} versus $MSLP_{mi}$ for NW Pacific typhoons for Period I, 1959-1969. Best-fit linear regression and Atkinson and Holliday curves are overlayed.

Figure 4.21: V_{mi} versus $MSLP_{mi}$ for Atlantic hurricanes for Period I, 1959-1969. Best-fit linear regression and Atkinson and Holliday curves are overlayed.

Figure 4.22: V_{mi} and $MSLP_{mi}$ for NW Pacific typhoons for Period II, 1970-1986. Best-fit linear regression and Atkinson and Holliday curves are overlayed.

Individual Storms Max Winds vs MSLP* (1970-86)
(Hurricanes Only)

*At time of Max Intensity

Figure 4.23: V_{mi} versus $MSLP_{mi}$ for Atlantic hurricanes for Period II, 1970-1986. Best-fit linear regression and Atkinson and Holliday curves are overlayed.

All Individual Cyclone Maximum Winds vs MSLP* (1987-1999)
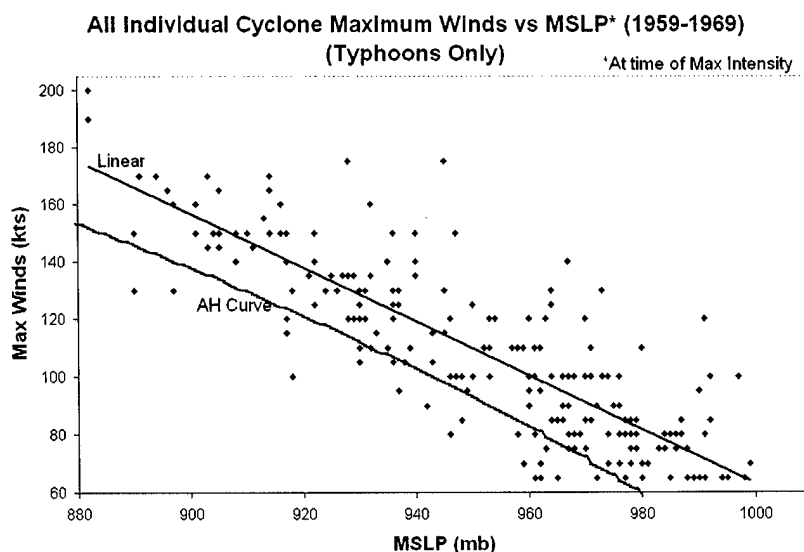**(Typhoons Only)**

*At time of Max Intensity

Figure 4.24: V_{mi} and $MSLP_{mi}$ for NW Pacific typhoons for Period III, 1987-1999. Best-fit linear regression and Atkinson and Holliday curves are overlayed.

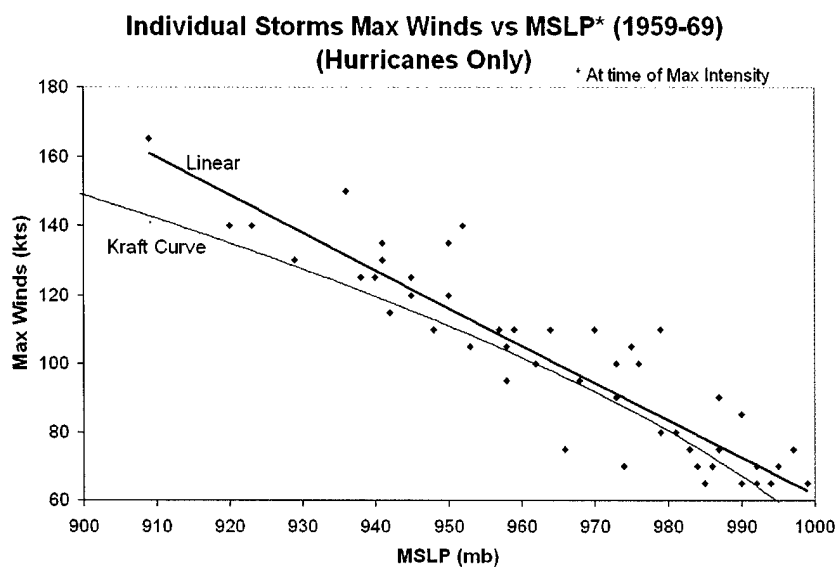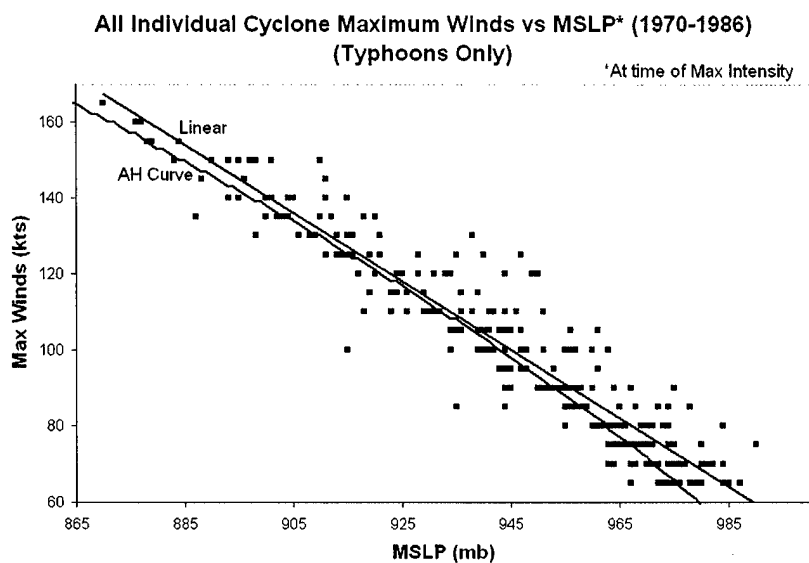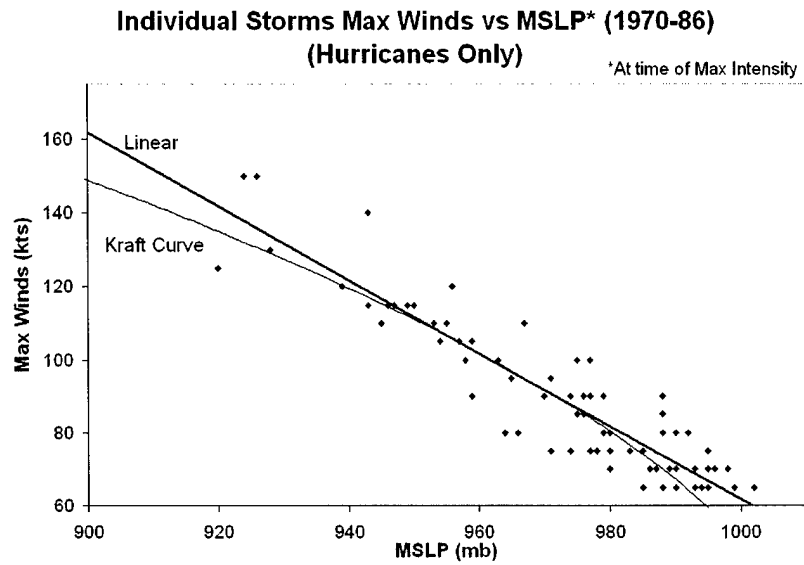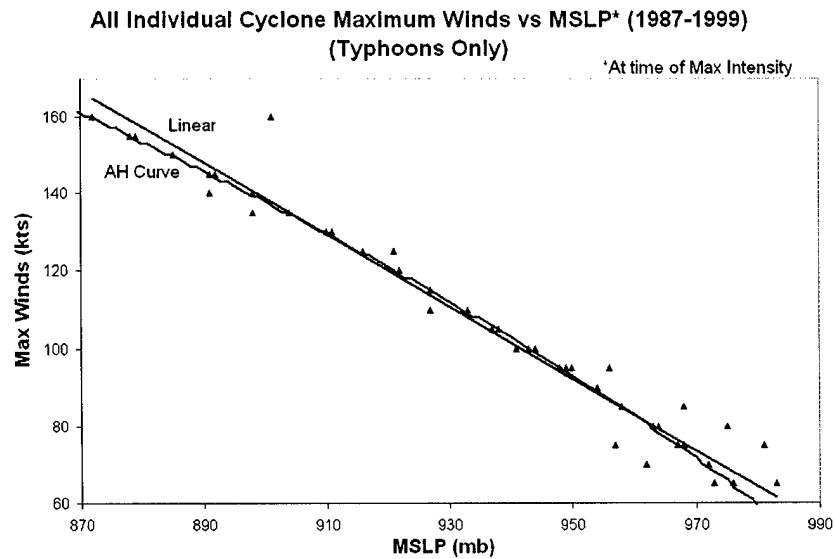**Individual Storms Max Winds vs MSLP* (1987-1999)**
Hurricanes Only
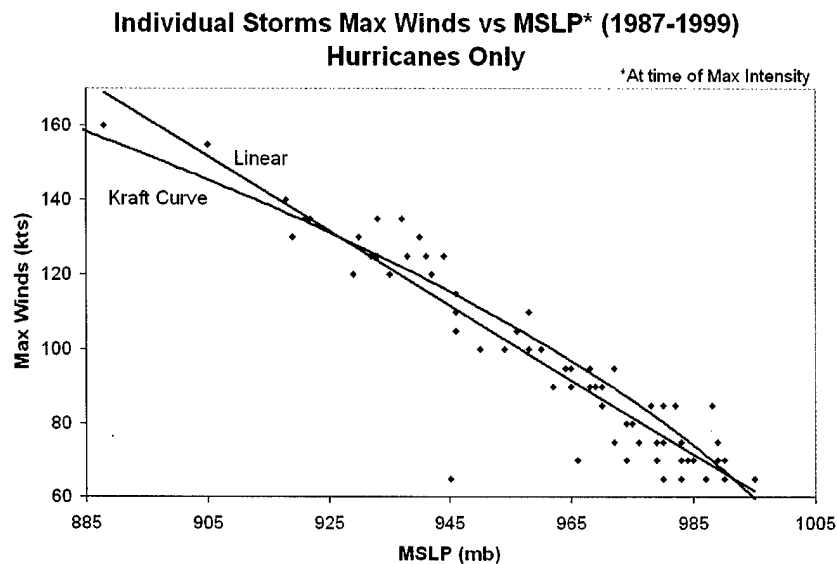
Figure 4.25: V_{mi} versus $MSLP_{mi}$ for Atlantic hurricanes for Period III, 1987-1999. Best-fit linear regression and Atkinson and Holliday curves are overlayed.

4.6 Summary

The variability of a tropical cyclone's structure as it goes through its life cycle must be accommodated while making an analysis or forecast of the storm's intensity. This study separates Atlantic storm data for 1995–1999 into specific life cycle segments to devise a simple but more accurate wind-pressure relationship to be used operationally by forecasters and analysts. Distinct wind-pressure relationships were found for deepening versus filling storms. These deepening and filling wind-pressure relationships also had distinct modes of latitudinal variability, which were captured in a comparison with Landsea et al's study of storm properties versus by latitude. Intensifying storms did not vary as much as filling storms when compared by latitude. Filling storms south of 25° North latitude tended to have higher winds for a given minimum sea level pressure than did filling storms north of 25°. Recommendations for acommodating of Landsea et al's results in the present study's equations were proposed and similar adjustments can and should be made for other TC basins. Further research on larger data sets in those regions will be required for accurate adjustments and still other adjustments may be necessary in the

future as more data are collected from aircraft, GPS dropwindsondes, satellites, and more advanced instruments developed during the next decades.

The disappearance variable modes of maximum surface wind-minimum sea level pressure interactions in the NW Pacific due to the loss of aircraft reconnaissance has been documented by the time period comparison. Specifically, while the North Atlantic has shown consistent modes of variability during the past three decades, the NW Pacific data have become dependent on the Atkinson and Holliday wind-pressure relationship since aircraft missions were halted in 1987. The overall impact of the absence of aircraft reconnaissance may not be known, but this is one example of how the NW Pacific best track data set is influenced.

Chapter 5

CONCLUSIONS AND RECOMMENDED FURTHER RESEARCH

The variability of the wind-pressure structure of tropical cyclones produces many challenges to TC forecasters. These difficulties are brought about by the gross measurement deficiencies over the tropical oceans. Currently, only the North Atlantic basin has aircraft reconnaissance flights while the other seven tropical basins are dependent on the subjective Dvorak satellite intensity scheme. While the Dvorak technique is a very successful first-guess estimate for cyclone intensity, it cannot accurately accommodate many of the various modes of variability which occur. This study has provided evidence that reveals the discrepancies between maximum intensities measured by aircraft versus values of maximum intensity measured by the Dvorak method (see also Appendix A). Differences between aircraft observed versus Dvorak estimates of MSLP of up to 45 mb are noted for some cases. This sort of discrepancy may lead to estimated wind differences up to 40 knots and alteration of outer radius wind strength. This may be the difference between a weak typhoon causing little damage and a strong typhoon causing a great deal of harm.

Estimating the MSLP from the maximum wind, or vice versa, is important for storm inner and outer-core wind estimates and model input. The single Kraft wind-pressure relationship used with the Dvorak technique to convert maximum wind estimation to MSLP is not able to account for all of the wind variability that can occur within individual cyclones.

It should be no surprise that the maximum wind-MSLP ratio of the Kraft, Dvorak and Atkinson-Holliday curves can frequently be unrepresentative. The radial pressure gradient and maximum winds near the radius of maximum winds (RMW) of a small intense cyclone can be greater than that of a cyclone with a much lower pressure. This is illustrated in

the top diagram of Fig. 5.1. Curve a is shown to have a stronger pressure gradient and height maximum wind (100 kts) at the RMW but less MSLP (960 mb) than the cyclone of curve b which has a MSLP of 940 mb and a maximum wind of only 70 knots.
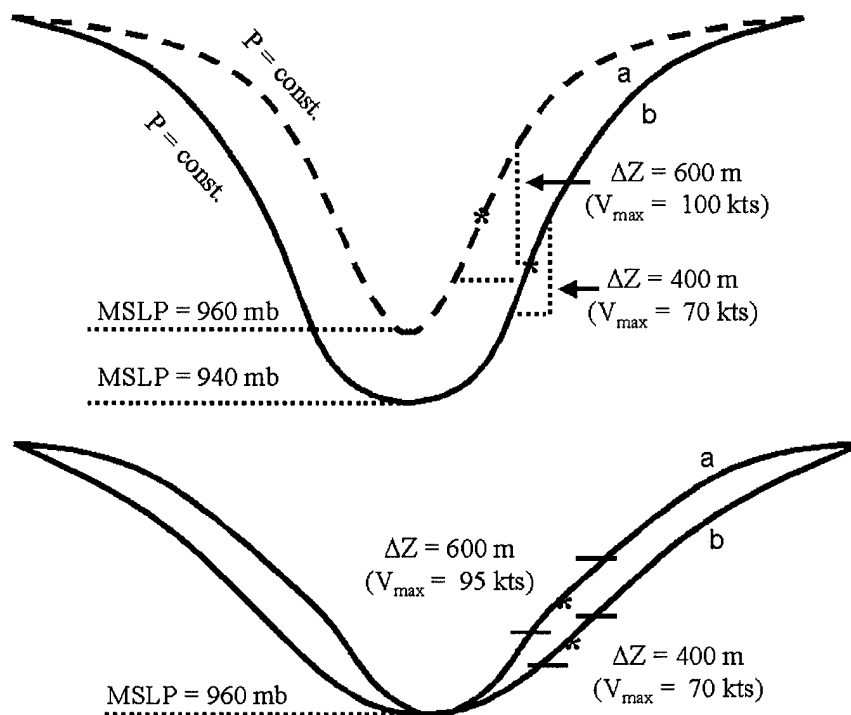

Figure 5.1: Illustration of how the radial gradient of constant pressure can vary from inner to outer-core causing the maximum wind to MSLP ratio to deviate from that specified by the Kraft, Atkinson-Holliday and Dvorak curves.

It would be beneficial if the maximum wind-MSLP relationship could be expressed as a single number which has a reference to the Kraft (K) relationship in the Atlantic and the Atkinson-Holliday (AH) relationship in the Pacific. Any observations showing an exact representation of these wind/pressure relationships are defined to be given by the ratio of 1.0. Should maximum winds be stronger than that specified K and AH curves, then this ratio would be greater than one. For example, a small intense cyclone might have wind 50 percent higher than the winds that would be specified by the MSLP. In this case the ratio would be 1.5. Or, if maximum winds were 50 percent weaker than the specified K

and AH curves give for a MSLP than the ratio of maximum wind to minimum pressure would be 0.5.

These ratios are defined for the Atlantic in terms of the standard wind-pressure Kraft curve and in the Pacific in terms of the standard AH curve as follows:

$$(Atlantic) \quad WPR_a = \frac{V_{ob}}{V_k} / \frac{\Delta P_{ob}}{\Delta P_k} \tag{5.1}$$

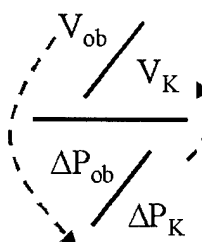$$(Pacific) \quad WPR_f = \frac{V_{ob}}{V_{AH}} / \frac{\Delta P_{ob}}{\Delta P_{AH}} \tag{5.2}$$

If aircraft reconnaissance is available to observe the maximum winds (V_{ob}) and the observed MSLP minus environmental pressure difference (ΔP_{ob}) one can then solve for the wind-pressure ratio (WPR) in each ocean basin. Two examples will now be given, one for a small intense Atlantic cyclone where the observed maximum wind (V_o) is 110 knots and the observed MSLP is 973 mb given a (ΔP_{ob}) of 40 mb (1013 environmental SLP minus 973 cyclone MSLP). The (V_o) measurements give a Kraft derived cyclone MSLP of 958 mb (1013 mb - 958 b) = 55 mb. The observed MSLP of 973 mb gives a Kraft maximum wind of 90 knots. Figure 5.2 shows the substitution of these four parameters into Eqs. 5.1 and 5.2. These substitutions give a WPR of 1.67. The maximum wind for this small intense cyclone is significantly higher than that specified by its central pressure.

A counter example can be taken for a large strong cyclone of the NW Pacific whose inner-core is not so intense. Figure 5.3 shows this calculation. The MSLP is much lower (1010 mb environmental pressure minus 940 mb observed pressure of ΔP_{ob} = 70 mb) than one would expect from the maximum wind as specified by the AH relationship. In this case the ratio is 0.3

<u>Radial Extent of Damaging Winds</u>. The radial extent of damaging winds can be expressed as the inverse of these WPR or $\frac{1}{WPR}$. The difference in the extent of radial winds between these two example cases would be given by $\frac{1}{0.32} / \frac{1}{1.67}$ or 5.22. The cyclone with the lowest WPR (0.32) has substantially greater extent of outer radius damaging winds than the cyclone with the high WPR (1.67).

LARGE STRONG CYCLONE
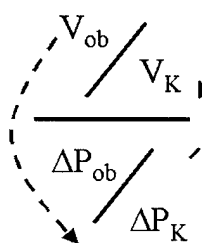
(Inner-Core not so Intense)

$$\left.\frac{V_{ob}/V_K}{\Delta P_{ob}/\Delta P_K}\right\} \text{ Ratio (RO)} = \frac{90/120}{70/30} = \frac{.75}{2.33} = \boxed{\textbf{0.32}}$$

$$V_{ob} = 90 \text{ kts } (\Delta P_K = 30 \text{ mb})$$

$$\Delta P_{ob} = 70 \text{ mb } (V_K = 120 \text{ kts})$$

Figure 5.2:

SMALL INTENSE CYCLONE

$$\left.\frac{V_{ob}/V_K}{\Delta P_{ob}/\Delta P_K}\right\} \text{ Ratio (RO)} = \frac{110/90}{40/55} = \frac{1.22}{.73} = \boxed{\textbf{1.67}}$$

$$V_{ob} = 110 \text{ kts } (\Delta P_K = 55 \text{ mb})$$

$$\Delta P_{ob} = 40 \text{ mb } (V_K = 90 \text{ kts})$$

Figure 5.3:

The bottom diagram if Fig. 5.1 illustrates how two cyclones with the same central pressure (960 mb) can have different maximum winds (95 kts versus 70 knots).

These need for new wind-pressure relationships that are applicable for the different stages in the life cycle of the TC, and variations with latitude are needed. First a stratification is made whether the storm is intensifying or filling. New wind-pressure relationships are then established. These new wind-pressure relationships indicate that the maximum wind for a given MSLP for a filling storm averages 9 knots less than the maximum wind for the same MSLP value for an intensifying storm. These differences range from 5 knots at 1005 mb up to nearly 11 knots at 870 mb. Storms were also compared in relation to eye size and, surprisingly, eye size had very little to do with the wind-pressure relationship.

Storm data were further broken into latitudinal groupings as prescribed by Landsea et al. It was found that Landsea et al's wind-pressure curve outperforms the others for storms south of 25°. The curve developed in the present study for filling and for deepening storms outperformed Kraft and Landsea et al. between 25 and 35° and for filling storms north of 35°. Kraft and Landsea et al's relationship overestimates winds between 35 and 45°, especially at weaker intensities. It is recommended that Landsea et al's relationship be used for all cases except in the three exceptions noted above for which the new filling and deepening curves from this study are proposed (See Table 5.1).

Table 5.1: Recommended V_m vs. MSLP relationships for corresponding storm tendency and latitude.

Type	<25	25–35	35–45
Deepening	Landsea et al.	New	Landsea et al.
Filling	Landsea et al.	New	New

In areas where aircraft are no longer flown into storms, these adjustments will add accuracy to model input and possibly provide an improvement in model initiation. For historical purposes, the proposed adjusted relationships may add some accuracy to the North Atlantic database in earlier periods when aircraft measurements were not available. Improved wind-pressure relationships may lead to more reliable remote sensing estimations. Studies are being conducted to see how the Advanced Microwave Sounding Unit

(AMSU) can estimate MSLP, and be related to the maximum surface winds (Brueske and Velden, 2000).

This study shows that a greater variability in the maximum wind versus MSLP ratio has occurred in the past 15 years in the Atlantic tropical basin than in the Northwest Pacific where aircraft penetrations are no longer conducted. This demonstrates the exclusive dependence of JTWC on the empirical intensity rules set up by Dvorak. These empirical rules do not accommodate all the variable wind to pressure conditions that can frequently exist in cyclone structure.

Future technology will likely add in the improvement of the wind-pressure relationship. The ability to monitor tropical cyclones via multiple remote sensing instruments is showing increased promise. Recent developments on the Advanced Microwave Sounding Unit (AMSU) and the satellite scatterometer are contributing real-time data that is beginning to add improvement to the Dvorak intensity estimates. The potential of high altitude unmanned aircraft with mounted radiometers flying over tropical cyclone centers to estimate the minimum sea level pressure (Gray 1971) is becoming more feasible. These aircraft would be able to resolve the eye, thus measuring a more accurate MSLP than current operational satellites. Since unmanned aircraft are completing trans-oceanic flights, they have the potential to monitor cyclones for many hours providing a non-stop data stream. It may also prove possible for lower troposphere small un-named vehicles such as the aerosonde (Holland 1999, 2000) to enter the typhoon and accurately and independently measure MSP.

REFERENCES

Aberson, S. D., and J. L. Franklin, 1999: Impact on hurricane track and intensity forecasts of GPS dropwindsonde observations from the first-season flights of the NOAA Gulfstream-IV jet aircraft. *Bull. of the Amer. Met. Soc.*, 80, 421-427.

Arakawa, H., 1952: Mame Taifu or midget typhoon (small storms of typhoon intensity). *Geophysical Magazine*, 24, 463-474.

Atkinson, G. D. and Holliday, C. R., 1977: Tropical cyclone minimum sea level pressure maximum sustained wind relationship for western North Pacific. *Monthly Weather Review*, 105, 421-427.

Black, M. L., and H. E. Willoughby, 1992: The concentric eyewall cycle of Hurricane Gilbert. *Mon. Wea. Rev.*, 120, 947-957.

Brand, S., 1972: Very large and very small typhoons of the western North Pacific Ocean. *J. Meteor. Soc. Japan*, 50, 332-341.

Brueske, K. F., and C. S. Velden, 2000: Tropical cyclone intensity estimation using the NOAA-KLM series advanced microwave sounding unit (AMSU): Preliminary results and future prospectus. *Preprints 24th Conf. on Hurricanes and Tropical Meteorology.*, Ft. Lauderdale, Amer. Meteor. Soc, 258-259.

Burpee, R. W., J. L. Franklin, S. J. Lord, R. E. Tuleya, and S. D. Aberson, 1996: The impact of Omego dropwindsondes on operational hurricane track forecast models. *Bull. of the Amer. Met. Soc.*, 77, 925-933. Cocks, S.B., 1997: The outer radius tangential winds of tropical cyclones. Dept. of Atmos. Sci. MS Thesis, Colo State Univ., Ft. Collins, CO, 102 pp.

Coxford, M. A. and G. M. Barnes, 1999: Strength estimates for Atlantic tropical cyclones. *Preprints 23rd Conf. on Hurricanes and Tropical Meteorology*, Dallas, Amer. Meteor. Soc.

Dvorak, V.F. 1975: Tropical cyclone intensity analysis and forecasting from satellite imagery. *Mon. Wea. Rev.*, 103, 420-430.

Dvorak, V.F. 1984: Tropical cyclone intensity analysis using satellite data. NOAA Technical Report NESDIS 11, US Dept of Commerce, Washington, DC, 47 pp.

Eastin, M. D., 1999: Instrument wetting errors in hurricanes and re-examination of inner-core thermodynamics. Dept. of Atmos. Sci. Paper No. 683, Colo. State Univ., Ft. Collins, CO, 80523, 203 pp.

Emanuek, K., 2000: A Statistical Analysis of Tropical Cyclone Intensity. *Mon. Wea. Rev.*, 128, 1139-1152.

Franklin, J. L. and M. L. Black, 1999: Wind profiles in hurricanes determined by GPS dropwindsondes. *Preprints 23d Conf. on Hurricanes and Tropical Meteorology.*, Dallas, Amer. Meter. Soc., 167-168.

Franklin, J. L., M. L. Black and K. Valde, 2000: Eyewall wind profiles in hurricanes determined by GPS dropwindsondes. *Preprints 24th Conf. on Hurricanes and Tropical Meteorology.*, Ft. Lauderdale, Amer. Meteor. Soc, 446-447.

Gray, W. M., C. Neumann, and T. L. Tsui, 1991: Assessment of the role of aircraft reconniassance on tropical cyclone analysis and forecasting. *Bull. of the Amer. Met. Soc.*, 72(12), 1867-1883.

Hawkins, H. F. and D. T. Rubsam, 1967: Hurricane Inez a classic "micro-hurricane". *Mariners Weather Log*, 11, 157-160.

Hock, T. F., and J. L. Franklin, 1999: The NCAR GPS dropwindsonde. *Bull. Amer. Meteor. Soc.*, 80, 407-420.

Holldand, G. J. 1980: An analytic model of the wind and pressure profiles in hurricanes. *Monthly Weather Review*, 108(8), 1212-1218.

Joint Typhoon Warning Center, 1959–1999: Annual Typhoon Report 1959–1999. US Naval Pacific Meteorology and Oceanography Center/Joint Typhoon Warning Center, Pearl Harbor, HI.

Knaff J. A., M. Demaria, J. P. Kossin, and V. E. Larson, 2001: A discussion of intensities associated with doughnut hurricanes. *Preprints, 54th Interdepartmental Hurricane Conference.*, Orlando.

Kraft, R. H., 1961: The hurricane's central pressure and highest wind. *Mar. Wea. Log*, 5, 155.

Kidder, S. Q. and Cauthors, 2000: Satellite analysis of tropical cyclones using the advanced microwave sounding unit (AMSU). *Bull. of the Amer. Met. Soc.*, 6, 1241-1259.

Kubat, G. B., 1995: Tropical cyclone intensity relationships. M.S. thesis, Dept. of Atmospheric Science, Colorado State University, 86 pp.

Lander, M. A., 1999: Some characteristics of tropical cyclone intensification as revealed by hourly digital Dvorak analysis. *Preprints, 23d Conf. on Hurr. and Trop. Met.*, Dallas, Amer. Met. Soc., 580-583.

Lander, M. A. 1999: A tropical cyclone with a very large eye. *Monthly Weather Review*, 127, 137-142.

Lander, M. A. 1999: A tropical cyclone with an enormous central cold cover. *Monthly Weather Review*, 127, 132-136.

Lander, Mark A. 2000: Midget tropical cyclones in the subtropics. *Preprints 24th Conf. on Hurricanes and Tropical Meteorology*, Fort Lauderdale, Amer. Meteor. Soc.

Landsea, C. W., C. Anderson, N. Charles, G. Clark, J. Partagas, P. Hungerford, C. Neumann and M. Zimmer, 2001: The Atlantic Hurricane Database Re-analysis Project -

Documentation for 1851-85 Addition to the HURDAT Database. *Hurricane Climate Variability and Forecasting*, R. Murnane, Ed., Columbia University Press, (submitted).

Leejoice, R. N. 2000: Hurricane inner-core structure as revealed by GPS dropwindsondes. M.S. thesis, Dept. of Atmospheric Science, Colorado State University, 55 pp.

Lubeck, O. M. and Shwechuk, J. D., 1980: Tropical cyclone minimum sea level pressure maximum sustained wind relationship. NAVOCEANCOMCEN TECH NOTE: JTWC 80-1.

Martin, J. D., and W. M. Gray, 1993: Tropical cyclone observation and forecasting with and without aircraft reconnaissance. *Weather Forecasting*, 8, 519-532.

Merrill, R.T. and W.M. Gray, 1982: A comparison of large and small tropical cyclones. Dept. of Atmos. Sci. Paper No. 352, Colo. State Univ., Ft. Collins, CO, 75 pp.

Merrill, R.T. and W.M. Gray, 1984: A comparison of large and small tropical cyclones. *Mon. Wea. Rev.*, 112, 1408-1418

Shea, D. J., and W. M. Gray, 1973: The hurricane's inner core region: I. Symmetric and asymmetric structure. *J. Atmos. Sci.*, 30, 1544-1564.

Shewchuck, J. D., Capt, USAF, and R. C. Weir, Ensign, USN, 1980: An evaluation of the Dvorak technique for estimating tropical cyclone intensity form satellite imagery. NOCC/JTWC 80-2, USNOCC, JTWC, COMNAV MARIANAS, Box 17 FPO San Francisco, CA 96630, 25 pp.

Shoemaker, D. N., W. M. Gray, and J. D. Scheaffer, 1990: Influence of synoptic track aircraft reconnaissance on JTWC tropical cyclone track forecast errors. *Weather and Forecasting*, 3, 503-507.

Takahashi, K., 1939: Distribution of pressure and wind in a typhoon. *J. Meteor. Soc. Japan*, Sec. 2, 17, 417–421.

Veldon, C. S., T. L. Olander, and R. M. Zehr, 1997: Development of an objective scheme to estimate tropical cyclone intensity from digital geostationary satellite infrared imagery. *Weather and Forecasting*, 1, 172-186.

Vickery, P. J., P. F. Skerlj, A. C. Steckley, and L. A. Twisdale, 2000: Hurricane wind field model for use in hurricane simulations. *J. of Structural Engineering*, 1203-1221.

Wang, C. Y. 1978: Sea-level pressure profile and gusts within a typhoon circulation. *Mon. Wea. Rev*, 106(7), 954-960.

Weatherford, C. L., 1985: Typhoon structural variability. Dept. of Atmos. Sci. Paper No. 391, Colo. State Univ., Ft. Collins, CO, 80523, 198 pp.

Weatherford, C. L., 1989: The structural evolution of typhoons. Dept. of Atmos. Sci. Paper No. 446, Colo. State Univ., Ft. Collins, CO 80523, 77 pp.

Weatherford, C. L. and W. M. Gray, 1988a: Typhoon structure as revealed by aircraft reconnaissance. Part I: Data analysis and Climatology. *Mon. Wea. Rev.*, 116, 1032-1043

Weatherford, C. L. and W. M. Gray, 1988b: Typhoon structure as revealed by aircraft reconnaissance. Part II: Structural Variability. *Mon. Wea. Rev.*, 116, 1044-1056

Willoughby, H. E., J. A. Clos, and M. G. Shoreibah, 1982: Concentric eye walls, secondary wind maxima, and the evolution of the hurricane vortex. *Journal of the Atmospheric Sciences*, 39(2), 395-411.

Zehr, R. M., 1995: Improving objective satellite estimates of tropical cyclone intensity. *Extended abstracts, 21st Conf. on Hurr. and Met*, San Diego, J25-J28.

Zehr, R. M. 1995: Satellite Analysis of tropical cyclones–more quantitative and more thorough techniques. *Preprints, 22nd Conf. on Hurricanes*, 25-26.

Appendix A

NORTHWEST PACIFIC DVORAK, BEST TRACK, AND AIRCRAFT

This Appendix provides time depictions of Northwest Pacific storms (1979–1986) using best track data (solid line), aircraft reported minimum sea level pressures (circle), and Dvorak satellite intensity estimates (X) to show how aircraft measurements influence satellite analyses of cyclone intensity. In the examples given, aircraft measurements regularly cause an adjustment of satellite estimates by ± 5 to 10 mb. Some differences are up to 40 mb and/or 40 knots.

Without aircraft reconnaissance in the Northwest Pacific, these differences have not been accounted for during the past 15 years. Appendix B provides examples from best track and Dvorak estimates from 1995-1999 showing how the best track follows Dvorak much closer than it did before reconnaissance data were discontinued. In some cases, aircraft information may have significantly changed best track intensity data, but we will never know.
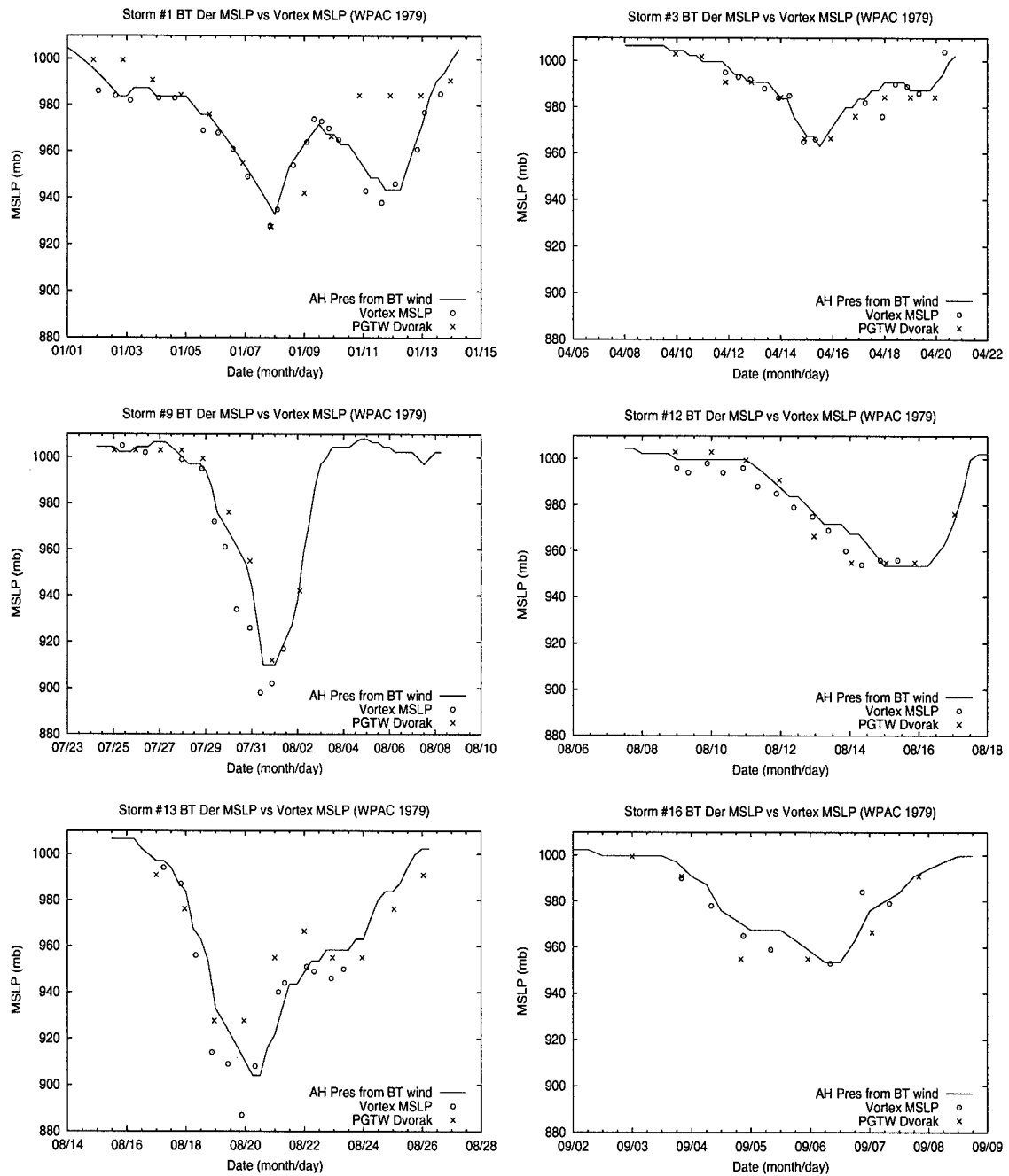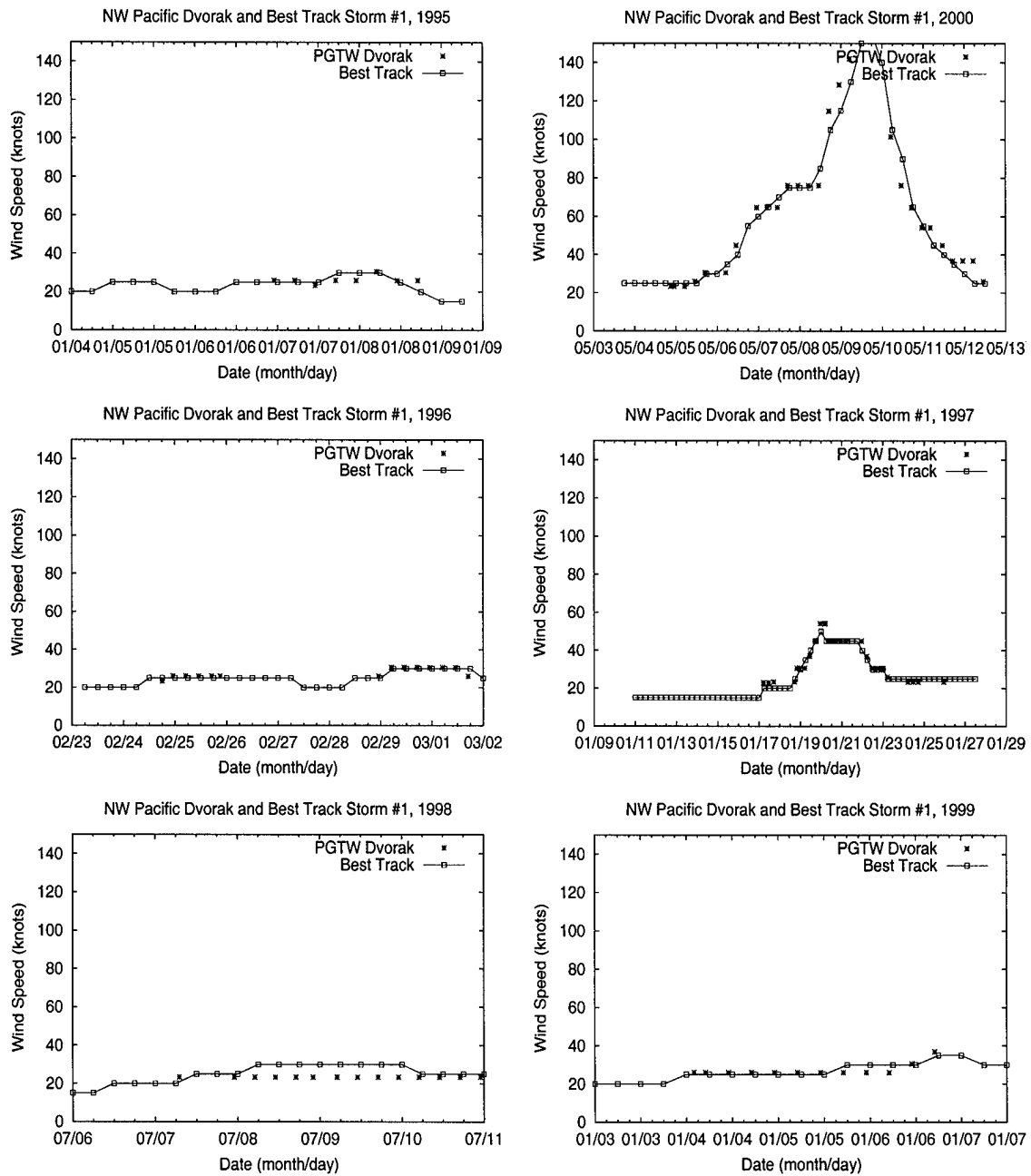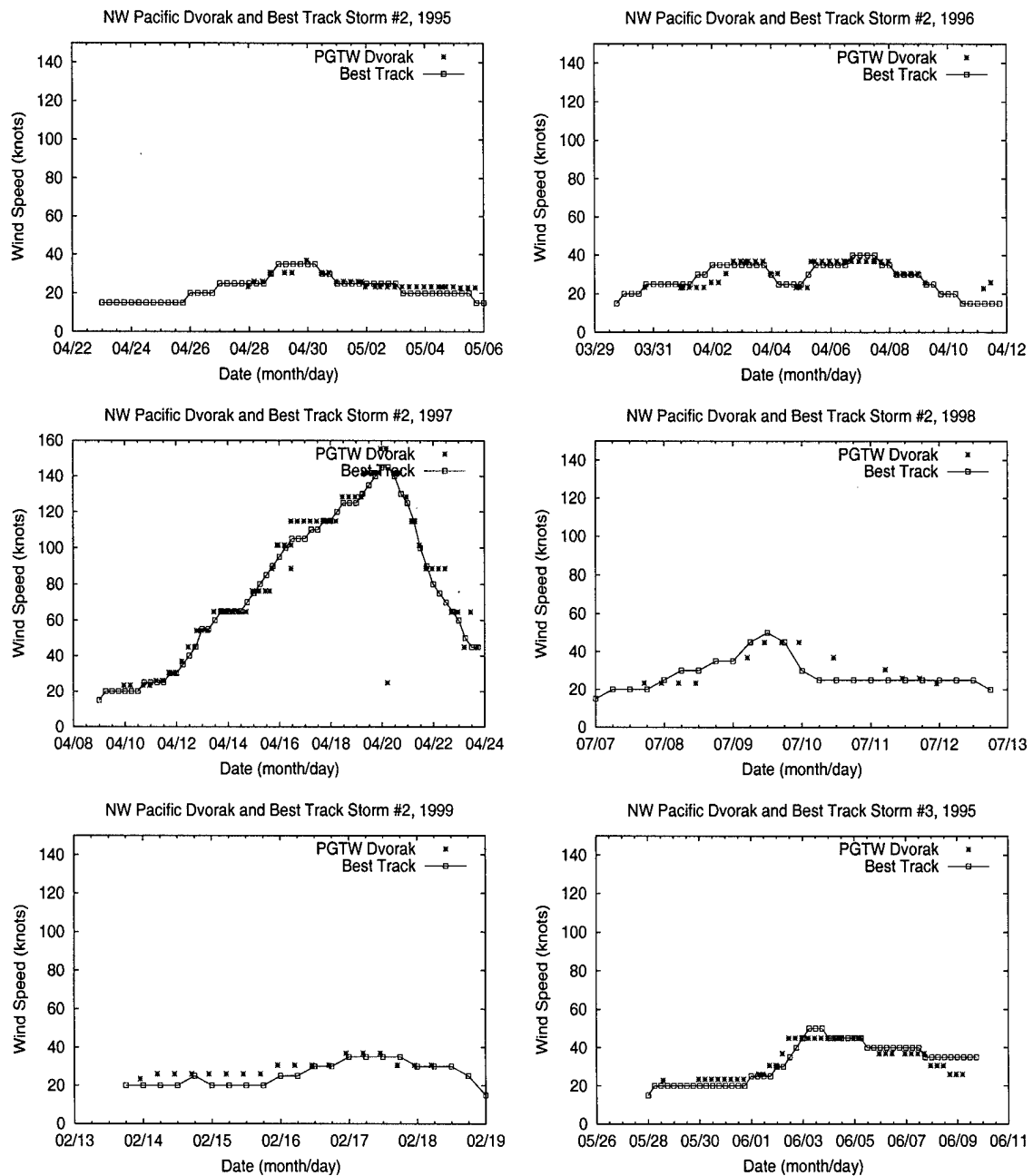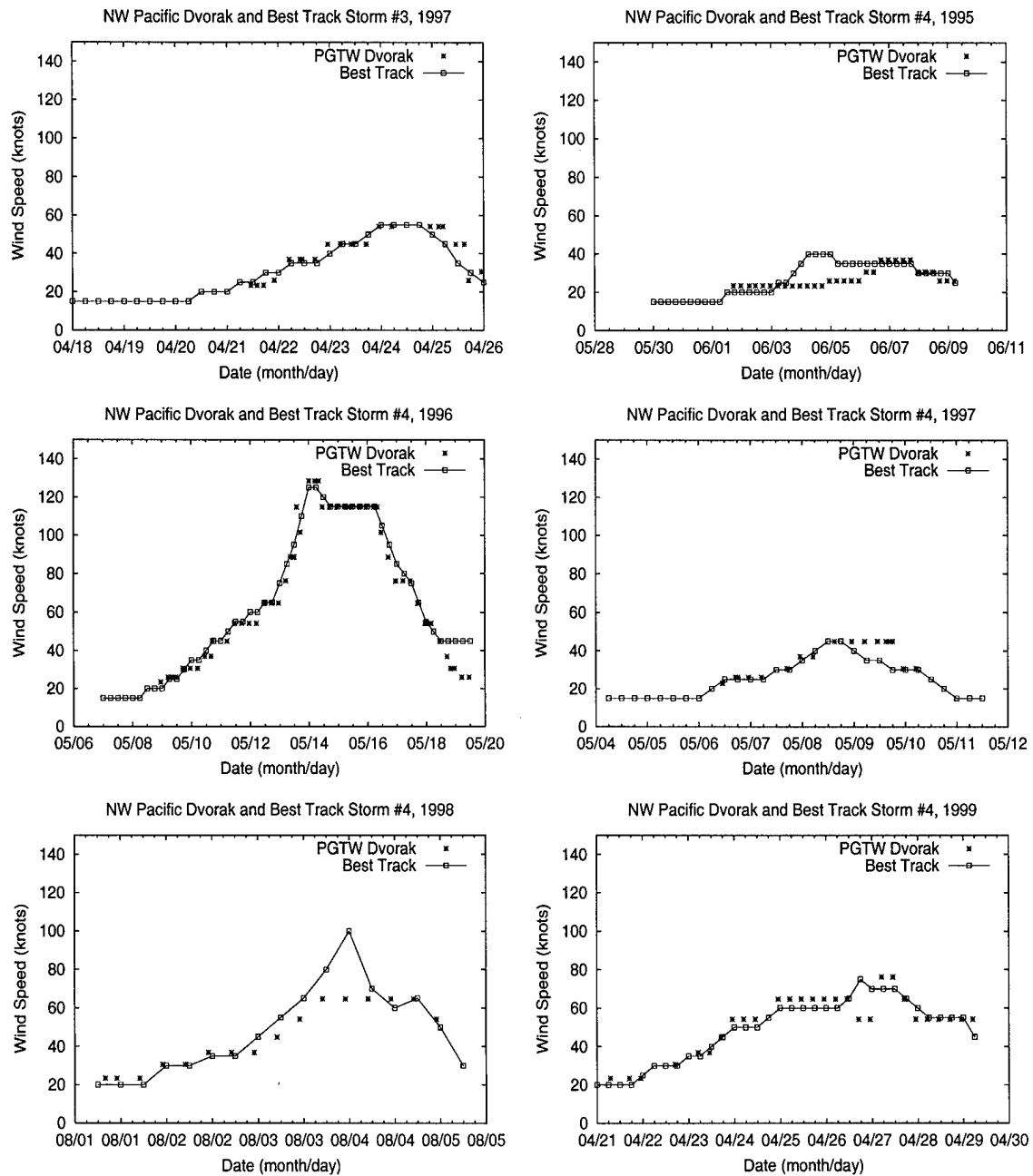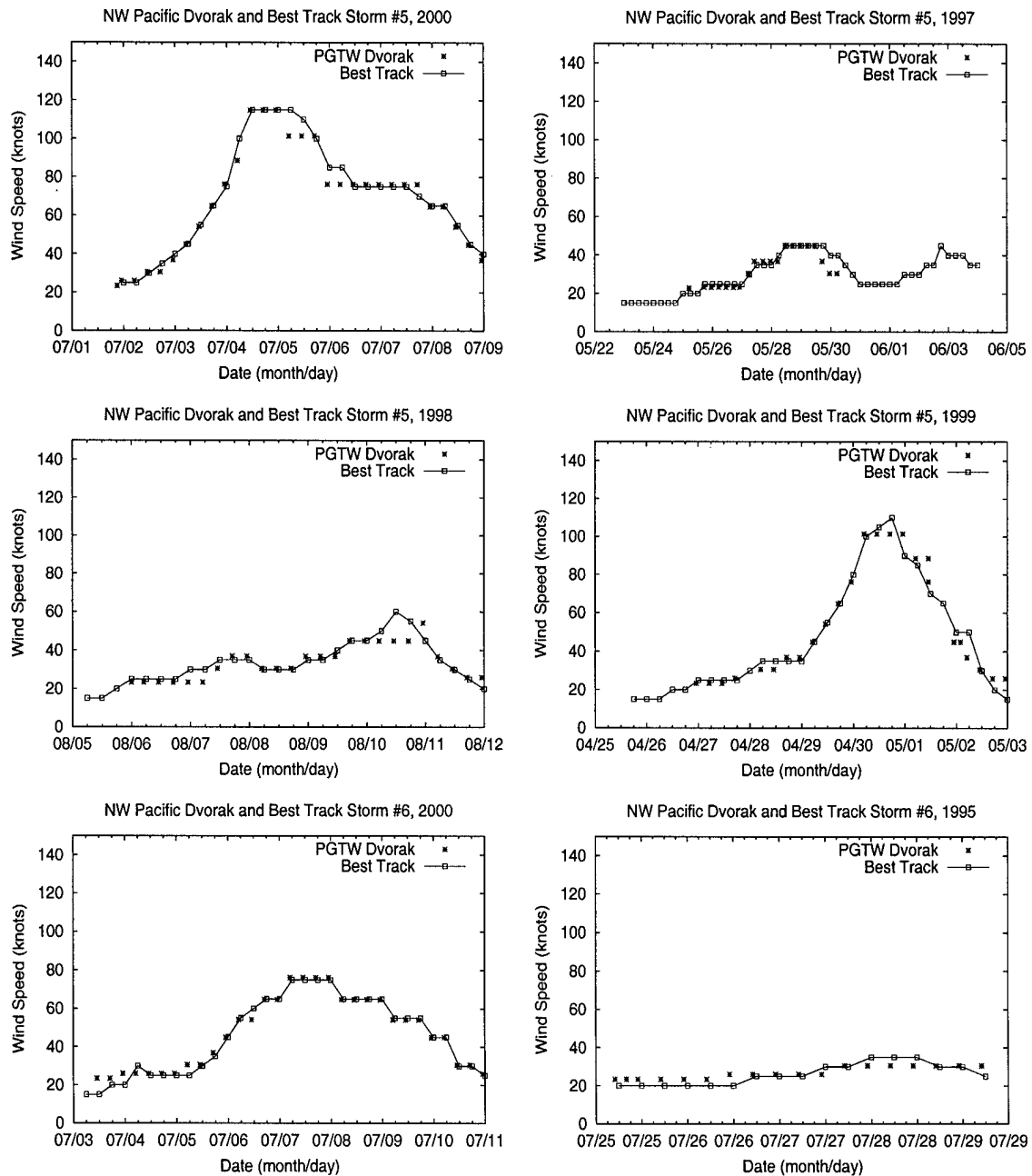
Figure A.1:
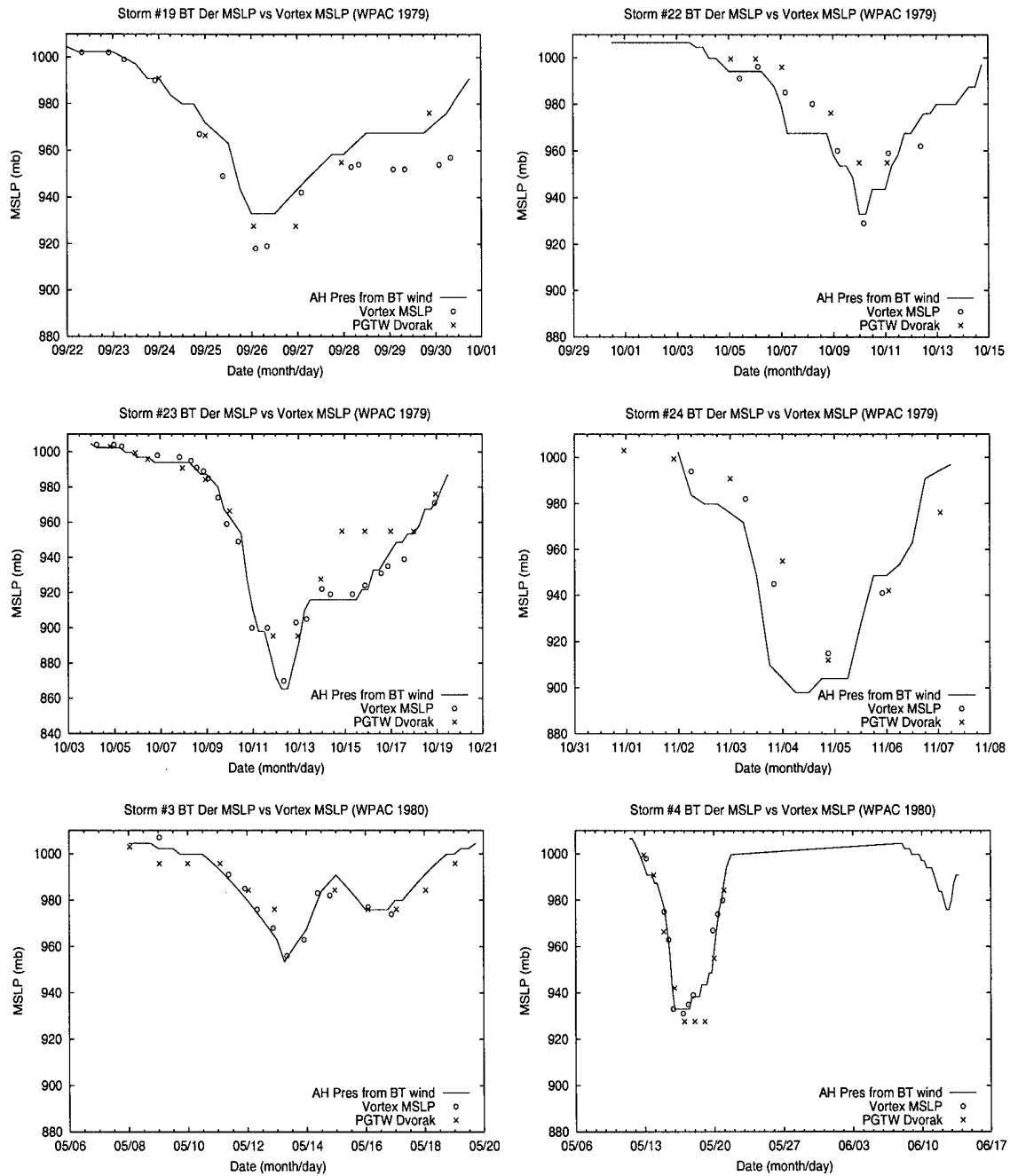
Figure A.2:
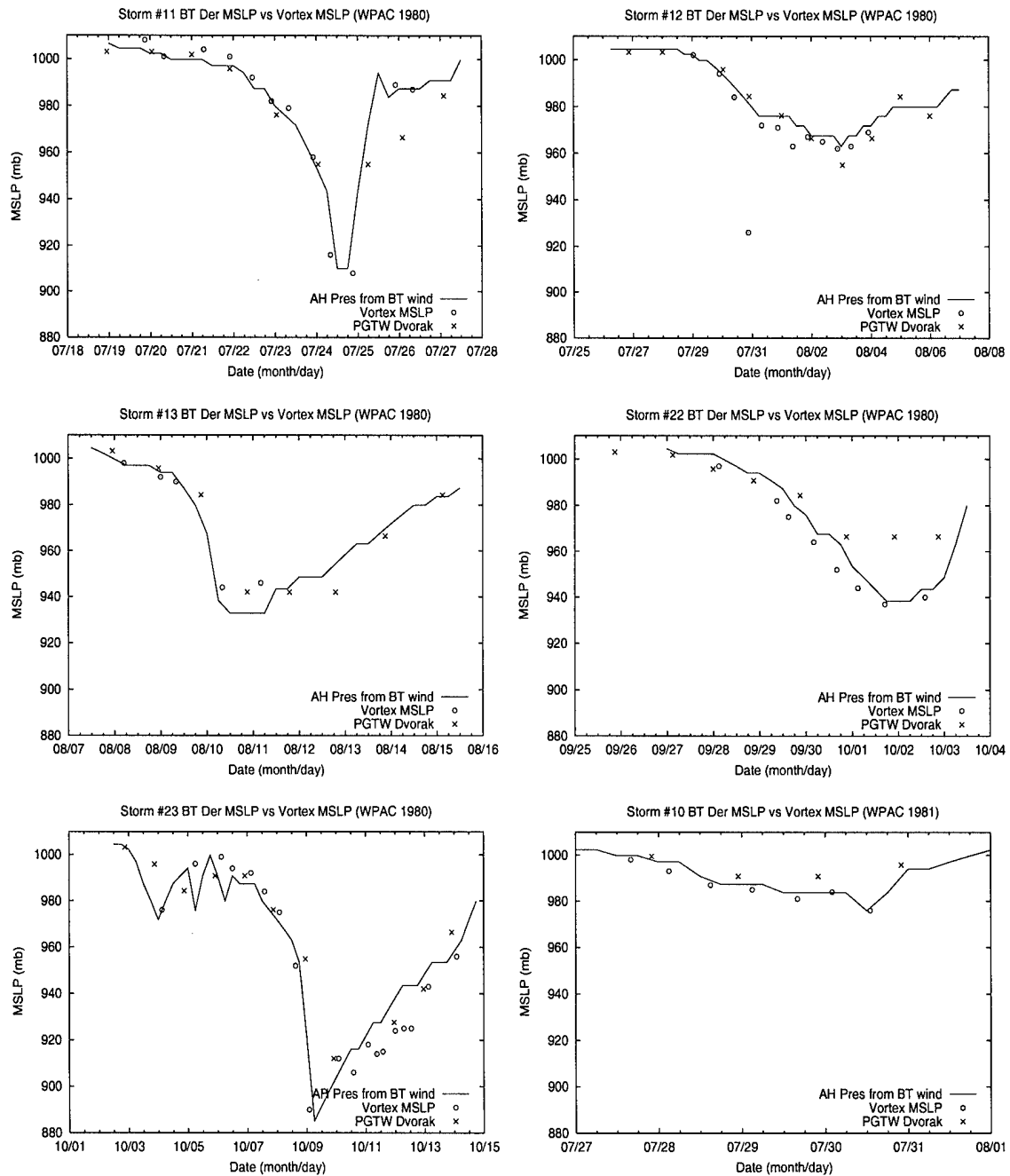
Figure A.3:
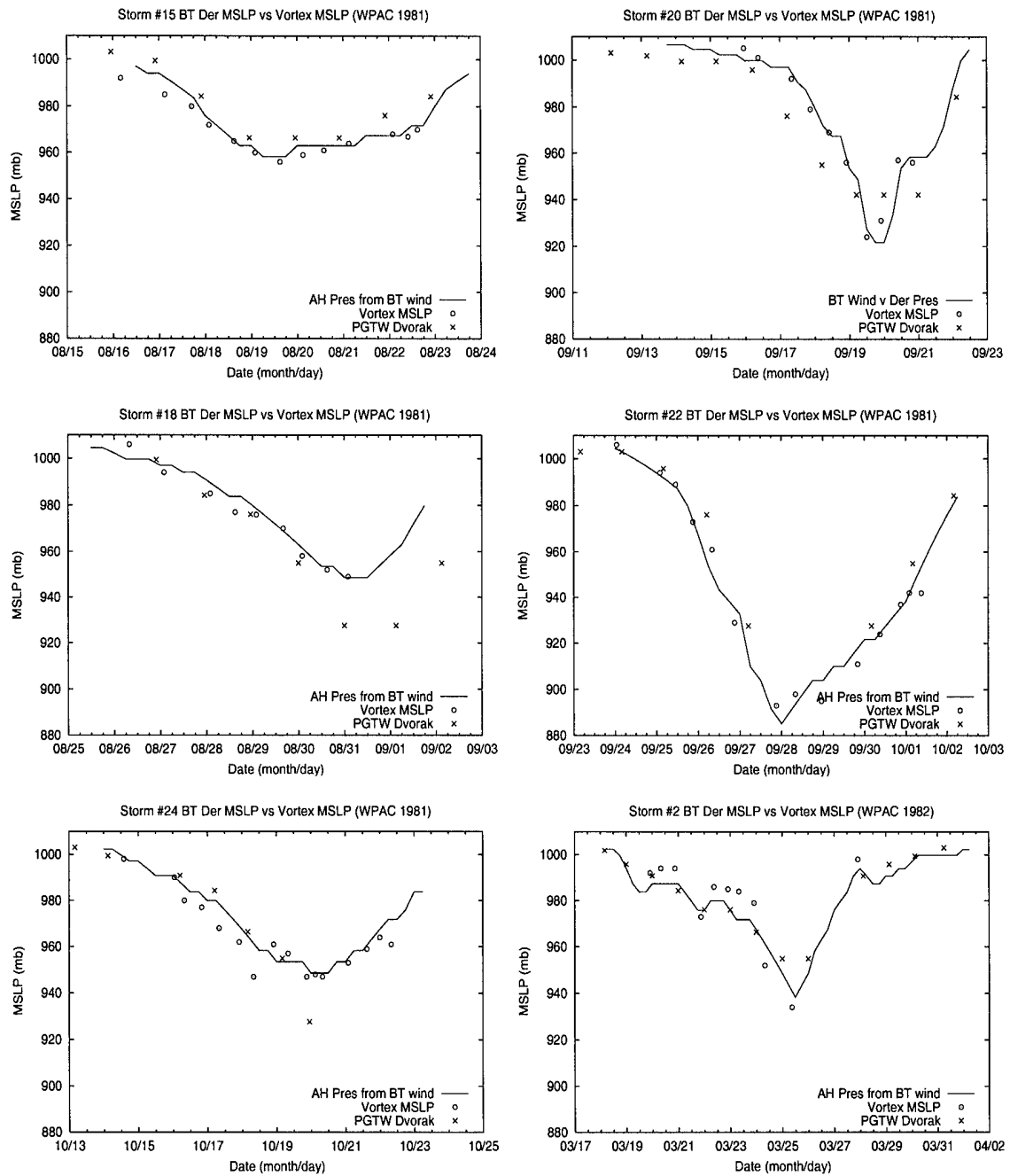
Figure A.4:
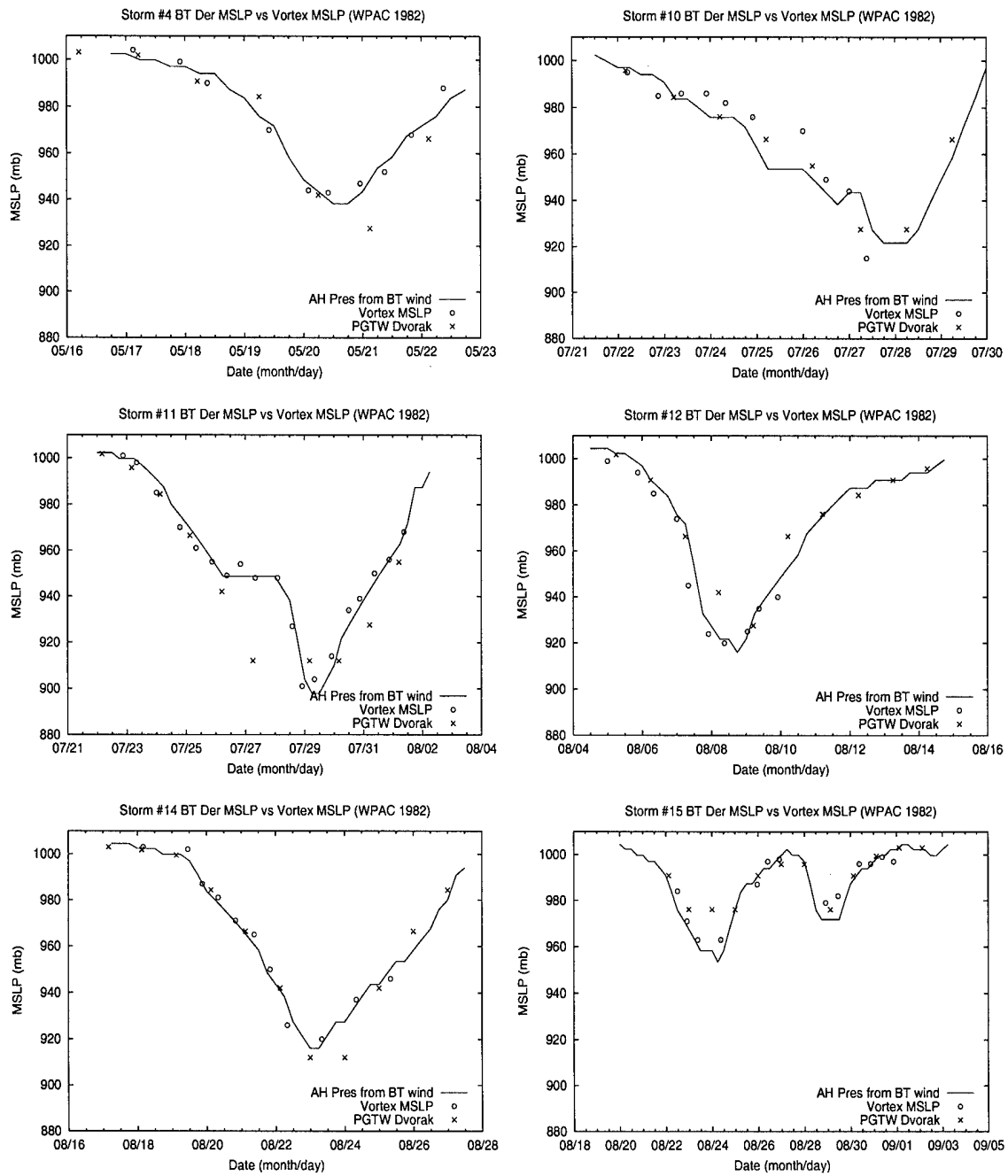
Figure A.5:
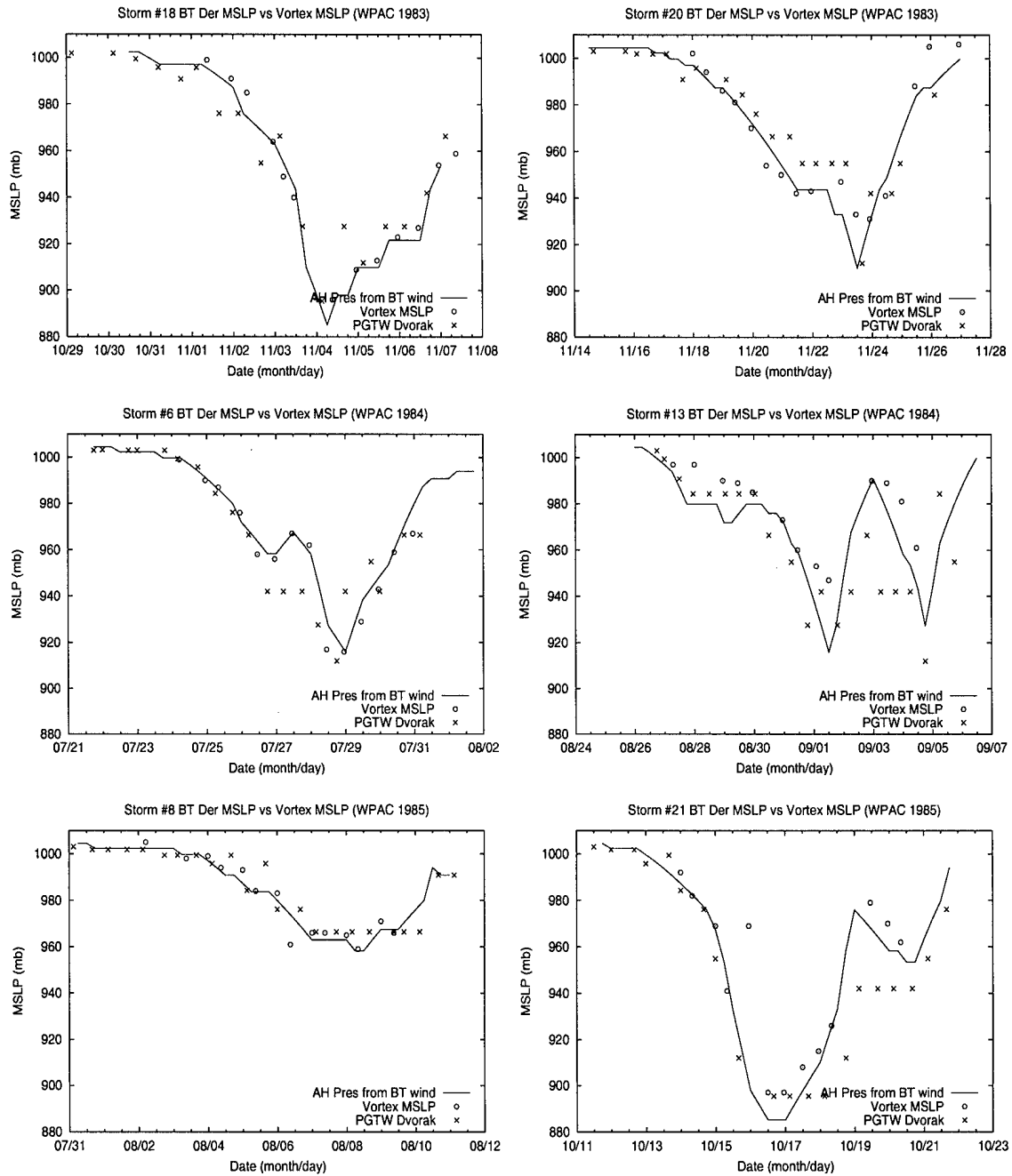
Figure A.6:
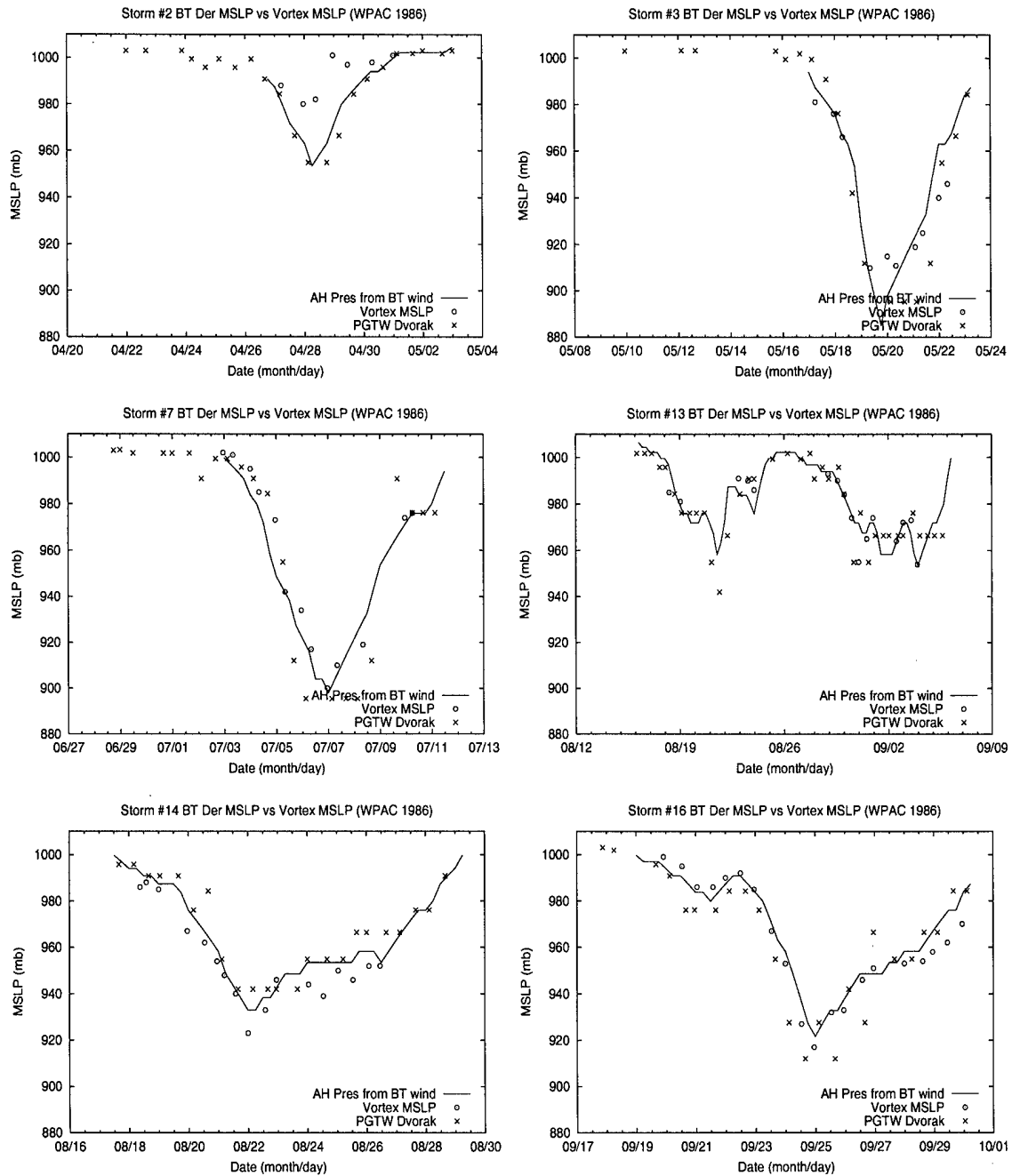
Figure A.7:

Appendix B

NORTHWEST PACIFIC DVORAK AND BEST TRACK, 1995-1999

This appendix provides time depictions of western North Pacific storms using Best Track data (solid line with squares) and the Joint Typhoon Warning Center (JTWC) Dvorak satellite intensity estimates (X) from 1995-1999. PGTW is the identifier for the JTWC Dvorak estimate. The figures reveal how JTWC has become exclusively depended on the Dvorak intensity estimate over the past five years. In comparison to the figures in Appendix A, the difference between Best Track and Dvorak intensity estimates are much smaller. Also, cases of large differences of up to 40 kts have become rare in the last five years. Analysts operating in basins without aircraft reconnaissance rarely have the data available to adjust their satellite intensity estimates.
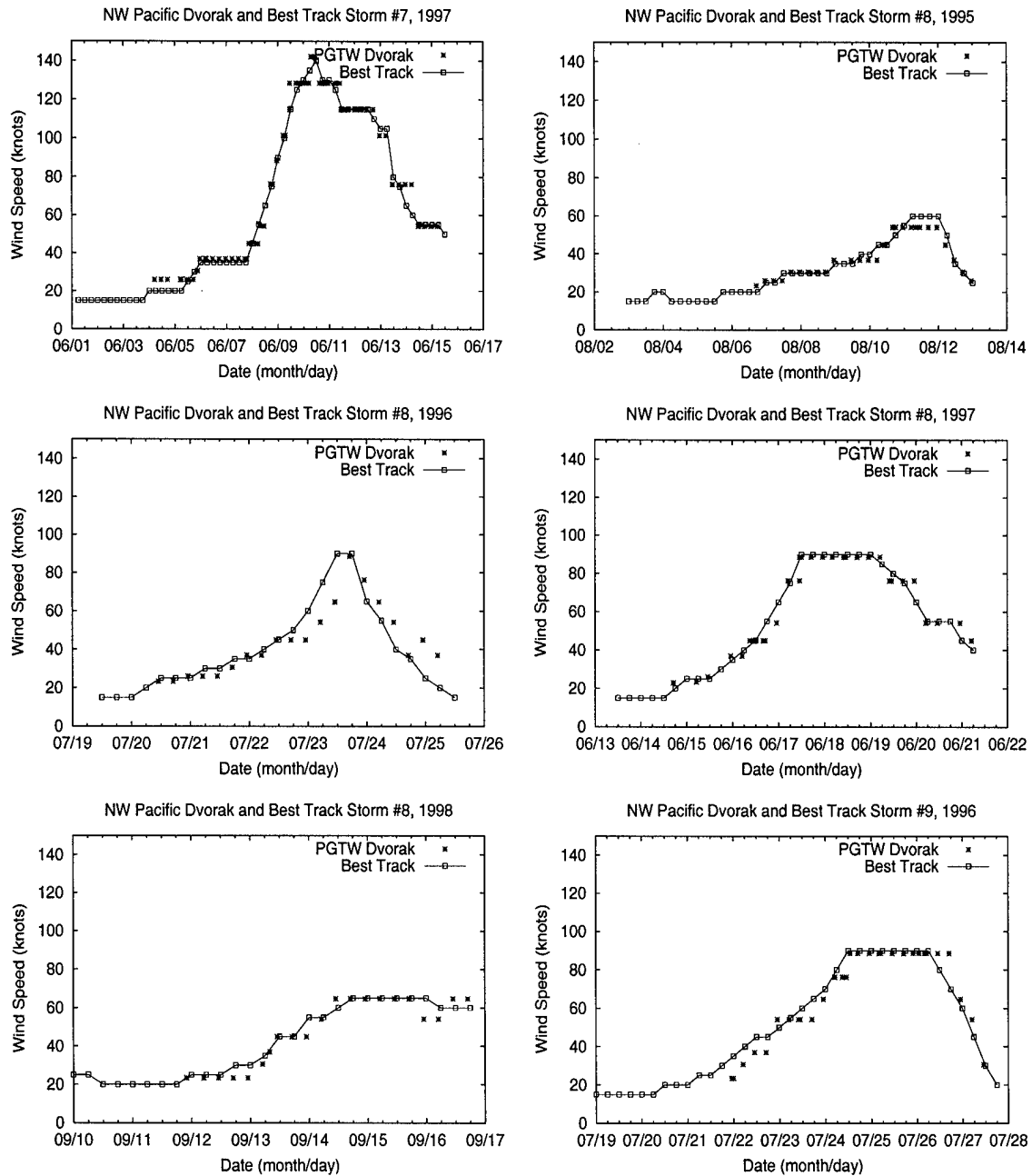
Figure B.1:
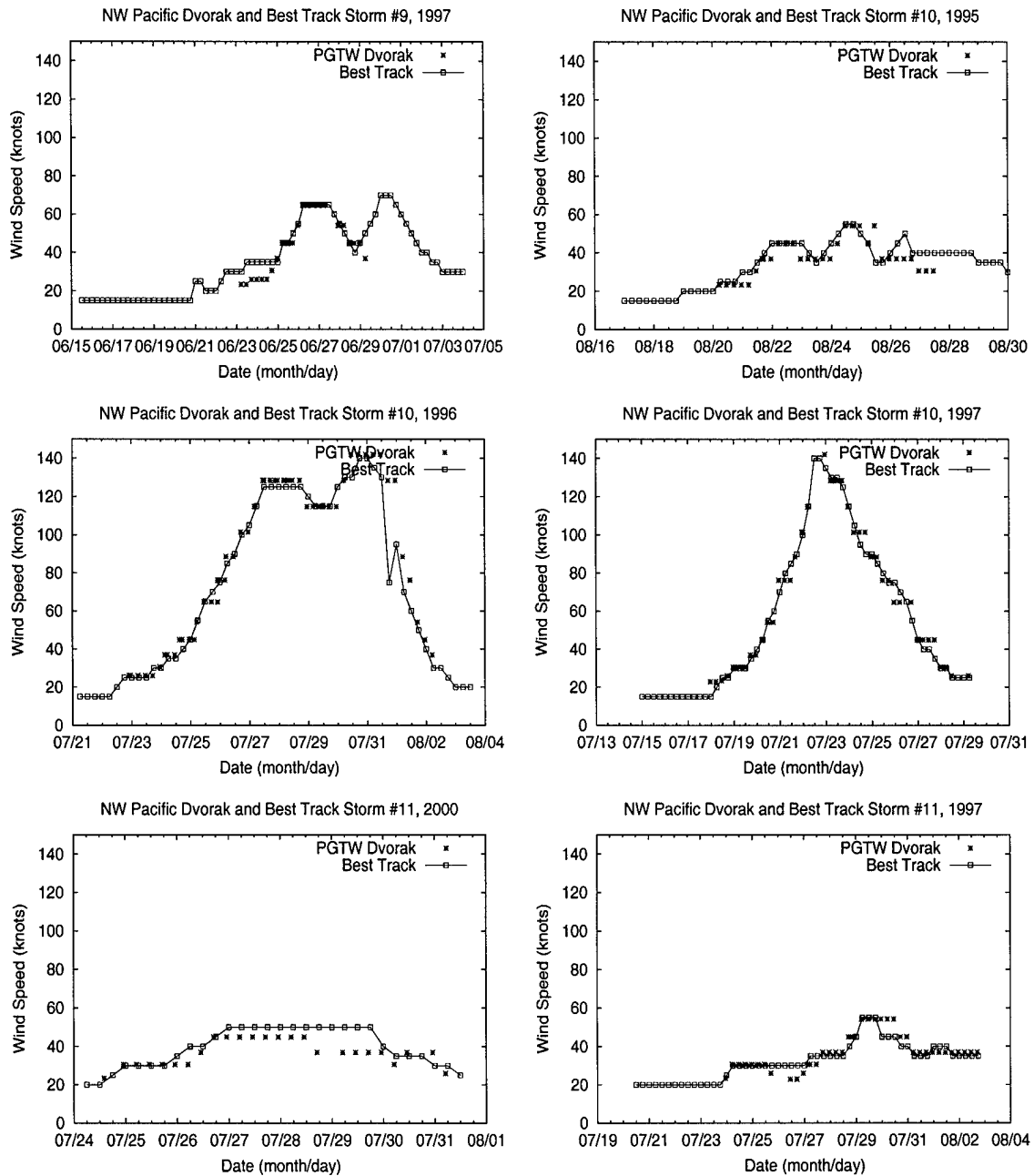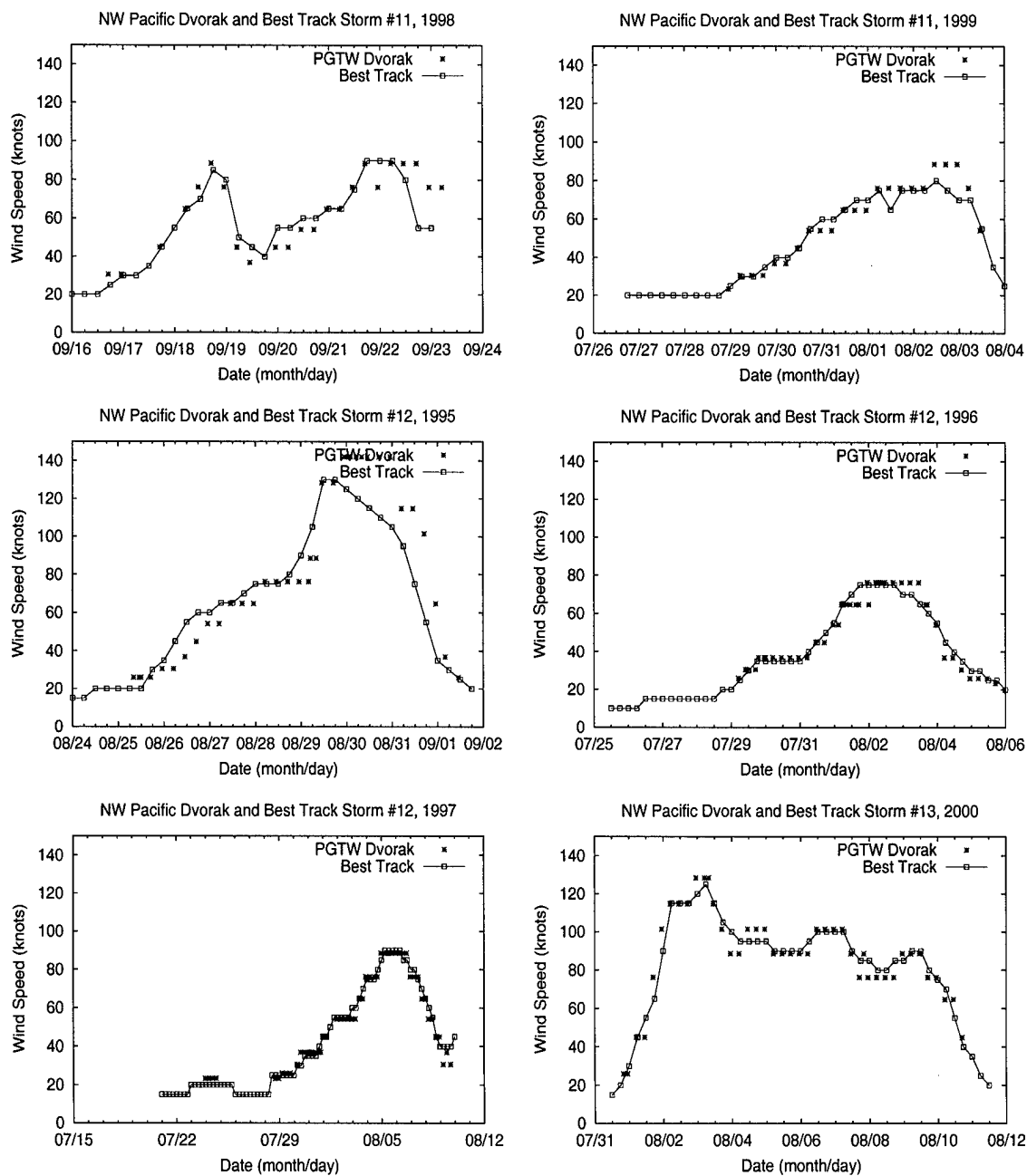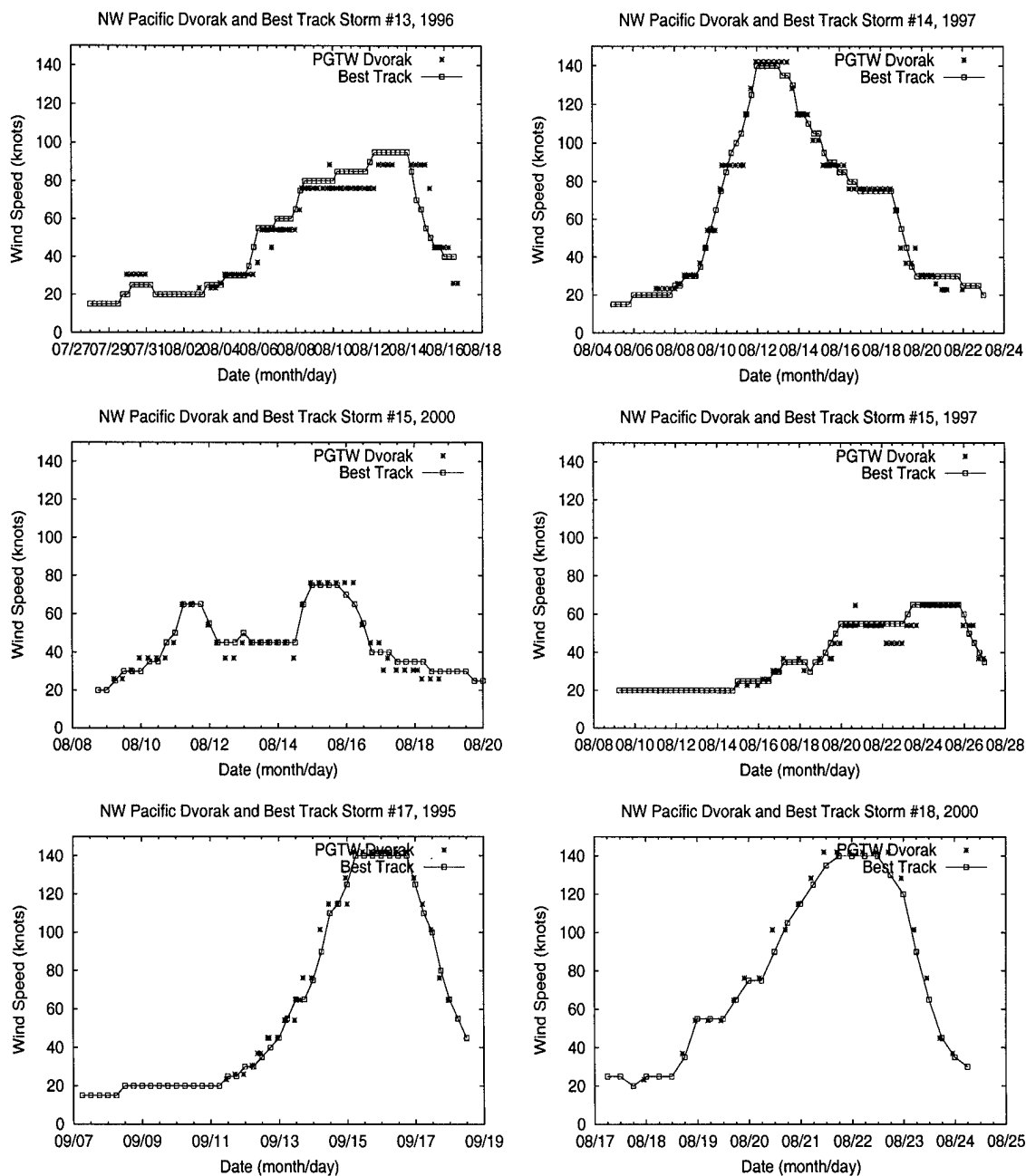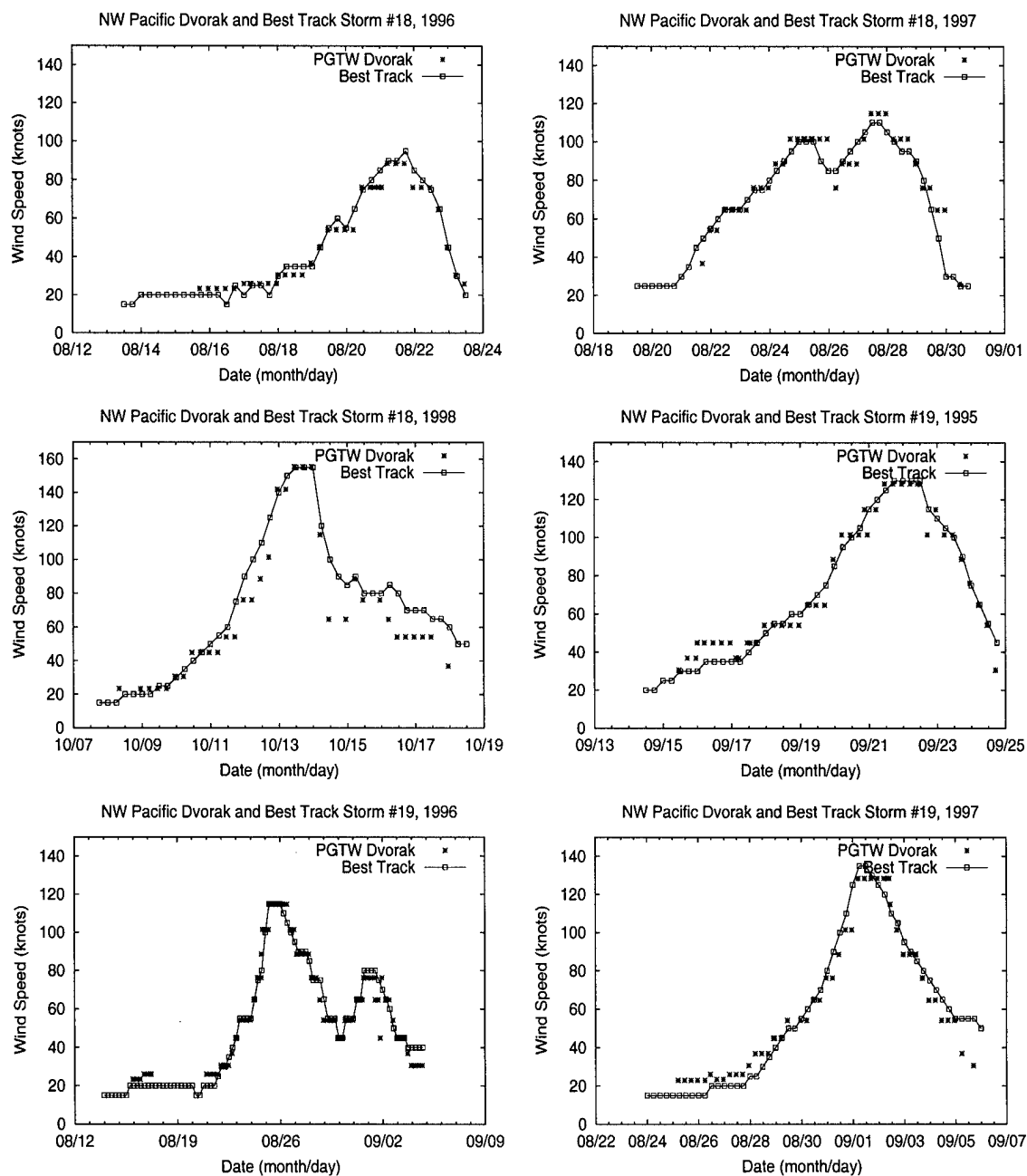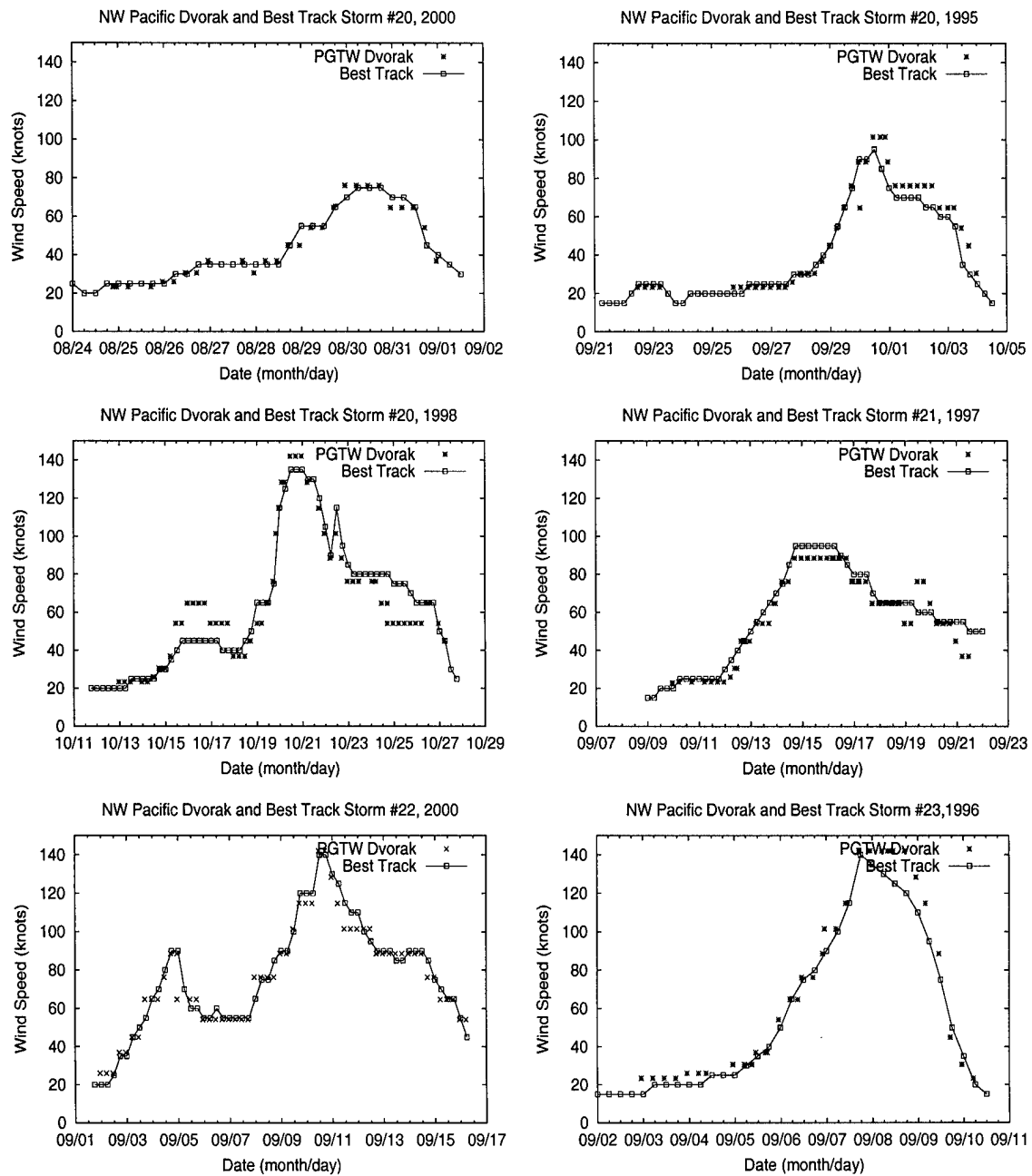
Figure B.2:

Figure B.3:

Figure B.4:
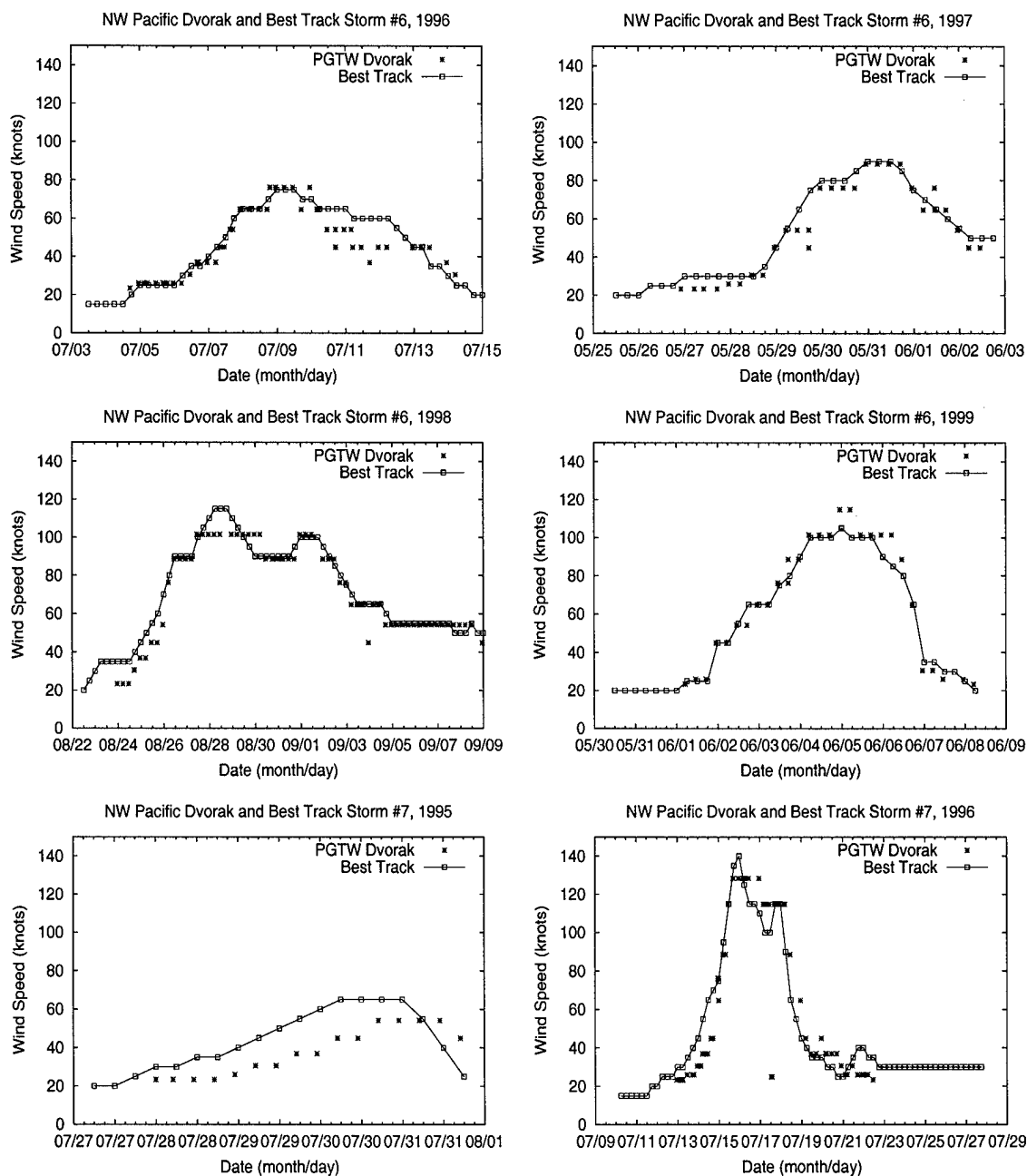
Figure B.5:

Figure B.6:

Figure B.7:

Figure B.8:

Figure B.9:

Figure B.10:

Figure B.11:

NW Pacific Dvorak and Best Track Storm #24, 1997

NW Pacific Dvorak and Best Track Storm #24, 1998

Figure B.12: